Rereplication in Cancer Cells:

Mechanisms, Regulation, and Therapeutic Opportunities

Mouadh Benamar

University of Virginia

School of Medicine

A Dissertation presented to
the Graduate Faculty of the University of Virginia
for the Degree of Doctor of Philosophy

Department of Biochemistry and Molecular Genetics

Department of Radiation Oncology

University of Virginia

June 2020

I. Abstract

Faithful and accurate transmission of the genetic information and maintenance of genomic integrity requires DNA duplication to proceed with remarkable fidelity. Excessive or incomplete DNA replication, that were not properly resolved by the cell, can result in genomic instability, developmental abnormalities, and cancer. Eukaryotic cells have evolved a multitude of regulatory mechanisms that work in concert to ensure a timely and accurate DNA replication and coordinate progression through S-phase. Failure to limit DNA replication to a single round per cell cycle results from erroneous origin re-firing leading to rereplication. Excessive rereplication is toxic to cells due to the accumulation of replication intermediates and stalled replication forks, and can lead to DNA breaks, chromosomal abnormalities, apoptosis, senescence and tumorigenesis. Amongst the regulatory mechanisms that guards against origin re-licensing is the degradation, during S-phase of the cycle, of key replicative factors via the ubiquitin proteasomal system.

Ubiquitin-mediated proteolysis is a highly regulated mechanism that controls the degradation of most cellular proteins with remarkable timing and specificity. $CRL4^{CDT2}$ E3 ubiquitin ligase plays a critical role in preventing excessive origin re-licensing in the same S-phase through the degradation of the licensing factor CDT1, the histone mono-methyltransferase SET8, and the CDK inhibitor p21. Our work shows that the expression of CDT2, the $CRL4^{CDT2}$ substrate adaptor, is elevated in melanoma and head and neck squamous cell carcinoma (HNSCC), and its elevated expression in melanoma correlates with poor patient outcome. Inactivation of $CRL4^{CDT2}$, via CDT2 depletion or pharmacological inhibition using MLN4924 (Pevonedistat), an inhibitor of the activity of all cullin-based E3 ligases, suppresses melanoma proliferation through the induction of a

p21 and SET8-dependent rereplication and senescence. We showed that MLN4924 suppresses melanoma tumor growth irrespective of the BRAF/NRAS mutational status. We have also shown that MLN4924-induced toxicity, both *in vitro* and *in vivo,* is mediated through failure to degrade p21 or SET8 during S-phase. We found that MLN4924 synergizes with the BRAF kinase inhibitor vemurafenib to suppress BRAF melanomas *in vivo* and is effective against vemurafenib-resistant melanomas. We have also shown that MLN4924 inhibits and radio-sensitizes HPV-negative HNSCC *in vivo*. Subsequent analysis demonstrates that rereplication is sufficient to confer radiation sensitivity in HNSCC.

My recent work with ionizing radiation (IR) identified rereplication as an underlying mechanism for inducing cytotoxicity in a subset of cancer cells of various epithelial origins. I have shown that DNA double-strand breaks (DSBs) are sufficient to induce rereplication in these cancer cells. The DSB-induced rereplication, or DIRR, correlates with IR-induced toxicity in melanoma cells, and is thus likely to impact the efficacy of radiotherapy in clinical settings. Mechanistically, we show that DIRR does not involve origin re-firing, and likely initiated by unshielded, hyper-resected broken DNA ends invading non-homologous sequences early in S-phase.

In summary, using various cancer model systems, my studies have shown how rereplication induction in cancer cells can exhibit anti-tumorigenic activities and demonstrate that it mediates the efficacy of new therapeutic agents (MLN4924), IR and other DSB-inducing chemotherapies.

II. Acknowledgments:

The work presented in this dissertation could not have been possible without the invaluable contribution and the overwhelming support I received from my family, colleagues, advisor, committee members, the UVA research community, and the Charlottesville friends and community throughout my tenure as a graduate student.

To my current and former lab members, words cannot describe the great teammates I had the pleasure to work with. It all began many years ago when I first joined the Abbas lab as a laboratory technician. Since then, and throughout my time as a technician and a graduate student, I had the privilege to work with incredible colleagues and exceptional talents. To Rebeka Eki, thank you for not only being an incredible colleague, but also a wonderful friend. You are a unique and talented researcher with a remarkable personality, and I am certain you will become a great scientist. To Dr. Fadila Guessous and Dr. Kang Ping, thank you for everything you have taught me and the critical assistance you provided me in various aspects of lab, especially in regards to animal work. To our former lab members Vanessa Vanderdys, Dr. Mahmut Parlak, and Dr. Jinho: thank you for your help, contribution, assistance, support, and above all the great work environment. And, of course, I wish to express my deepest appreciation and gratitude to my advisor and mentor: Dr. Tarek Abbas. Thank you Tarek for your guidance and unwavering support throughout my time in your lab. None of this would have been possible without your mentorship, contribution, and persistent help. Your patience, encouragement, ambitious character, and dedication to your work helped shape the scientist I aspire to be.

To my thesis committee members; Dr. Craig Slingluff, Dr. Bryce Paschal, and Dr. Patrick Grant, thank you for your valuable input during my committee meetings and your continued support and mentorship throughout my time as a student. To everyone in the Biomedical Sciences Graduate Program (BIMS), the Department of Biochemistry and Molecular Genetics (BMG), and the Department of Radiation Oncology, with special regards to Dr. Anindya Dutta, Dr. James Larner, and their lab members, and to Dr. Joel Hockensmith, and Dr. Janet Cross: Thank you for your relentless support and assistance throughout my time as a student. It was an honor and a privilege for me to have the opportunity to work in a program that cultivates a nourishing and supportive educational and work environment to its students, and in a department that facilitates the collaboration with various teams of incredible, talented, and ambitious scientists and researchers.

Finally I cannot express my thanks to my family, my mother, Hafidha; my father, Amor; and my brother: Fadhel, and to my extended family members in Algeria. Your unparalleled support and profound belief in my work kept me going in the most difficult times of my career. And to my Charlottesville friends and community, thank you for your persistent encouragement, continuous support, advice, and help throughout my career. I could not have done any of this without your help. Your help and support inspire me to dream more, learn more, and become more.

III. Publication Information

The following publications were used as a basis for these chapters:

Chapter II:

- Mouadh Benamar, Fadila Guessous, Kangping Du, Patrick Corbett, Joseph Obeid, Daniel Gioeli, Craig L. Slingluff Jr and Tarek Abbas. *"Inactivation of the CRL4-CDT2-SET8/p21 Ubiquitylation and Degradation Axis Underlies the Therapeutic Efficacy of Pevonedistat in Melanoma"* EBioMedicine, 2016 Aug;10:85-100. doi: 10.1016/j.ebiom.2016.06.023.

Chapter III:

- Vanessa Vanderdys, Amir Allak, Fadila Guessous, Mouadh Benamar, Paul W. Read, Mark J.Jameson and Tarek Abbas. *"The Neddylation Inhibitor Pevonedistat (MLN4924) Suppresses and Radiosensitizes Head and Neck Squamous Carcinoma Cells and Tumors"* Mol Cancer Ther August 24 2017 DOI: 10.1158/1535-7163.MCT-17-0083

Chapter IV:

- Mouadh Benamar, Rebeka Eki, Kangping Du, Vanessa Vanderdys, and Tarek Abbas. "*DNA double-strand breaks drives rereplication induction in cancer cells through a hyper-resection-mediated and origin-independent mechanism*." *Manuscript under review*.

IV. List of Abbreviations:

4-OHT	4-Hydroxytamoxifen
53BP1	p53-binding protein 1
APC/C	Anaphase Promoter Complex or Cyclosome
ATM	ataxia telangiectasia mutated kinase
ATP	Adenosine triphosphate
BAH	bromo-adjacent homology
BRAF	B-Raf Serine/Threonine Kinase
BrdU	bromodeoxyuridine
CDC6	cell division cycle 6
CDK	Cyclin Dependent Kinase
CDT1	CDC10-dependent transcript 1
CRISPR	Clustered regularly interspaced short palindromic repeats
CRL4	Cullin 4-RING E3 ubiquitin Ligase
CsCl	cesium chloride
CtIP	CtBP-interacting protein
DDK	Dbf4-dependent CDC7 Kinase
DIRR	DSB-induced rereplication
DNA-PKcs	the catalytic subunit of the nuclear serine-threonine protein kinase
DSB	DNA double-strand breaks
DTB	Double Thymidine block
EXO1	Exonuclease 1
FACS	Fluorescence-activated cell sorting
Gy	Gray; unit of ionizing radiation dose; the 1 Joule per Kilogram
H4K20me1	mono-methylated histone H4 at the lysine 20 residue
H4K20me2	di-methylated histone H4 at the lysine 20 residue
H4K20me3	tri-methylated histone H4 at the lysine 20 residue
HNSCC	head and neck squamous cell carcinoma
HPV	Human papillomavirus
HR	Homologous recombination repair
IR	ionizing radiation
Ki-67	proliferation marker
MCM2-7	mini-chromosomal maintenance complex
MDC1	mediator of DNA damage checkpoint proteins 1
MLN4924	or Penovedistat, selective inhibitor of the Neddylation Activating Enzyme (NAE1),
NAE1	neddylation activation enzyme 1
NEDD8	ubiquitin-like moiety required for neddylation
NHEJ	nonhomologous end joining repair
NRAS	N-ras proto-oncogene GTPase

NU7441	chemical inhibitor of DNA-PKcs kinase activity
ORC	Origin Recognition Complex
p16	CDKN2A, Cyclin-dependent kinase inhibitor 2A
p21	CDKN1A, Cyclin dependent kinase inhibitor 1
PCNA	Proliferating cell nuclear antigen
Pevonedistat	or MLN4924, selective inhibitor of the Neddylation Activating Enzyme (NAE1),
PI	propidium iodide
PIP box	PCNA-interacting peptide, or PIP degron
PLX4720	or Vemurafenib: Small molecule Inhibitor that specifically targets BRAF Kinase harboring V600E mutation
POL	DNA Polymerase
Pre-RCs	pre-replicative complexes
PTMs	post-translational modifications
RB1	retnoblastoma protein 1
ROS	Reactive Oxygen Species
SCF	CRL1 or SKP1-Cullin1-F-Box protein
SET8	histone methyltransferase PR-Set7
SHLD	Shieldin subunit
shRNA	short hairpin RNA
siRNA	small interfering RNA
SKP2	FBX-L1 or S-phase kinase associated protein 2
SSBs	single strand breaks
ssDNA	single stranded DNA
TCGA	The Cancer Genome Atlas
TMA	tissue microarray
U2OS	human osteosarcoma cell line
UPS	The Ubiquitin-Proteasome System Proteolytic Pathway
Vemurafenib	or PLX4720 : Small molecule Inhibitor that specifically targets BRAF Kinase harboring V600E mutation
WT	Wild type
β-gal	β-galactosidase

V. Table of Contents

VI.

Chapter I:

Introduction

Regulation of DNA Replication Initiation in Eukaryotic Cells

1. Overview of DNA Replication Initiation In Eukaryotes

Faithful duplication and accurate transmission of the genetic and epigenetic information from one cell to its daughter cells is integral for maintaining genetic stability and cellular viability. Excessive or incomplete DNA replication or failure to restrict the duplication of the genome to a single round per cell cycle can results in catastrophic consequences such as genomic instability, developmental abnormalities, and cancer. Extensive studies have identified a number of key cell cycle regulators and molecular processes that oversee and timely and accurate DNA replication and coordinate a smooth progression through S phase (Limas and Cook 2019; Marks, Fu, and Aladjem 2017). How does the cell "know" when and where to initiate DNA replication? What are the key factors involved? And how does it limit DNA replication to a single round per cell cycle?

Several studies have outlined the steps involved in the initiation of DNA replication in eukaryotic cells (Leonard and Mechali 2013): (1) **Recognition of replication origins**: identification of the chromosomal loci where DNA replication is initiated; (2) **Replication or origin licensing:** recruitment of key DNA-binding proteins that serve as a platform for the loading of the replicative MCM2-7 helicase; and (3) **Helicase activation and origin firing**: recruitment of additional factors that activate the replicative helicase and facilitate DNA unwinding and initiation of DNA synthesis. These distinct steps in replication initiation **(Figure 1.1)** are briefly described below.

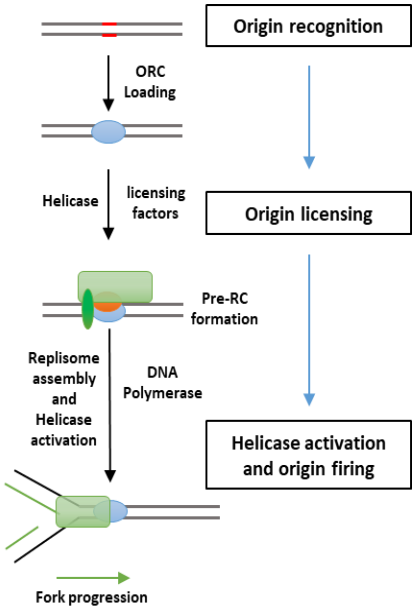

Figure 1.1: Summary of the key steps in DNA replication

1.1. Origins of DNA Replication:

DNA replication is initiated at numerous and specific chromosomal loci in the genome termed origins of replication. The number and nature of replication origins needed for efficient genome duplication varies depending on the chromosome size. The small circular bacterial and archaeal chromosome usually contains a single replication origin, while the eukaryotic genome contains from 400 origins (as in yeasts) to up to 50,000 in humans (Leonard and Mechali 2013). Due to the size of the eukaryotic genome, an efficient and timely DNA replication requires the coordinated co-activation of multiple origins per chromosome.

Unlike prokaryotes and budding yeasts, metazoan replication origins do not share a unique distinct consensus sequence, and, instead, are more plastic and exhibit high heterogeneity (Fragkos et al. 2015). However, DNA sequences are not the only determinant of replication initiation sites and highly activated replicative origins in vertebrates have been shown to share certain chromatin and epigenetic features, such as CpG islands, G-quadruplexes, transcription start sites, strand asymmetry, origin G-rich repeated elements (OGREs), and regions of DNase hypersensitivity (Marks, Fu, and Aladjem 2017). It has been estimated that only 20% of all metazoans potential origin sites initiate replication in a given cell cycle, and origin choice appears to be dictated primarily by chromatin context and cell lineage (Cayrou et al. 2015). Flexibility of origin usage, and the presence of excess “passive” or “dormant” replication origins, that are rarely used to initiate DNA replication, appear to play a role in genome preservation, and those passive

origins might act as backup initiation sites that can be activated during replication stress (Marks, Fu, and Aladjem 2017; Fragkos et al. 2015).

1.2. Epigenetic Regulation of Replication Origins:

Open, and often transcriptionally active, chromatin structures are believed to be the most favorable for origins of replication, and certain histone post-translational modifications (PTMs) are strong predictors of origin utilization and play a major role in regulating chromatin compaction. Histone phosphorylation was shown to correlate with chromatin condensation while histone acetylation leads to less compact and relaxed chromatin due to the disruption of histone-DNA electrostatic interactions (Shoaib et al. 2018). Recent genome-wide studies have demonstrated that origin sites are associated with local histone marks such as acetylated H4K5 and H4K12 catalyzed by the histone acetyltransferase HBO1, and methylated H4K20 catalyzed by histone methyltransferase PR-Set7 (SET8) (Sherstyuk, Shevchenko, and Zakian 2014; Shoaib et al. 2018). Other histone markers associated with replication origins include H3K4me1/2/3, H3K36me3, H3K9ac, H3K18ac, and H3K27ac (Smith et al. 2016). It is important to note that most findings regarding the role of histone features in chromatin structure result from genome-wide association studies with cell cycle progression, and are primarily correlative, but the precise mechanistic roles most histone PTMs play in chromatin condensation/decondensation, and whether they dictate origin regulation may require further investigation (Shoaib et al. 2018).

1.3. Origin Licensing:

The licensing of replication origins refers to the stepwise assembly of a set of DNA-binding proteins to form pre-replicative complexes (Pre-RCs) at the various origin initiation sites starting from late mitosis and throughout the G1 phase of each cell cycle **(Figure 1.1)**. Components of the Pre-RC, which are orthologous in all eukaryotes, include the DNA-binding Origin Recognition Complex (ORC, six subunits ORC1-6), representing a scaffold that facilitate the recruitment of a conserved group of accessory proteins, helicases, and polymerases that catalyze the initiation of DNA replication (Marks, Fu, and Aladjem 2017). At the end of mitosis and during the M/G1 transition, ORC directly binds to open chromatin at replication origins, which as a result recruits two licensing factors: the cell division cycle 6 (CDC6) and the CDC10-dependent transcript 1 (CDT1). Two inactive hexamer replicative helicases (mini-chromosomal maintenance complex MCM2-7) are then loaded onto each replication origin to form the pre-RCs. The inactive MCM helicases remain stably bound to DNA until the end of G1, and will be activated or "fired" in S-phase (Sheu, Kinney, and Stillman 2016; Limas and Cook 2019).

1.4. Histone Modification in Origin Licensing - H4K20 methylation:

In higher eukaryotes, loading of the ORC complex and the rest of the licensing factors onto replication origins is associated with local histone modifications rather than a unique consensus DNA sequence at origin sites. For instance, ORC1 was shown to contain a bromo-adjacent homology (BAH) domain that recognizes the di-methylated histone H4 at the lysine 20 residue (H4K20me2), a modification that was found to be enriched at origins of replication (Kuo et al. 2012). Mutation in the ORC1 BAH domain, which

abrogates the ability of ORC1 to recognize H4K20me2, decreases ORC1 loading and occupancy at replication origins and impairs cell cycle progression (Kuo et al. 2012). Depletion of the mono-methyltransferase SET8, which results in a genome-wide reduction in H4K20 methylation, leads to defects in origin licensing (Limas and Cook 2019). It is important to note that the methylation of H4K20 was found to enhance MCM2-7 loading, but the histone mark alone was insufficient to define a functional replication origin (Brustel et al. 2017). On the other hand, excessive H4K20 methylation as a result of the uncontrolled expression of SET8 results in de-regulated origin licensing, and re-replication (discussed later in this chapter) (Limas and Cook 2019).

The expression of the core components of the pre-RC is controlled on the transcriptional level by members of the E2F transcription factors, which are activated as a result of Cyclin D/CDK4-6 activity after mitogen stimulation. The activity of each origin licensing factor is tightly regulated by various PTMs (phosphorylation and ubiquitylation) to ensure timely and proper licensing and avoid premature or excessive firing (Limas and Cook 2019).

1.5. Helicase Activation and Origin Firing:

To ensure the timely and efficient DNA replication in higher eukaryotes, thousands of origins are “licensed” throughout G1, and activated at different times during S-phase. Helicase activation or “origin firing” requires a series of phosphorylation events that establishes the replication fork machinery (promote the recruitment of polymerases and accessory replication factors), and initiate DNA synthesis in a bidirectional fashion from each origin (Limas and Cook 2019). As a result of the activity of S-phase kinases, such as

Cyclin-Dependent Kinase 2 (CDK2) and Dbf4-dependent CDC7 Kinase (DDK), additional factors including CDC45, MCM10, and the GINS complex (Sld5, Psf1, Psf2, Psf3) are recruited to the inactive MCM hexamers to form the active helicase complex (CMG; CDC45-MCM-GINS) (Tanaka and Araki 2013; Sheu, Kinney, and Stillman 2016). Origin firing requires additional factors, such as TopBP1, Treslin, RECQL4, MCM10, and DNA polymerase (Pol ε). Finally, after the recruitment PCNA, RPA, and RFC, the replisome is fully activated and the bidirectional progression of the replication forks commences on both DNA strands (Limas and Cook 2019).

2. Negative Regulation of DNA Replication: The Ubiquitin-Proteasome System (UPS)

All proteins within the cell are maintained in a dynamic state and are continuously created, modified, and degraded with remarkable timing and specificity. Active and proper balancing between synthesis and degradation of cellular proteins is a primary mechanism in regulating most cellular processes. Major intracellular proteolytic systems used in protein homeostasis include (1) the endo-lysosomal degradation pathway, (2) autophagy, and (3) the ubiquitin proteolytic pathway (Schwartz and Ciechanover 2009) .

2.1. The Ubiquitin-Proteasome Proteolytic Pathway:

Ubiquitin-proteasomal degradation is a highly regulated and irreversible process that governs the downregulation of most cellular proteins (Figure 1.2). Ubiquitin proteolysis occurs in two major steps: (1) Ubiquitin conjugation or labeling via the covalent attachment of a single or multiple ubiquitin molecules to the targeted substrate protein, (2) degradation of ubiquitylated or labeled substrates via the 26S proteasome

complex (Schwartz and Ciechanover 2009). Ubiquitin conjugation to the substrate occurs in three consecutive enzymatic steps. (1) First, the ubiquitin moiety, a highly conserved 76-amino acid polypeptide, is "activated" by the E1 ubiquitin-activating enzyme. (2) Second, an E2 ubiquitin-conjugating enzyme carries or transfers the activated ubiquitin to

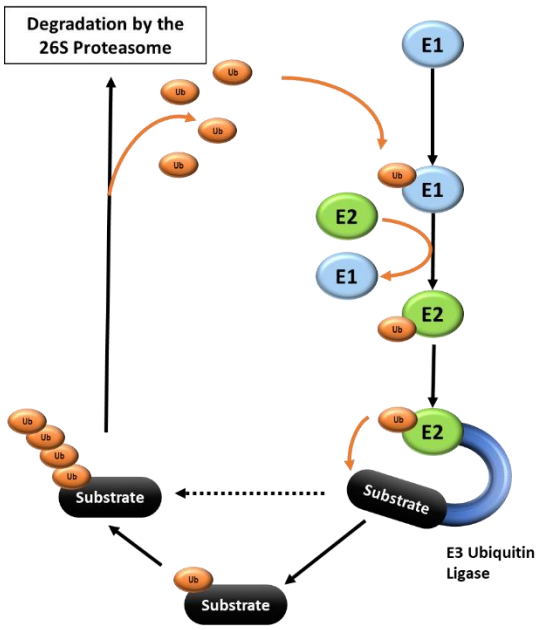

Figure 1.2: Summary the Ubiquitin-Proteasome Proteolytic Pathway

a highly selective E3 ubiquitin ligase which (3) mediate the covalent attachment of the ubiquitin moiety to the substrate targeted for degradation (Schwartz and Ciechanover 2009). The resulting polyubiquitin chains feature at least five different topologies depending on the ubiquitin lysine residue used for chain extension (Figure 1.2). The canonical Lys48-linked ubiquitin chain, which adopts a tightly packed conformation, typically targets the substrate for degradation via the 26S proteasome. Other forms of ubiquitin linkages (such as Lys6, Lys11, Lys27, Lys29, Lys33, Lys63, Met1, and monoubiquitylation) which can form different chains with variable conformations and

configurations have also been implicated in non-proteolytic processes such as protein interaction, activation, and localization (Komander and Rape 2012; Kliza and Husnjak 2020; Akutsu, Dikic, and Bremm 2016) (Table 1).

Table 1 Ubiquitin Linkage Types and physiological functions
(Akutsu, Dikic, and Bremm 2016)

Ub Linkage	Examples of physiological processes	Examples of E3 ligases with preference for this linkage
K6	DNA damage response	BRCA1
K11	Cell cycle control, proteasomal degradation (less common)	APC/C
K27	Nuclear translocation, DNA damage response	RNF168
K29	Wnt signaling	Smurf1, UBE3C
K33	TCR signaling, post-Golgi trafficking, kinase signaling	Cul3-KLHL20, AREL1
K48	Typical signaling for proteasomal degradation	SCF, E6AP
K63	Endocytosis, protein trafficking, innate immunity, NFkB signaling	TRAF6
M1	innate immunity, NFkB signaling, angiognenesis, authophagy	LUBAC

The polyubiquitin chain architectures and linkages are thought to be determined by the conjugating E2 enzymes , while the E3 ubiquitin ligases are known to confer substrate specificity (Rieser, Cordier, and Walczak 2013). E3s are classified into at least two main types: HECT (Homology to E6AP C terminus) and RING (Really interesting new gene). While both E3s recruit the substrate and bring it into contact with E2s, HECT E3 enzyme

directly participate in the reaction of transferring the ubiquitin moiety to the substrate (Skaar, Pagan, and Pagano 2014). The human genome contains at least 20 E2s and roughly 1000 E3 ligases, but only a few of these enzymes have been characterized (Schwartz and Ciechanover 2009).

2.2. The Cullin-RING E3 Ubiquitin Ligases:

Cullin-RING E3 ubiquitin ligases (CRLs) represent the largest family of E3 ligases and are involved in regulating various cellular processes, including cellular progression through the cell cycle. CRLs contain four main subunits. The first subunit is the evolutionary conserved **Cullin scaffold**, for which the human genome encodes 6 types (CUL1, 2, 3, 4A, 4B, 5) and two atypical ones (CUL7, and 9). The second subunit, the **RING finger domain** (RBX1 and/or RBX2 bound to two zinc atoms), interacts with the Cullin at the C-terminus. One of four **adaptor proteins** (Skp1 (S-phase kinase-associated protein 1), Elongin B, Elongin C, or DDB1 (damaged DNA binding protein 1) represent the third subunit. Each adaptor proteins interacts with a particular Cullin at the N-terminus. For example, Skp1 typically interacts with CUL1 and CUL7, while DDB1 is often linked with CUL4A and 4B (Chen et al. 2015). The E3 specificity is conferred by the fourth subunit, **the substrate recognition receptor**, for which more than 400 proteins have been identified in the human genome. These include 78 F-box proteins for CUL1, 80 SOCs for CRL2/5, more than 200 BTBs for CRL3, and 90 DCAFs (DDB1 and Cul4-associated Factors) for CRL4A/B (Chen et al. 2015).

Tumors can take advantage of the ubiquitin-proteasome system (UPS) to achieve uncontrolled proliferation or resistance to apoptosis (Heo, Eki, and Abbas 2016).

Deregulations of CRLs have been shown to play a role in oncogenesis due to their central role in regulating cell cycle progression, proliferation, and survival. Proteins such as SKP2 and CUL4A are considered oncogenic, and were found to be frequently overexpressed in tumors, while FBXW7 and VHL act as tumor suppressors and were found to be mutated or inactivated in tumors (Table 2) (Chen et al. 2015).

Table 2. Examples of Cullin-based E3 ubiquitin ligases with an anti-cancer therapeutic potential

Cullin	**Examples of Adaptors and Substrate Receptors**	**Examples of substrates**
CUL1	SKP2, β-TrCP, FBW7	p21, p27, phosphorylated CDT1, cyclin E, mTOR, c-MYC, c-JUN
CUL2/5	VHL	HIF1α
CUL3	KEAP1	NRF2
CUL4A	DDB2/CDT2	CDT1, p21, SET8,

Reference: (Soucy, Smith, and Rolfe 2009)

2.3. Key E3 Ubiquitin Ligases Involved in Regulation of DNA Replication:

Cell cycle progression is primarily regulated by the activity and the levels of various cyclin-dependent kinases (CDKs), CDK-interacting proteins, and CDK inhibitors (Nakayama and Nakayama 2006). The activity of each CDK is mediated by the presence of its cyclin partner and the specific CDK inhibitor, and by certain protein modifications, such as phosphorylation. The levels of cyclins, CDK inhibitors, and other cell cycle

regulators oscillate during each phase of the cell cycle as a result of a delicate balance between synthesis and proteolysis via the UPS (Nakayama and Nakayama 2006). The E3 ubiquitin ligases **APC/C complex** (Anaphase Promoter Complex or Cyclosome) and **SCF** (CRL1 or SKP1-Cullin1-F-Box protein) and are among the best well-characterized ligases responsible for driving cell cycle progression by impacting DNA replication and controlling the periodic proteolysis of cyclins and cell cycle regulators (Lee and Diehl 2014; Chen et al. 2015; Abbas 2019).

2.4. APC/C E3 Ubiquitin Ligase:

APC/C (Anaphase promoting complex/cyclosome) is the largest multi-subunit E3 ubiquitin ligase whose activity is critical in regulating DNA replication and driving cell cycle progression (Robbins and Cross 2010). APC/C interacts with two main substrate receptors CDC20 (during mitosis) and CDH1 (late mitosis and throughout G1 phase) (Robbins and Cross 2010). Normal cell cycle progression requires APC/C to be active from late mitosis and inactive by the G1/S transition. APC/C is needed at early G1 to maintain a low CDK activity required for the proper initiation of DNA replication. By the end of G1, APC/C is inactivated due to the rise in activity of its negative regulators, such as E2F1-dependent transcription of the APC/C inhibitor EMI1 and Cyclin E-CDK2. The full inactivation of APC/C at the G1/S transition is regarded as a “point of no return” in S-phase entry (Limas and Cook 2019).

2.5. SCF^{SKP2} E3 Ligase:

The SCF^{SKP2} E3 ubiquitin ligase, which is composed of an SCF ligase associated with the substrate receptor SKP2 (FBX-L1 or S-phase kinase associated protein 2), is

another essential driver of DNA replication initiation and is directly involved in the proteolysis of key components of the pre-RCs (Abbas and Dutta 2017). The timely degradation of pre-RC components ensures that origin licensing occurs only from late mitosis to G1 and is prevented during the rest of the cell cycle. SCF^{SKP2} also promotes DNA replication through the ubiquitin-dependent degradation of CDK inhibitors such as p21, p27, and p57 (Table 2) (Abbas and Dutta 2017).

Since SCF^{SKP2} is responsible for the negative regulation of many replication initiation factors, the degradation of its substrate receptor SKP2 by APC/C^{CDH1} during late M and G1 is necessary to stabilize replicative factors and facilitate pre-RC assembly. For instance, ORC1, the largest subunit of the ORC complex, is targeted for degradation by SCF^{SKP2}. Therefore, ORC1 levels remain stable in G1 where SKP2 is kept low by APC/C^{CDH1} but is degraded in S-phase when APC/C is inactive and SKP2 is stable (Abbas and Dutta 2017).

2.5.1. $CRL4^{CDT2}$ E3 Ubiquitin Ligase:

The $CRL4^{CDT2}$ E3 ubiquitin ligase is an emerging major coordinator of cell cycle progression and genomic instability (Abbas and Dutta 2011). Recent studies have demonstrated the critical role the cullin 4-based E3 ubiquitin ligase $CRL4^{CDT2}$ plays in preventing aberrant origin relicensing and preserving the integrity of the genome by degrading positive regulators of origin licensing (Abbas and Dutta 2011). The core structure of cullin 4 E3 ligases is very similar to other cullin-based SCF ligases (Higa and Zhang 2007). CRL4 ligases are composed of a core Cullin 4 (A or B) scaffold protein attached to one Ring finger domain (RBX1 or RBX2) needed to bind the E2 conjugating

enzyme carrying the activated ubiquitin moiety, and a DDB1 adaptor protein (DNA damage-specific protein-1) responsible for binding one of many DCAFs, such as CDT2 (Higa and Zhang 2007).

$CRL4^{CDT2}$ is a unique E3 ligase that recognizes its substrates (namely CDT1, p21, and SET8) only when they are interacting with the chromatin-bound PCNA (Proliferating cell nuclear antigen) through a PIP box motif (PCNA-interacting peptide, or PIP degron) (Table 2) (Senga et al. 2006; Arias and Walter 2006; Abbas, Keaton, and Dutta 2013; Abbas and Dutta 2011). The chromatin-bound PCNA requirement of $CRL4^{CDT2}$ substrate recognition therefore limits the ligase's activity to S-phase and in response to certain types of DNA damage (Senga et al. 2006; Arias and Walter 2006; Abbas, Keaton, and Dutta 2013; Abbas and Dutta 2011). By promoting the degradation of these key replication factors during S-phase, $CRL4^{CDT2}$ prevents replication relicensing until DNA replication and the subsequent chromosomal segregation are completed.

3. Negative Regulation of the Pre-RC Components to Prevent Rereplication

Eukaryotic cells have evolved multiple mechanisms to maintain a tight control on DNA replication initiation and the level and activity of replicative factors, such as CDT1 and CDC6, throughout the cell cycle. This strict regulation aims to avert DNA re-replication by preventing any erroneous re-licensing of the same DNA or licensing of newly replicated DNA until the end of mitosis. This timely regulation is mediated by the activity of the key E3 ubiquitin ligases described above and driven by the oscillating levels of CDKs throughout the cell cycle.

3.1. CDK Levels

Origin licensing and the sequential assembly of Pre-RCs (ORCs, CDC6, CDT1, MCM2-7) begins at the end of mitosis and continue through G1 (Figure 1.1). The phosphorylation of pre-RCs components by CDK inhibits origin licensing by either promoting the nuclear export of phosphorylated licensing factors, such as CDC6, or by facilitating their proteolysis via the UPS. Therefore, in order for origin licensing to proceed normally, CDK activity must remain low. From late mitosis to the end of G1, CDK activity is maintained low due to the increased levels of CDK inhibitors (such as p21 and p27) and the activity of the APC/C^{CDH1} E3 ligase which promotes the degradation of mitotic Cyclins (A and B) and the CDC25A phosphatase (Abbas and Dutta 2017). By the end of G1 and through S-phase, CDK activity is restored due to the inactivation of its negative regulators. At the end of G1, CDK inhibitors p21 and p27 are targeted for degradation by SCF^{SKP2}, and p21 is also degraded in S-phase by $CRL4^{CDT2}$ (Elzen and Pines 2001; Abbas and Dutta 2009). By the end of G1, increased levels of CDK lead to the phosphorylation of pRb (by Cyclin D1/CDK4 and 6, and Cyclin E/CDK2), which promotes the transcription of E2F1 target genes needed to prevent origin re-licensing (such as EMI1 and Geminin) and drive S-phase entry and progression (such as Cyclin E) (Abbas and Dutta 2017).

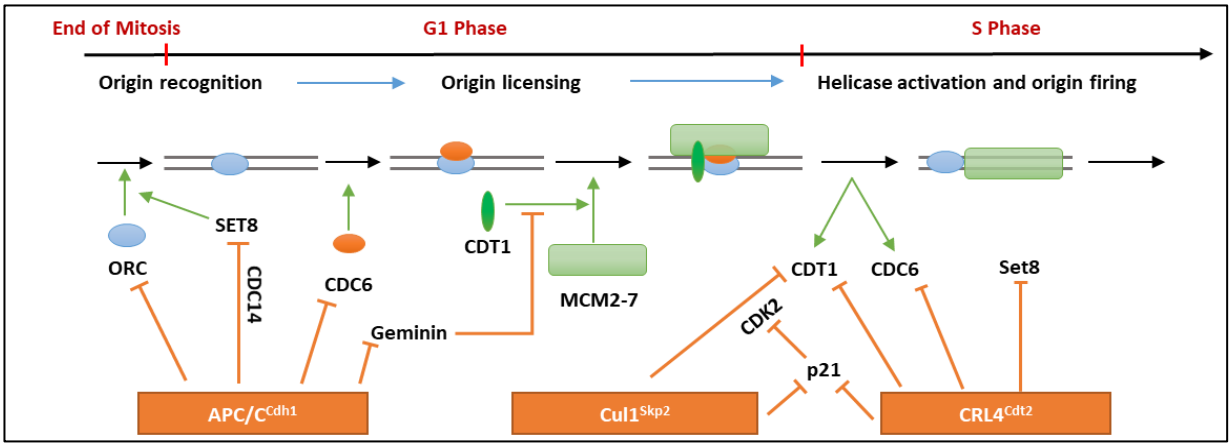

Figure 1.3 DNA Replication initiation regulation by CRLs (modified from: Abbas and Dutta, 2017).

3.2. CDC6

Starting from the G1/S transition, mammalian CDC6 is phosphorylated by CDK, triggering its nuclear export to the cytoplasm (Mailand and Diffley 2005). This prevents relicensing until the levels of CDK are down in mitosis. Studies have also shown that CDC6 is degraded by APC/C^{CDH1} in G1 (Figure 1.3), but this is inhibited following its phosphorylation by Cyclin E/CDK2 (Mailand and Diffley 2005). During S-phase, chromatin-bound CDC6 is targeted for degradation via the $CRL4^{CDT2}$ E3 ligase via its interaction with PCNA (Clijsters and Wolthuis 2014) (Figure 1.3). CDC6 is also ubiquitylated by $SCF^{CyclinF}$ E3 ligase in G2 and early mitosis, and this degradation was shown to be critical in preventing re-replication (Clijsters and Wolthuis 2014; Walter et al. 2016).

3.3. CDT1

CDT1 is another key factor in origin licensing and helicase loading. The timely degradation or inhibition of CDT1 activity is critical to prevent origin-relicensing (Abbas and Dutta 2017). At the G1/S transition, CDT1 is phosphorylated by CDK (Cyclin A/CDK2), creating a “phospho-degron” motif recognized by SKP2, which promotes its proteolysis by SCF^{SKP2} E3 ligase (Liu et al. 2004) (Figure 1.3). The activity of SKP2 and the subsequent phosphorylation mediated proteolysis of CDT1 is facilitated by the inhibition of APC/C activity through EMI1 (early mitotic inhibitor 1) at this stage of the cell cycle.

During S-phase, CDT1 is ubiquitylated via the $CRL4^{CDT2}$ ligase (Senga et al. 2006) (Figure 1.3). As mentioned above, $CRL4^{CDT2}$ recognizes the chromatin-bound CDT1

through its interaction with PCNA via a PIP (PCNA-interacting peptide) motif or PIP degron (Abbas, Keaton, and Dutta 2013). $CRL4^{CDT2}$-mediated proteolysis of CDT1 is found in all eukaryotes, except for budding yeast who appears to lack an ortholog of CDT2 (Zaidi et al. 2008). Studies have shown that the inhibition of the $CRL4^{CDT2}$-mediated degradation of CDT1 is sufficient to induce re-replication and genomic instability, highlighting the critical importance this regulatory mechanism plays in preventing origin-re-licensing and promoting healthy cell cycle progression (Abbas and Dutta 2017).

CDT1 activity is also inhibited in S-phase through the interaction with a small protein called geminin (Figure 1.3). The binding of geminin to CDT1 sterically hinders the loading of a second helicase at the same replication origin site (Tada et al. 2001; Abbas and Dutta 2017). Geminin levels are maintained low in G1 by the APC/C^{CDH1} ligase. By the end of G1, due to the increase in E2F1-dependent transcription and CDK-mediated suppression of the APC/C^{CDH1}, Geminin levels are restored and remain stable until the end of mitosis, where it is degraded after the resurgence of APC/C^{CDH1} ligase and remains low throughout G1 (McGarry and Kirschner 1998).

4. The Consequences of Deregulated Origin Licensing: DNA Rereplication

4.1. DNA Re-replication

As mentioned earlier, eukaryotic cells have evolved multiple mechanisms to strictly regulate replication factors and ensure that DNA sequences are duplicated once and only once per cell cycle. Due to the large size of the mammalian genome, S-phase progression takes several hours and a single molecular mechanism is not sufficient to prevent all possible instances of re-licensing. The presence of a multitude of regulatory mechanisms that operate in a parallel fashion aim to minimize the probability of origin re-licensing in case one mechanism is compromised. Failure to prevent re-initiation of DNA replication, or origin re-firing, results in re-replication and genomic instability (Figure 1.4). On the other hand, failure to properly assemble pre-RCs at sufficient replication origins inhibits cell proliferation and results in growth arrest. The consequences of re-replication can be

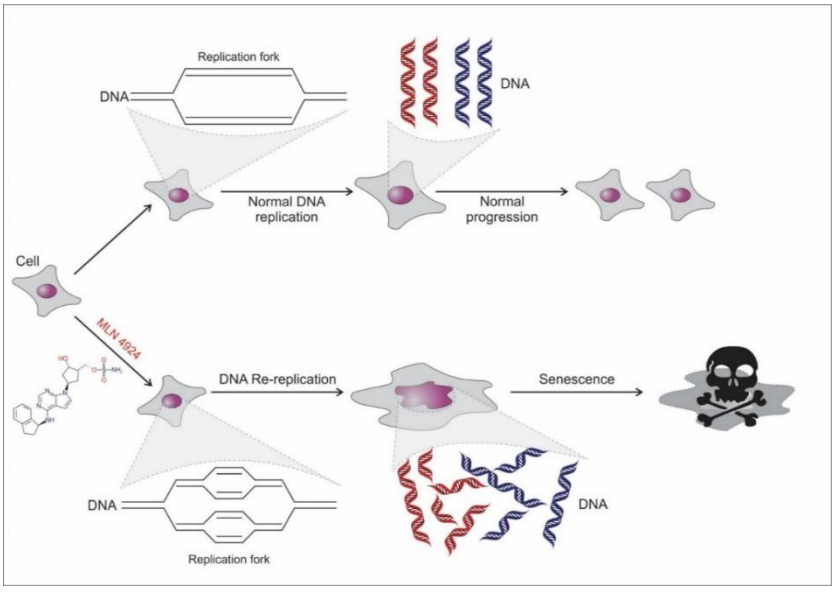

Figure 1.4 Schematic depicting DNA re-replication, resulting from an abnormal re-initiation of DNA replication within the same cell division cycle.

devastating to the cell and include stalled and collapsed replication forks, chromosome breakage, DNA breaks, mutagenesis, gene amplification, apoptosis, senescence, and oncogenesis (Liontos et al. 2007; Bui and Li 2019; Truong and Wu 2011; Abbas, Keaton, and Dutta 2013). Deregulated expression of replication initiation proteins has been observed in several human malignancies, and the overexpression of several of these lead to the transformation of premalignant cells and promote tumorigenesis *in vivo* (Bui and Li 2019; Liontos et al. 2007).

4.2. Perturbations that Result in Re-replication:

Rereplication has been shown to be induced pharmacologically or through genetic manipulations of proteins that control origin licensing. Excessive origin licensing caused by the overexpression of CDT1 or depletion of its negative regulators (geminin or CDT2), has been shown to cause deleterious effects resulting from the accumulation of DNA damage, cell cycle checkpoint activation, and apoptosis (Abbas and Dutta 2011; W. Zhu and Dutta 2006; Abbas, Keaton, and Dutta 2013). Studies have shown that the inactivation of CDT1 degradation via SCF^{SKP2}, which requires CDT1 phosphorylation by cyclin A-CDK2, however, is insufficient to induce rereplication, presumably due to the fact that CDT1 is still degraded by $CRL4^{CDT2}$ (Takeda, Parvin, and Dutta 2005). In G2 where CDT1 reaccumulates and the levels of CDKs are high, geminin-mediated inhibition of CDT1 is particularly important in preventing re-licensing and re-firing of already replicated DNA (Machida and Dutta 2007). Rereplication was also shown to be induced in cells with the overexpression a stable mutant of CDC6, or inactivation of its E3 ligase $SCF^{CyclinF}$, particularity in the absence of geminin (Walter et al. 2016).

In addition to CDT1 and CDC6, another $CRL4^{CDT2}$ target whose degradation is essential in preventing rereplication is the mono-methyltransferase SET8 (Pr-Set7) (Abbas et al. 2010; Tardat et al. 2010) (Figure 1.3). Chromatin-bound SET8 is normally targeted for degradation by $CRL4^{CDT2}$ at the G1/S transition and during S-phase. Expression of a $CRL4^{CDT2}$-insensitive, non-degradable, but catalytically active form of SET8 is sufficient to induce robust rereplication in multiple cell lines (Abbas et al. 2010; Tardat et al. 2010).

4.3. Pharmacological Induction of Rereplication

One of the most common examples of pharmacological agents causing anti-proliferative effect in cancer as a result of rereplication is a small molecule inhibitor called MLN4924 (Pevonedistat or TAK-924, from Millennium pharmaceuticals, Inc.). MLN4924, an adenosine sulfamate derivative, is a first-in-class, selective inhibitor of the Neddylation Activating Enzyme (NAE1) required for various cellular processes, including the activation of Cullin-based E3 ubiquitin ligases (Soucy, Smith, and Rolfe 2009).

4.3.1. Neddylation:

The activation of CRLs requires a PTM termed Neddylation, which is the covalent attachment of a ubiquitin-like moiety NEDD8 (neural precursor cell expressed, developmentally down-regulated 8) to the Cullin scaffold. Similar to ubiquitylation, neddylation requires a three-step enzymatic process which includes: (1) ATP-dependent "activation" of NEDD8 through a NEDD8-activating enzyme E1 (NAE1) forming an NAE-NEDD8 thioester. (2) The activated NEDD8 is then transferred to an E2 conjugating enzyme (UBC12 or UBE2F). (3) Finally, NEDD8 is covalently attached to the target

substrate (such as the C-terminus of a cullin protein) through a NEDD8-E3 ligase (Chen et al. 2015; Soucy, Smith, and Rolfe 2009).

Structural studies have shown that the neddylation of cullins causes a conformational change in the N-terminus that brings the E2 enzyme in close proximity to the substrate to facilitate ubiquitin transfer (Duda et al. 2008). Neddylation is increasingly becoming an attractive anticancer target due to recent studies showing the levels of catalytic neddylation enzymes are upregulated in several human cancers associated with poor survival (e.g. breast, lung, glioblastoma, and liver cancers) (Zhou and Jia 2020).

4.3.2. MLN4924

MLN4924 has been shown to selectively inhibit NAE1 by forming a covalent adduct with NEDD8, which prevents the formation of the NAE-NEDD8 thioester bond (Soucy, Smith, and Rolfe 2009). Inhibition of NAE1, and thus CRLs, results in the accumulation of CRL ubiquitylation substrates. Due to the regulatory roles CRL ligases play in DNA replication, repair, and cell cycle progression, the disruption of their activity by MLN4924 led to the disruption of S-phase, induction of rereplication, accumulation of DNA damage, senescence, and cell death (Soucy, Smith, and Rolfe 2009). MLN4924 also exhibited strong anti-tumor activity in mouse models and is currently in multiple clinical trials for hematologic and solid malignancies (Soucy, Smith, and Rolfe 2009; Soucy et al. 2009; Abbas and Dutta 2017).

4.4. Consequences of DNA Rereplication:

DNA replication is a critical step in cellular development and cells are highly sensitive and intolerant to any event, however rare, that disrupts this delicate process and leads to DNA rereplication. Several studies have shown that the induction of DNA rereplication leads to the activation of cell cycle checkpoints to prevent genomic instabilities and protect cells against potentially harmful replication intermediates (Truong and Wu 2011).

4.4.1. DNA Damage and Checkpoints Activation:

In mammalian cells, rereplication induced after CDT1 overexpression, or the depletion of geminin or CDT2 was shown to result in an increase of H2AX phosphorylation, suggesting the generation of DNA lesions including ssDNA and DSBs (Archambault et al. 2005; Liu et al. 2007; Benamar et al. 2016; Vanderdys et al. 2018). Several studies have shown that, upon Cdt1 overexpression, RPA-bound ssDNA is

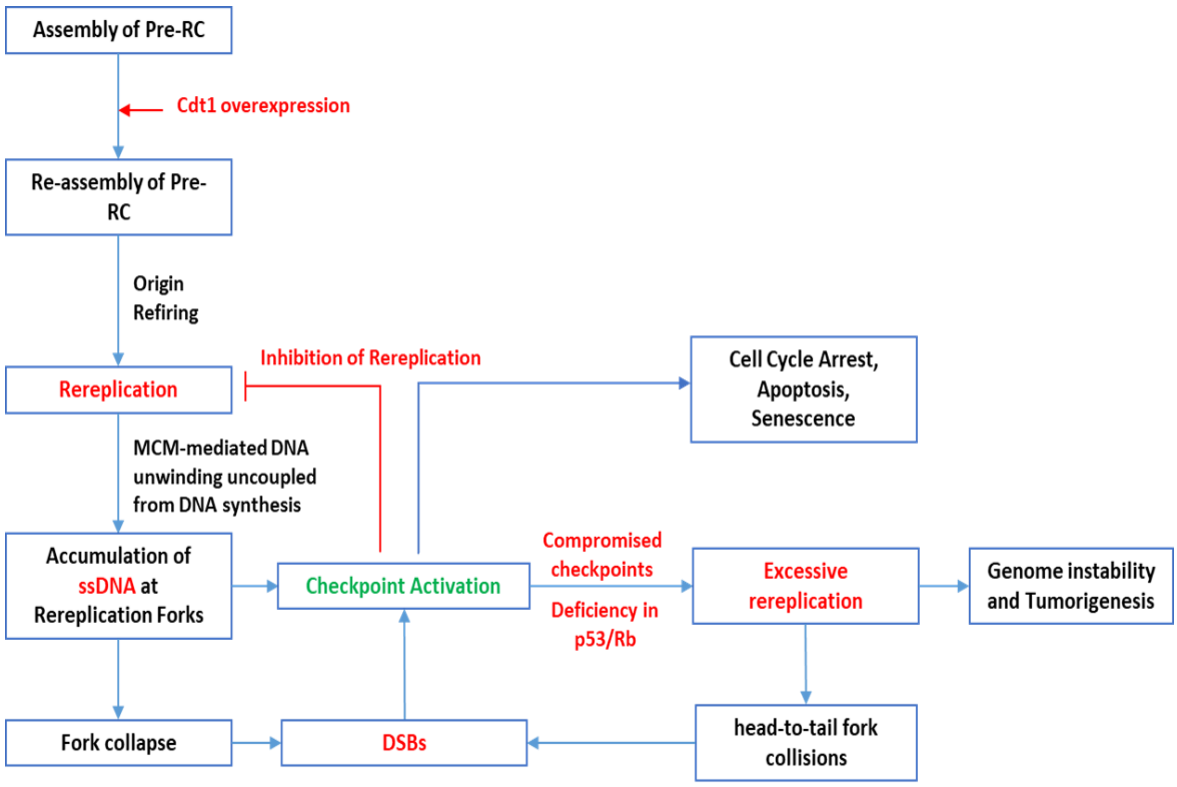

Figure 1.5: ATR-mediated S-phase checkpoint prevents rereplication caused by deregulated origin licensing. Adapted from (Truong and Wu 2011).

detected at an early stage and is generated as a result of the MCM-mediated unscheduled DNA unwinding of re-licensed origins that may exceed the rate or capacity of available DNA polymerases. This ssDNA formation serves as an early signal that triggers ATR checkpoint activation to prevent further rereplication, and is eventually followed by ATM activation that act synergistically with ATR to arrest cells in G2/M (Liu et al. 2007). As shown in Xenopus egg extracts, DSBs are subsequently generated at a later stage as a result of head-to-tail collisions of replication forks chasing each other or when new forks encounter Okazaki fragments leading to the accumulation of DNA fragments (Davidson, Li, and Blow 2006; Liu et al. 2007) (Figure 1.5).

Both ATM and ATR are important checkpoint kinases that play overlapping but non-redundant roles in detecting abnormal DNA lesions. While ATM is activated as a result of DSBs, ATR responds primarily to accumulation of ssDNA at stalled forks (Cimprich and Cortez 2008). Inactivation of ATR/CHK1, but not ATM/CHK2, was shown to lead to extensive rereplication (Liu et al. 2007). The inhibition of the expression of factors involved in ATR activation, such as RAD17 and ATR-interacting protein (ATRIP), reduced CHK1 phosphorylation induced by CDT1 overexpression, caused more rereplication in U2OS, and was sufficient to induce rereplication in cell lines, such as A549, that are otherwise resistant to rereplication induced by CDT1-overexpression. These findings highlight the role ATR-mediated S-phase checkpoint activation plays in early detection and prevention of rereplication beyond licensing control, and is consistent with the observations that rereplication is more profound in ATR-deficient cells where it leads to more checkpoint activation and severe DNA lesions (Liu et al. 2007).

In budding yeast, it has been shown that the induction of rereplication by disrupting pre-RC formation (by interfering with cdc6 proteolysis, MCM nuclear exclusion, or ORC2/6 phosphorylation) leads to cell cycle arrest, RAD53 activation, and halted nuclear division (Archambault et al. 2005). This rereplication is further stimulated in the absence of the ATR homologue *Mec1* (Archambault et al. 2005). In higher eukaryotes, overexpression of licensing factors such as CDT1, CDC6, or Cyclin A triggers the activation of the ATM/ATR/CHK2 DNA damage checkpoint pathway that aims to activate p53 and the CDK2 inhibitor p21 to suppress rereplication (Vaziri et al. 2003). In addition, it was also shown that CDK2 inactivation during S-phase leads to an unexpected MCM loading onto chromatin followed by the activation of the ATM/ATR-p53 pathway (an intra-S-phase checkpoint) needed to suppress rereplication (Y. Zhu et al. 2004). Rereplication induced by the geminin depletion triggers the activation of the G2/M checkpoint leading to the inhibition of Cyclin B/CDK1 activity via CHK1 and CDC25C in a p53-independent manner (W. Zhu, Chen, and Dutta 2004).

ATR-mediated checkpoint activation, whether as a result of CDT1 overexpression or following DNA damage, was also shown to induce RB1 dephosphorylation, potentially as a result of ATR-mediated CDK downregulation. CDT1 overexpression in cells expressing shRNA against RB1 was shown to result in substantial rereplication in certain tumor cell lines, such as T98G and A549, that are otherwise resistant to rereplication induced after CDT1 overexpression (Liu et al. 2007). RB1 is likely to inhibit DNA replication via multiple mechanisms. Hypo-phosphorylated RB1 binds to E2F transcription factor family and inhibits the transcription of replicative factors including DNA

polymerases, ORC1, MCMs, CDC6, and CDT1, or cell cycle proteins such as CDKs and cyclins (Liu et al. 2007; Yoshida and Inoue 2004; Leone et al. 1998; Helin 1998). After DNA damage, RB1 interacts with PCNA and disrupts its replicative role potentially as a means to free PCNA to relocalize to DNA break sites (Angus et al. 2004). RB1 additionally interacts with MCM7 and DNA polymerase α, and relocalizes to replication origins after DNA damage (Avni et al. 2003; Gladden and Diehl 2003). These findings collectively show the role RB1 plays in preventing rereplication as a result of ATR checkpoint activation.

ATR activation in response to DNA rereplication is essential to prevent genomic instability. ATR-mediated S phase checkpoint protects against rereplication either directly through phosphorylation of replicative factors or indirectly through its downstream effectors p53 and RB1 (Truong and Wu 2011). As such, ATR-mediated checkpoint serves as a replicative surveillance machinery that keeps rereplication to a minimum and protects against replication errors that lead to origin re-firing and fork collision during normal cell cycle, and allows checkpoint-mediated repair to remove duplicated sequences and repair rereplication-associated lesions. Both ATR- and ATM-mediated G2/M checkpoints ensures repair of DNA lesions, establishes normal licensing control, and prevents over-replicated DNA from being carried through mitosis (Liu et al. 2007; W. Zhu and Dutta 2006).

5. DNA Rereplication and Tumorigenesis

Deregulated overexpression of replication licensing regulators has been readily observed in many cancer types and was shown to promote malignancies. CDT1 and CDC6 overexpression has been documented in non-small cell lung tumors, colon cancer, mantle cell lymphoma, and head and neck carcinomas (Karakaidos et al. 2004; Pinyol et al. 2006; Liontos et al. 2007). A set of analysis in 75 cases of non-small cell lung carcinomas showed that at least 40% of tumors have overexpression of CDT1 and CDC6 independently, and this observation is likely due to the upregulation of their transcription activator E2F1 in tumors (Karakaidos et al. 2004). Additional studies have shown that certain non-tumorigenic cell lines, such as mouse embryonic fibroblasts NIH3T3, readily form tumors in mice after CDT1 overexpression. These cells displayed numerous structural chromosomal abnormalities, translocations, inversions, and mutations (Arentson et al. 2002; Seo et al. 2005). CDC6 and CDT1 expression levels in different precancerous and cancerous stages of colon, lung, and head-and-neck tumors, showed a two-fold mRNA increase in hyperplasia and at least four-fold increase in the protein levels in dysplasia and carcinoma compared to adjacent normal tissues. No correlation, however, was observed between Ki67 proliferation index and the elevated expression of these factors (Liontos et al. 2007). These results suggest that the overexpression of licensing factors may driver tumorigenesis and not only represent a mere byproduct of increased proliferation.

Unscheduled DNA replication induced as a result of overexpression of licensing factors or the expression of various oncogenes (e.g. CDC25A, Cyclin E and $HRAS^{V12}$) at pre-cancerous stages activates the cell cycle checkpoints and the DNA damage response,

which activates senescence and apoptosis to protect against harmful rereplication-associated DNA lesions. The loss of this antitumor barrier under those conditions was shown to promotes tumorigenesis (Bartkova et al. 2005; 2006; Di Micco et al. 2006). For instance, the loss of p53 or inactivation of the p53/p14(ARF) pathway was often observed in tumors with unbalanced licensing signature characterized by overexpression of CDT1 and CDC6 (Pinyol et al. 2006). These studies highlight that the loss of replication control, either as a result of oncogenes or deregulated origin licensing, is a common phenomenon at the early stages of tumorigenesis.

Deregulated licensing control and the resulting rereplication is shown to carry an oncogenic potential and is readily observed at the early stages of tumorigenesis (Truong and Wu 2011). The rereplication-induced genomic instability and the accumulation of DNA lesions and mutations that disrupt checkpoint activation can abrogate the cellular anti-tumor barrier and promote tumorigenesis (Truong and Wu 2011).

6. References:

Abbas, Tarek. 2019. “The Role of Ubiquitylation and SUMOylation in DNA Replication.” In *SUMOylation and Ubiquitination: Current and Emerging Concepts*. Caister Academic Press. https://doi.org/10.21775/9781912530120.14.

Abbas, Tarek, and Anindya Dutta. 2009. “P21 in Cancer: Intricate Networks and Multiple Activities.” *Nature Reviews Cancer*. Nature Publishing Group. https://doi.org/10.1038/nrc2657.

Abbas, Tarek, and Anindya Dutta. 2011. “CRL4Cdt2: Master Coordinator of Cell Cycle Progression and Genome Stability.” *Cell Cycle*. Taylor and Francis Inc. https://doi.org/10.4161/cc.10.2.14530.

Abbas, Tarek, and Anindya Dutta. 2017. “Regulation of Mammalian DNA Replication via the Ubiquitin-Proteasome System.” In *Advances in Experimental Medicine and Biology*, 1042:421–54. Springer New York LLC. https://doi.org/10.1007/978-981-10-6955-0_19.

Abbas, Tarek, Mignon A. Keaton, and Anindya Dutta. 2013. “Genomic Instability in Cancer.” *Cold Spring Harbor Perspectives in Biology* 5 (3): a012914. https://doi.org/10.1101/cshperspect.a012914.

Abbas, Tarek, Etsuko Shibata, Jonghoon Park, Sudhakar Jha, Neerja Karnani, and Anindya Dutta. 2010. “CRL4Cdt2 Regulates Cell Proliferation and Histone Gene Expression by Targeting PR-Set7/Set8 for Degradation.” *Molecular Cell* 40 (1): 9–21. https://doi.org/10.1016/j.molcel.2010.09.014.

Akutsu, Masato, Ivan Dikic, and Anja Bremm. 2016. “Ubiquitin Chain Diversity at a Glance.” *Journal of Cell Science* 129 (5): 875–80. https://doi.org/10.1242/jcs.183954.

Angus, S. P., C. N. Mayhew, D. A. Solomon, W. A. Braden, M. P. Markey, Y. Okuno, M. C. Cardoso, D. M. Gilbert, and E. S. Knudsen. 2004. “RB Reversibly Inhibits DNA Replication via Two Temporally Distinct Mechanisms.” *Molecular and Cellular*

Biology 24 (12): 5404–20. https://doi.org/10.1128/mcb.24.12.5404-5420.2004.

Archambault, V., A. E. Ikui, B. J. Drapkin, and F. R. Cross. 2005. "Disruption of Mechanisms That Prevent Rereplication Triggers a DNA Damage Response." *Molecular and Cellular Biology* 25 (15): 6707–21. https://doi.org/10.1128/mcb.25.15.6707-6721.2005.

Arentson, Elizabeth, Patrick Faloon, Junghee Seo, Eunpyo Moon, Joey M Studts, Daved H Fremont, and Kyunghee Choi. 2002. "Oncogenic Potential of the DNA Replication Licensing Protein CDT1." *Oncogene* 21 (8): 1150–58. https://doi.org/10.1038/sj.onc.1205175.

Arias, Emily E., and Johannes C. Walter. 2006. "PCNA Functions as a Molecular Platform to Trigger Cdt1 Destruction and Prevent Re-Replication." *Nature Cell Biology* 8 (1): 84–90. https://doi.org/10.1038/ncb1346.

Avni, Dror, Hong Yang, Fabio Martelli, Francesco Hofmann, Wael M. ElShamy, Shridar Ganesan, Ralph Scully, and David M. Livingston. 2003. "Active Localization of the Retinoblastoma Protein in Chromatin and Its Response to S Phase DNA Damage." *Molecular Cell* 12 (3): 735–46. https://doi.org/10.1016/S1097-2765(03)00355-1.

Bartkova, Jirina, Zuzana Hořejší, Karen Koed, Alwin Krämer, Frederic Tort, Karsten Zleger, Per Guldberg, et al. 2005. "DNA Damage Response as a Candidate Anti-Cancer Barrier in Early Human Tumorigenesis." *Nature* 434 (7035): 864–70. https://doi.org/10.1038/nature03482.

Bartkova, Jirina, Nousin Rezaei, Michalis Liontos, Panagiotis Karakaidos, Dimitris Kletsas, Natalia Issaeva, Leandros Vassilios F. Vassiliou, et al. 2006. "Oncogene-Induced Senescence Is Part of the Tumorigenesis Barrier Imposed by DNA Damage Checkpoints." *Nature* 444 (7119): 633–37. https://doi.org/10.1038/nature05268.

Benamar, Mouadh, Fadila Guessous, Kangping Du, Patrick Corbett, Joseph Obeid, Daniel Gioeli, Craig L. Slingluff, and Tarek Abbas. 2016. "Inactivation of the CRL4-CDT2-SET8/P21 Ubiquitylation and Degradation Axis Underlies the Therapeutic Efficacy of

Pevonedistat in Melanoma." *EBioMedicine* 10 (August): 85–100. https://doi.org/10.1016/j.ebiom.2016.06.023.

Brustel, Julien, Nina Kirstein, Fanny Izard, Charlotte Grimaud, Paulina Prorok, Christelle Cayrou, Gunnar Schotta, et al. 2017. "Histone H4K20 Tri-methylation at Late-firing Origins Ensures Timely Heterochromatin Replication." *The EMBO Journal* 36 (18): 2726–41. https://doi.org/10.15252/embj.201796541.

Bui, Duyen T., and Joachim J. Li. 2019. "DNA Rereplication Is Susceptible to Nucleotide-Level Mutagenesis." *Genetics* 212 (2): 445–60. https://doi.org/10.1534/genetics.119.302194.

Cayrou, Christelle, Benoit Ballester, Isabelle Peiffer, Romain Fenouil, Philippe Coulombe, Jean Christophe Andrau, Jacques Van Helden, and Marcel Méchali. 2015. "The Chromatin Environment Shapes DNA Replication Origin Organization and Defines Origin Classes." *Genome Research* 25 (12): 1873–85. https://doi.org/10.1101/gr.192799.115.

Chen, Zhi, Jie Sui, Fan Zhang, and Caiguo Zhang. 2015. "Cullin Family Proteins and Tumorigenesis: Genetic Association and Molecular Mechanisms." *Journal of Cancer*. Ivyspring International Publisher. https://doi.org/10.7150/jca.11076.

Cimprich, Karlene A., and David Cortez. 2008. "ATR: An Essential Regulator of Genome Integrity." *Nature Reviews Molecular Cell Biology*. Nature Publishing Group. https://doi.org/10.1038/nrm2450.

Clijsters, Linda, and Rob Wolthuis. 2014. "PIP-Box-Mediated Degradation Prohibits Re-Accumulation of Cdc6 during S Phase." *Journal of Cell Science* 127 (6): 1336–45. https://doi.org/10.1242/jcs.145862.

Davidson, Iain F., Anatoliy Li, and J. Julian Blow. 2006. "Deregulated Replication Licensing Causes DNA Fragmentation Consistent with Head-to-Tail Fork Collision." *Molecular Cell* 24 (3): 433–43. https://doi.org/10.1016/j.molcel.2006.09.010.

Duda, David M., Laura A. Borg, Daniel C. Scott, Harold W. Hunt, Michal Hammel, and

Brenda A. Schulman. 2008. “Structural Insights into NEDD8 Activation of Cullin-RING Ligases: Conformational Control of Conjugation.” *Cell* 134 (6): 995–1006. https://doi.org/10.1016/j.cell.2008.07.022.

Elzen, Nicole Den, and Jonathon Pines. 2001. “Cyclin A Is Destroyed in Prometaphase and Can Delay Chromosome Alignment and Anaphase.” *Journal of Cell Biology* 153 (1): 121–35. https://doi.org/10.1083/jcb.153.1.121.

Fragkos, Michalis, Olivier Ganier, Philippe Coulombe, and Marcel Méchali. 2015. “DNA Replication Origin Activation in Space and Time.” *Nature Reviews Molecular Cell Biology*. Nature Publishing Group. https://doi.org/10.1038/nrm4002.

Gladden, Andrew B., and J. Alan Diehl. 2003. “The Cyclin D1-Dependent Kinase Associates with the Pre-Replication Complex and Modulates RB-MCM7 Binding.” *Journal of Biological Chemistry* 278 (11): 9754–60. https://doi.org/10.1074/jbc.M212088200.

Helin, Kristian. 1998. “Regulation of Cell Proliferation by the E2F Transcription Factors.” *Current Opinion in Genetics and Development* 8 (1): 28–35. https://doi.org/10.1016/S0959-437X(98)80058-0.

Heo, Jinho, Rebeka Eki, and Tarek Abbas. 2016. “Deregulation of F-Box Proteins and Its Consequence on Cancer Development, Progression and Metastasis.” *Seminars in Cancer Biology*. Academic Press. https://doi.org/10.1016/j.semcancer.2015.09.015.

Higa, Leigh, and Hui Zhang. 2007. “Stealing the Spotlight: CUL4-DDB1 Ubiquitin Ligase Docks WD40-Repeat Proteins to Destroy.” *Cell Division*. BioMed Central. https://doi.org/10.1186/1747-1028-2-5.

Karakaidos, Panagiotis, Stavros Taraviras, Leandros V. Vassiliou, Panayotis Zacharatos, Nikolaos G. Kastrinakis, Dionysia Kougiou, Mirsini Kouloukoussa, et al. 2004. “Overexpression of the Replication Licensing Regulators HCdt1 and HCdc6 Characterizes a Subset of Non-Small-Cell Lung Carcinomas: Synergistic Effect with Mutant P53 on Tumor Growth and Chromosomal Instability - Evidence of E2F-1

Transcriptional Control over HCdt1." *American Journal of Pathology* 165 (4): 1351–65. https://doi.org/10.1016/S0002-9440(10)63393-7.

Kliza, Katarzyna, and Koraljka Husnjak. 2020. "Resolving the Complexity of Ubiquitin Networks." *Frontiers in Molecular Biosciences*. Frontiers Media S.A. https://doi.org/10.3389/fmolb.2020.00021.

Komander, David, and Michael Rape. 2012. "The Ubiquitin Code." *Annual Review of Biochemistry* 81 (1): 203–29. https://doi.org/10.1146/annurev-biochem-060310-170328.

Kuo, Alex J., Jikui Song, Peggie Cheung, Satoko Ishibe-Murakami, Sayumi Yamazoe, James K. Chen, Dinshaw J. Patel, and Or Gozani. 2012. "The BAH Domain of ORC1 Links H4K20me2 to DNA Replication Licensing and Meier-Gorlin Syndrome." *Nature* 484 (7392): 115–19. https://doi.org/10.1038/nature10956.

Lee, E. K., and J. A. Diehl. 2014. "SCFs in the New Millennium." *Oncogene*. Nature Publishing Group. https://doi.org/10.1038/onc.2013.144.

Leonard, Alan C., and Marcel Mechali. 2013. "DNA Replication Origins." *Cold Spring Harbor Perspectives in Medicine* 3 (10): a010116. https://doi.org/10.1101/cshperspect.a010116.

Leone, Gustavo, James DeGregori, Zhen Yan, Laszlo Jakoi, Seiichi Ishida, R. Sanders Williams, and Joseph R. Nevins. 1998. "E2F3 Activity Is Regulated during the Cell Cycle and Is Required for the Induction of S Phase." *Genes and Development* 12 (14): 2120–30. https://doi.org/10.1101/gad.12.14.2120.

Limas, Juanita C., and Jeanette Gowen Cook. 2019. "Preparation for DNA Replication: The Key to a Successful S Phase." *FEBS Letters* 593 (20): 2853–67. https://doi.org/10.1002/1873-3468.13619.

Liontos, Michalis, Marilena Koutsami, Maria Sideridou, Konstantinos Evangelou, Dimitris Kletsas, Brynn Levy, Athanassios Kotsinas, et al. 2007. "Deregulated Overexpression of HCdt1 and HCdc6 Promotes Malignant Behavior." *Cancer Research* 67 (22):

10899–909. https://doi.org/10.1158/0008-5472.CAN-07-2837.

Liu, Enbo, Alan Yueh Luen Lee, Takuya Chiba, Erin Olson, Peiqing Sun, and Xiaohua Wu. 2007. "The ATR-Mediated S Phase Checkpoint Prevents Rereplication in Mammalian Cells When Licensing Control Is Disrupted." *Journal of Cell Biology* 179 (4): 643–57. https://doi.org/10.1083/jcb.200704138.

Liu, Enbo, Xianghong Li, Feng Yan, Qiping Zhao, and Xiaohua Wu. 2004. "Cyclin-Dependent Kinases Phosphorylate Human Cdt1 and Induce Its Degradation." *Journal of Biological Chemistry* 279 (17): 17283–88. https://doi.org/10.1074/jbc.C300549200.

Machida, Yuichi J., and Anindya Dutta. 2007. "The APC/C Inhibitor, Emi1, Is Essential for Prevention of Rereplication." *Genes and Development* 21 (2): 184–94. https://doi.org/10.1101/gad.1495007.

Mailand, Niels, and John F.X. Diffley. 2005. "CDKs Promote DNA Replication Origin Licensing in Human Cells by Protecting Cdc6 from APC/C-Dependent Proteolysis." *Cell* 122 (6): 915–26. https://doi.org/10.1016/j.cell.2005.08.013.

Marks, Anna B., Haiqing Fu, and Mirit I. Aladjem. 2017. "Regulation of Replication Origins." In *Advances in Experimental Medicine and Biology*, 1042:43–59. Springer New York LLC. https://doi.org/10.1007/978-981-10-6955-0_2.

McGarry, Thomas J., and Marc W. Kirschner. 1998. "Geminin, an Inhibitor of DNA Replication, Is Degraded during Mitosis." *Cell* 93 (6): 1043–53. https://doi.org/10.1016/S0092-8674(00)81209-X.

Micco, Raffaella Di, Marzia Fumagalli, Angelo Cicalese, Sara Piccinin, Patrizia Gasparini, Chiara Luise, Catherine Schurra, et al. 2006. "Oncogene-Induced Senescence Is a DNA Damage Response Triggered by DNA Hyper-Replication." *Nature* 444 (7119): 638–42. https://doi.org/10.1038/nature05327.

Nakayama, Keiichi I., and Keiko Nakayama. 2006. "Ubiquitin Ligases: Cell-Cycle Control and Cancer." *Nature Reviews Cancer*. Nature Publishing Group. https://doi.org/10.1038/nrc1881.

Pinyol, Magda, Itziar Salaverria, Silvia Bea, Verónica Fernández, Lluís Colomo, Elías Campo, and Pedro Jares. 2006. "Unbalanced Expression of Licensing DNA Replication Factors Occurs in a Subset of Mantle Cell Lymphomas with Genomic Instability." *International Journal of Cancer* 119 (12): 2768–74. https://doi.org/10.1002/ijc.22146.

Rieser, Eva, Stefanie M. Cordier, and Henning Walczak. 2013. "Linear Ubiquitination: A Newly Discovered Regulator of Cell Signalling." *Trends in Biochemical Sciences*. Elsevier Current Trends. https://doi.org/10.1016/j.tibs.2012.11.007.

Robbins, Jonathan A., and Frederick R. Cross. 2010. "Regulated Degradation of the APC Coactivator Cdc20." *Cell Division* 5 (1): 23. https://doi.org/10.1186/1747-1028-5-23.

Schwartz, Alan L., and Aaron Ciechanover. 2009. "Targeting Proteins for Destruction by the Ubiquitin System: Implications for Human Pathobiology." *Annual Review of Pharmacology and Toxicology* 49 (1): 73–96. https://doi.org/10.1146/annurev.pharmtox.051208.165340.

Senga, Takeshi, Umasundari Sivaprasad, Wenge Zhu, Jong Park Jong, Emily E. Arias, Johannes C. Walter, and Anindya Dutta. 2006. "PCNA Is a Cofactor for CDT1 Degradation by CUL4/DDB1-Mediated N-Terminal Ubiquitination." *Journal of Biological Chemistry* 281 (10): 6246–52. https://doi.org/10.1074/jbc.M512705200.

Seo, Junghee, Yun S. Chung, Girdhar G. Sharma, Eunpyo Moon, Walter R. Burack, Tej K. Pandita, and Kyunghee Choi. 2005. "Cdt1 Transgenic Mice Develop Lymphoblastic Lymphoma in the Absence of P53." *Oncogene* 24 (55): 8176–86. https://doi.org/10.1038/sj.onc.1208881.

Sherstyuk, Vladimir V., Alexander I. Shevchenko, and Suren M. Zakian. 2014. "Epigenetic Landscape for Initiation of DNA Replication." *Chromosoma*. Springer Science and Business Media Deutschland GmbH. https://doi.org/10.1007/s00412-013-0448-3.

Sheu, Yi Jun, Justin B. Kinney, and Bruce Stillman. 2016. "Concerted Activities of Mcm4,

Sld3, and Dbf4 in Control of Origin Activation and DNA Replication Fork Progression." *Genome Research* 26 (3): 315–30. https://doi.org/10.1101/gr.195248.115.

Shoaib, Muhammad, David Walter, Peter J. Gillespie, Fanny Izard, Birthe Fahrenkrog, David Lleres, Mads Lerdrup, et al. 2018. "Histone H4K20 Methylation Mediated Chromatin Compaction Threshold Ensures Genome Integrity by Limiting DNA Replication Licensing." *Nature Communications* 9 (1): 1–11. https://doi.org/10.1038/s41467-018-06066-8.

Skaar, Jeffrey R., Julia K. Pagan, and Michele Pagano. 2014. "SCF Ubiquitin Ligase-Targeted Therapies." *Nature Reviews Drug Discovery*. Nature Publishing Group. https://doi.org/10.1038/nrd4432.

Smith, Owen K., Ryanguk Kim, Haiqing Fu, Melvenia M. Martin, Chii Mei Lin, Koichi Utani, Ya Zhang, et al. 2016. "Distinct Epigenetic Features of Differentiation-Regulated Replication Origins." *Epigenetics and Chromatin* 9 (1): 18. https://doi.org/10.1186/s13072-016-0067-3.

Soucy, Teresa A., Peter G. Smith, Michael A. Milhollen, Allison J. Berger, James M. Gavin, Sharmila Adhikari, James E. Brownell, et al. 2009. "An Inhibitor of NEDD8-Activating Enzyme as a New Approach to Treat Cancer." *Nature* 458 (7239): 732–36. https://doi.org/10.1038/nature07884.

Soucy, Teresa A., Peter G. Smith, and Mark Rolfe. 2009. "Targeting NEDD8-Activated Cullin-RING Ligases for the Treatment of Cancer." *Clinical Cancer Research*. American Association for Cancer Research. https://doi.org/10.1158/1078-0432.CCR-09-0343.

Tada, Shusuke, Anatoliy Li, Domenico Maiorano, Marcel Méchali, and J. Julian Blow. 2001. "Repression of Origin Assembly in Metaphase Depends on Inhibition of RLF-B/Cdt1 by Geminin." *Nature Cell Biology* 3 (2): 107–13. https://doi.org/10.1038/35055000.

Takeda, David Y., Jeffrey D. Parvin, and Anindya Dutta. 2005. "Degradation of Cdt1 during S Phase Is Skp2-Independent and Is Required for Efficient Progression of Mammalian Cells through S Phase." *Journal of Biological Chemistry* 280 (24): 23416–23. https://doi.org/10.1074/jbc.M501208200.

Tanaka, Seiji, and Hiroyuki Araki. 2013. "Helicase Activation and Establishment of Replication Forks at Chromosomal Origins of Replication." *Cold Spring Harbor Perspectives in Biology* 5 (12): a010371. https://doi.org/10.1101/cshperspect.a010371.

Tardat, Mathieu, Julien Brustel, Olivier Kirsh, Christine Lefevbre, Mary Callanan, Claude Sardet, and Eric Julien. 2010. "The Histone H4 Lys 20 Methyltransferase PR-Set7 Regulates Replication Origins in Mammalian Cells." *Nature Cell Biology* 12 (11): 1086–93. https://doi.org/10.1038/ncb2113.

Truong, Lan N., and Xiaohua Wu. 2011. "Prevention of DNA Re-Replication in Eukaryotic Cells." *Journal of Molecular Cell Biology* 3 (1): 13–22. https://doi.org/10.1093/JMCB/MJQ052.

Vanderdys, Vanessa, Amir Allak, Fadila Guessous, Mouadh Benamar, Paul W. Read, Mark J. Jameson, and Tarek Abbas. 2018. "The Neddylation Inhibitor Pevonedistat (MLN4924) Suppresses and Radiosensitizes Head and Neck Squamous Carcinoma Cells and Tumors." *Molecular Cancer Therapeutics* 17 (2): 368–80. https://doi.org/10.1158/1535-7163.MCT-17-0083.

Vaziri, Cyrus, Sandeep Saxena, Yesu Jeon, Charles Lee, Kazutaka Murata, Yuichi Machida, Nikhil Wagle, Deog Su Hwang, and Anindya Dutta. 2003. "A P53-Dependent Checkpoint Pathway Prevents Rereplication." *Molecular Cell* 11 (4): 997–1008. https://doi.org/10.1016/s1097-2765(03)00099-6.

Walter, David, Saskia Hoffmann, Eirini Stavroula Komseli, Juri Rappsilber, Vassilis Gorgoulis, and Claus Storgaard Sørensen. 2016. "SCFCyclin F-Dependent Degradation of CDC6 Suppresses DNA Re-Replication." *Nature Communications* 7

(1): 1–10. https://doi.org/10.1038/ncomms10530.

Yoshida, Kenichi, and Ituro Inoue. 2004. “Regulation of Geminin and Cdt1 Expression by E2F Transcription Factors.” *Oncogene* 23 (21): 3802–12. https://doi.org/10.1038/sj.onc.1207488.

Zaidi, Iram Waris, Gwénaël Rabut, Ana Poveda, Hartmut Scheel, Johan Malmström, Helle Ulrich, Kay Hofmann, Philippe Pasero, Matthias Peter, and Brian Luke. 2008. “Rtt101 and Mms1 in Budding Yeast Form a CUL4-DDB1 -like Ubiquitin Ligase That Promotes Replication through Damaged DNA.” *EMBO Reports* 9 (10): 1034–40. https://doi.org/10.1038/embor.2008.155.

Zhou, Lisha, and Lijun Jia. 2020. “Targeting Protein Neddylation for Cancer Therapy.” In *Advances in Experimental Medicine and Biology*, 1217:297–315. Springer. https://doi.org/10.1007/978-981-15-1025-0_18.

Zhu, W., Y. Chen, and A. Dutta. 2004. “Rereplication by Depletion of Geminin Is Seen Regardless of P53 Status and Activates a G2/M Checkpoint.” *Molecular and Cellular Biology* 24 (16): 7140–50. https://doi.org/10.1128/mcb.24.16.7140-7150.2004.

Zhu, W., and A. Dutta. 2006. “An ATR- and BRCA1-Mediated Fanconi Anemia Pathway Is Required for Activating the G2/M Checkpoint and DNA Damage Repair upon Rereplication.” *Molecular and Cellular Biology* 26 (12): 4601–11. https://doi.org/10.1128/mcb.02141-05.

Zhu, Y., C. Alvarez, R. Doll, H. Kurata, X. M. Schebye, D. Parry, and E. Lees. 2004. “Intra-S-Phase Checkpoint Activation by Direct CDK2 Inhibition.” *Molecular and Cellular Biology* 24 (14): 6268–77. https://doi.org/10.1128/mcb.24.14.6268-6277.2004.

VII.

Chapter II:

The Therapeutic Efficacy of Targeting the $CRL4^{CDT2}$ E3 Ligase in Melanoma

1. Abstract

Ubiquitin-mediated proteolytic degradation is a highly regulated process that ensures selective and timely turnover of most cellular proteins necessary to maintain proper cell homeostasis and preserve genomic integrity. The $CRL4^{CDT2}$ E3 ubiquitin ligase is emerging as a master regulator of cell proliferation involved protecting against aberrant DNA replication and maintaining healthy cell cycle progression. The timely $CRL4^{CDT2}$-mediated proteolysis of its substrates CDT1, p21, and SET8 is critical to prevent excessive origin relicensing during the same S-phase leading to rereplication, a lethal phenomenon that results in various forms of genomic instabilities, senescence, and apoptosis. Our work shows that the $CRL4^{CDT2}$ substrate adaptor, CDT2, is elevated in cutaneous melanoma and its expression correlates with poor overall and disease-free survival. We showed that $CRL4^{CDT2}$ inactivation, via CDT2 depletion or pharmacological inhibition using MLN4924, a specific inhibitor of neddylation that is required for the activity of all cullin-based E3 ligases, suppress melanoma proliferation through the induction of a p21- and SET8-dependent rereplication and senescence. We found that transient exposure of at least 12 hours to MLN4924 is sufficient to irreversibly inhibit cell proliferation and induce rereplication and senescence in melanoma cells, but not in immortalized melanocytes. Using melanoma cell lines with hypomorphic deletions of p21 or SET8, we showed that MLN4924-induced toxicity is mediated through the $CRL4^{CDT2}$-mediated stabilization of p21 or SET8 *in vitro* and in nude mice. MLN4924 inhibits melanoma tumor growth irrespective of BRAF/NRAS mutational status and synergizes with BRAF kinase inhibitor PLX4720 to suppress BRAF melanomas *in vivo*. In addition, PLX4720-resistant

melanomas remain sensitive to MLN4924-induced growth suppression and rereplication. Collectively, our results show that MLN4924-induced toxicity in melanoma is mediated primarily through the disruption of the $CRL4^{CDT2}$-p21/SET8 degradation axis, and its therapeutic efficacy can benefit a broad patient population including individual with tumors that relapsed from conventional vemurafenib therapy.

2. Introduction:

2.1. Melanoma

Melanoma is one of the most aggressive forms of skin cancer estimated to affect at least 100,000 newly diagnosed patients and cause 6,850 deaths in the United States alone in 2020 (PDQ Adult Treatment Editorial Board 2002). It is the most common cancer among young adults (ages 25 to 29), the third most common cancers among males, and is responsible for the vast majority of all skin cancer deaths (Miller et al. 2019; PDQ Adult Treatment Editorial Board 2002). Even though patient with a primary local tumor have a five-year survival rate of 99%, it drops significantly to between 19% and 25% after metastasis ("Cancer Facts and Figures" 2020; Miller et al. 2019).

Over half of melanoma cases have an activating mutation in the BRAF serine/threonine kinase, with V600E being the most common, while 15-25% of melanomas have a mutation in NRAS (Davies and Samuels 2010). Both BRAF and NRAS are involved in the MAPK/ERK signaling pathway (RAS-RAF-MEK-MAPK) whose activation stimulates cell proliferation, survival, and inhibits cell death. NRAS also activates the PI3K (phosphatidyl-inositol 3-kinase) pathway (Solus and Kraft 2013). Certain melanomas have additional and less prevalent mutations in the genes encoding SCF receptor tyrosine kinase (KIT), neurofibromin (NF1), or GNAQ/GNA11, all of which interact with the MAPK pathway. In addition, 20-40% of melanoma cases have a loss or reduced expression of the tumor suppressor and phosphatase PTEN (phosphatase and tensin homologue). Inactivating mutations in CDKN2A (p16) and loss of p53 both were found to cooperate with NRAS-mutated melanoma cases (Solus and Kraft 2013).

Patients harboring the BRAF-V600E mutations provide a therapeutic target with BRAF/MEK inhibitors such as vemurafenib (PLX4032), a low molecular weight molecule that binds to the ATP-binding site of BRAF-V600E kinase and inhibits its activity. Patients treated with vemurafenib show a median progression-free survival of 7 months with a median overall survival rate of up to 14 months (Garbe and Eigentler 2018). Despite their rapid clinical results, most BRAF/MEK inhibitors are associated with high rates of resistance in the majority of patients. Due to the significant therapeutic resistance, and the absence of valid inhibitors against non-BRAF melanomas (Goldinger et al. 2013), it is critical to identify alternative therapeutic approaches against melanoma tumors irrespective of their mutational status.

2.2. DNA Replication Regulation via the Ubiquitin Proteasome System

Eukaryotic cells have evolved multiple mechanisms to maintain healthy cell cycle progression and preserve genomic integrity. Ubiquitin-mediated proteolysis via the 26S proteasome is a highly regulated cellular process that govern the degradation of most cellular proteins (Glickman and Ciechanover 2002). The $CRL4^{CDT2}$ ubiquitin ligase is one of the key E3 ubiquitin ligase involved in cell cycle progression, DNA replication, and DNA repair. Recent studies have demonstrated the critical role this E3 ligase plays in the proteolysis of positive regulators of the initiation of DNA replication such as CDT1 (Abbas and Dutta 2011; Abbas, Keaton, and Dutta 2013). $CRL4^{CDT2}$ also targets for degradation p21 and SET8 in S-phase to prevent DNA rereplication.. Substrate recognition of $CRL4^{CDT2}$ requires the interaction with the chromatin-bound PCNA which limits the ligase activity to S-phase and particular instances of DNA damage (Senga et al. 2006;

Arias and Walter 2006; Abbas, Keaton, and Dutta 2013; Abbas and Dutta 2011). This strict and timely $CRL4^{CDT2}$-mediated proteolysis of these substrates is critical to limit DNA replication to a single round per cell cycle and prevent erroneous replication re-initiation which leads to rereplication. The consequences of rereplication is often lethal to the cell and leads to multiple forms of genomic instabilities including DNA breaks, gene amplification, collapsed replication forks, chromosome breakage, senescence and apoptosis (Liontos et al. 2007; Bui and Li 2019; Truong and Wu 2011; Abbas, Keaton, and Dutta 2013).

Excessive origin relicensing leading to rereplication can be triggered through the deregulated expression of licensing factors, such as the overexpression of CDT1, or inactivation of $CRL4^{CDT2}$ through the downregulation of CDT2 (Abbas, Keaton, and Dutta 2013; Jin et al. 2006). $CRL4^{CDT2}$ can be inactivated pharmacologically using a small molecule inhibitor called MLN4924 (pevonedistat). The activation of Cullin-based E3 ubiquitin ligases requires a ubiquitination-like process termed Neddylation, which involves the covalent attachment of the ubiquitin-like NEDD8 moiety (neural precursor cell expressed, developmentally down-regulated 8) and is involved in various cellular processes. MLN4924 is a potent inhibitor of the neddylation activation enzyme (NAE1) which interrupts the activity of all CRL-based E3 ligases including $CRL4^{CDT2}$ (Soucy et al. 2009; Merlet et al. 2009). The inactivation of CRL4 activity by MLN4924 is toxic to cancer cells in vitro and in vivo and results in the accumulation of DNA damage and cell death and is currently in multiple clinical trials for hematologic and solid malignancies (NCT00722488, NCT00911066, NCT01011530) (Soucy et al. 2009; Lin et al. 2010). In

addition to inactivating CRL-mediated proteolysis, MLN4924 was found to inhibit various other pathways including NFκB, ATK, and mTOR. However, additional pre-clinical studies are needed to further uncover the underlying mechanisms that contributes to MLN4924's efficacy in melanoma (Godbersen et al. 2014; Gu et al. 2014; L. Li et al. 2014; H. Li et al. 2014; Milhollen et al. 2011; 2010; Soucy et al. 2009).

2.3. Overview of Key Findings:

In this chapter, we show that the substrate adapter CDT2 is overexpressed in malignant melanoma and its high expression correlates with poor patient outcome. We also show that the inactivation of $CRL4^{CDT2}$ by CDT2 knockdown or MLN4924 treatment inhibits melanoma proliferation regardless of the BRAF/NRAS mutational status, and induces rereplication and senescence is dependent on the stability of p21 and SET8. We also demonstrate that the efficacy of MLN4924 *in vivo* is dependent on the expression of p21 or SET8 independently. These results suggest that $CRL4^{CDT2}$ inactivation represents the primary mechanism of MLN4924-mediated toxicity in melanoma. We also show that MLN4924 synergizes with the BRAF inhibitor vemurafenib against melanoma tumors *in vivo* harboring this mutation $BRAF^{V600E}$, and is toxic to melanoma cell lines that are resistant to vemurafenib treatment.

3. Results:

3.1. The Expression of CDT2 is Elevated in Melanoma and Serves as a Negative Prognostic Marker

The most common and significant driver genetic alterations in cutaneous melanoma occur in both the MAPK and PI3K signaling pathways, both of which affect gene expression promoting survival, cell cycle entry, proliferation and other responses (Solus and Kraft 2013). We searched a series of gene expression databases in order to identify previously uncharacterized melanoma-specific alterations in genes involved in cell cycle progression and DNA replication downstream of the MAPK/PI3K pathways. The identification of new melanoma-specific deregulated genes could provide additional insight into melanomagenesis, promote novel molecular markers that facilitate the development of more efficient prognostic assays, and identify potential druggable targets outside of the MAPK/PI3K pathways to overcome acquired resistance in melanoma.

Using a publicly available database that examined the RNA expression profiles from 45 primary melanoma, 18 benign skin nevi, and 7 normal skin tissues (Talantov et al. 2005), we found that the levels of CDT2 to be elevated in 84% of melanoma samples compared to the non-malignant nevi and normal skin tissues (Fig. 2.1A-B). This observation was not specific to melanoma as CDT2 was also overexpressed in additional malignancies including pancreatic, brain, lung, breast, cervical and gastric tumors (Data not shown). By examining the CDT2 expression levels in a database of 471 primary and metastatic melanomas as part of The Cancer Genome Atlas (TCGA) available at cBioPortal (Cerami et al. 2012; Gao et al. 2013), we found that elevated expression levels

of CDT2 correlates with poor clinical outcome and lower probability of both overall and disease-free survival (Fig. 2.1C-D).

Furthermore, we looked at the CDT2 protein expression levels in a human tissue microarray (TMA). In this *in situ* analysis, we examined 138 melanoma samples derived from 100 patients (58 males and 42 females aged between 23 and 90) including 8 primary tumors and 92 metastatic melanomas compared to a set of non-malignant nevi tissues. We found that 117 out of 138 melanoma samples (84.7%) have significant elevation of nuclear CDT2 levels, which was more significant in the metastatic samples compared to the primary cutaneous melanomas, and was not detectable in the benign nevi (Fig. 2.1E-G). To test if the elevated CDT2 protein levels, similar to its mRNA expression, can be considered as an indicator of poor prognosis, we compared the CDT2 levels with the proliferative marker Ki-67 whose reactivity was shown to be a predictor of histological malignancy in melanoma (Moretti et al. 2001). We found a statistically significant positive correlation between CDT2 and Ki67 staining ($r = 0.447$, $p < 0.01$) (Fig. 2.1H). These results show that CDT2 is overexpressed in melanoma, in both the mRNA and the protein levels, and its expression can serve as a negative prognostic factor and a predictor of poor clinical outcome.

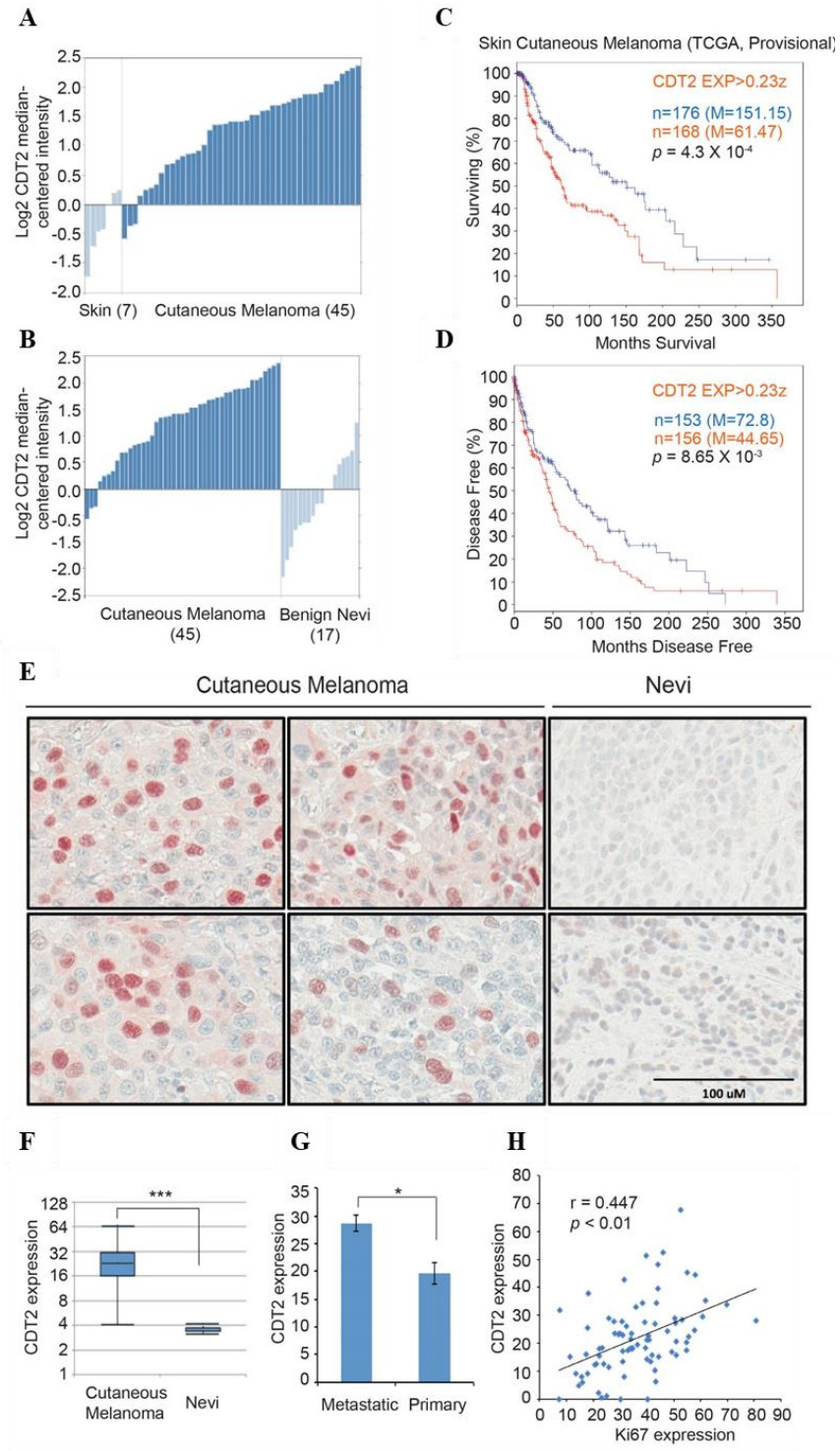
A
Log2 CDT2 median-centered intensity
Skin (7)
Cutaneous Melanoma (45)
B
Log2 CDT2 median-centered intensity
Cutaneous Melanoma (45)
Benign Nevi (17)
C
Skin Cutaneous Melanoma (TCGA, Provisional)
CDT2 EXP>0.23z
n=176 (M=151.15)
n=168 (M=61.47)
p = 4.3 X 10-4
Surviving (%)
Months Survival
D
CDT2 EXP>0.23z
n=153 (M=72.8)
n=156 (M=44.65)
p = 8.65 X 10-3
Disease Free (%)
Months Disease Free
E
Cutaneous Melanoma
Nevi
100 uM
F
CDT2 expression
***
Cutaneous Melanoma
Nevi
G
CDT2 expression
*
Metastatic
Primary
H
r = 0.447
p < 0.01
CDT2 expression
Ki67 expression

Figure 2.1: The Expression of CDT2 is Elevated in Melanoma and Serves as a Negative Prognostic Marker

A-B. mRNA Expression level of CDT2 in a set of cutaneous melanoma samples (45) compared to normal skin (A) or melanoma precursors (B) from a publicly available dataset at Oncomine (Talantov et al. 2005).

C-D. Survival curves representing overall survival (C) or disease-free survival (D) in patients with cutaneous melanoma stratified by CDT2 mRNA expression level. Red curves represent the group with the high CDT2 expressors (>0.23z), while the blue curve represents the low expressors (<0.23z). M= median survival (months), n = sample size (patient number). Data is publicly available from TCGA.

E-F. Representative tissue microarray (TMA) images (**E**) of melanoma (primary and metastatic), or nonmalignant nevi, samples stained for CDT2. Relative quantification of CDT2 expression in cutaneous melanoma samples compared to nevi is shown in the box plot in F.

G. Relative quantification of CDT2 expression from the TMA cohort in primary compared to metastatic samples.

H. Dot plot showing the correlation between CDT2 expression from the TMA set in E compared to Ki67 expression derived from the same set co-stained with Ki-67

3.2. CDT2 Is Required for Melanoma Cell Proliferation and Its Depletion Results in Rereplication and Senescence

CDT2, the substrate adapter of the $CRL4^{CDT2}$ E3 ubiquitin ligase, has been shown to be involved in the negative regulation of replication factors to prevent excessive DNA replication and the maintenance of proper S phase progression (Abbas, Keaton, and Dutta 2013; Jin et al. 2006). Activating mutations in the mitogenic pathways, such as BRAF and NRAS which are common in melanoma, were shown to result in oncogene-induced replication stress by increasing origin firing and generating asymmetric replication forks (Di Micco et al. 2006). We hypothesized that the elevated expression of CDT2 observed in melanoma tissues serves as a way to alleviate the oncogene-induced replication stress and maintain proper growth of tumor cells.

To test this hypothesis, we showed that siRNA-mediated silencing of the CDT2 expression suppressed cell proliferation in a panel of 9 melanoma cells with various mutational background, including the BRAF-mutant DM93 cells (Fig. 2.2A and data not shown). Flow cytometry analysis, using propidium iodide as a DNA marker, revealed that silencing CDT2 results in an increase in the population of cells with more than 4N DNA content, indicative of rereplication, in the same melanoma panel (Fig. 2.2B, D). Cell cycle analysis following a one-hour pulsing with bromodeoxyuridine (BrdU) confirmed the presence of a significant rereplication population (57%) post CDT2 knockdown in DM93 (Fig. 2.2C). A small apoptotic population was also observed in both flow cytometry analyses in multiple cell lines represented by a population of cells with less than G1 DNA content.

Oncogene-induced replication stress and DNA hyper replication were shown to result in increased DNA damage and cellular senescence (Gaillard, García-Muse, and Aguilera 2015; Di Micco et al. 2006; Tu et al. 2011). Using β-galactosidase (β-gal) staining assay, we showed that depletion of CDT2 resulted in significant increase of β-gal staining indicative of senescence in the majority of the melanoma cells tested (Fig. 2.2F–G). 28 to 48hrs following the siRNA-mediated knockdown of CDT2 in a set of melanoma cells, the protein levels of the $CRL4^{CDT2}$ degradation substrates such as p21 and SET8 was increased. This was accompanied with an increase in DNA damage (γH2AX) and checkpoint markers (phosphorylation of CHK1 and CHK2) (Fig. 2.2E) These results suggest that CDT2 is required for the proliferation of melanoma cells, regardless of their mutational background, and its depletion results in DNA rereplication, DNA damage and cellular senescence.

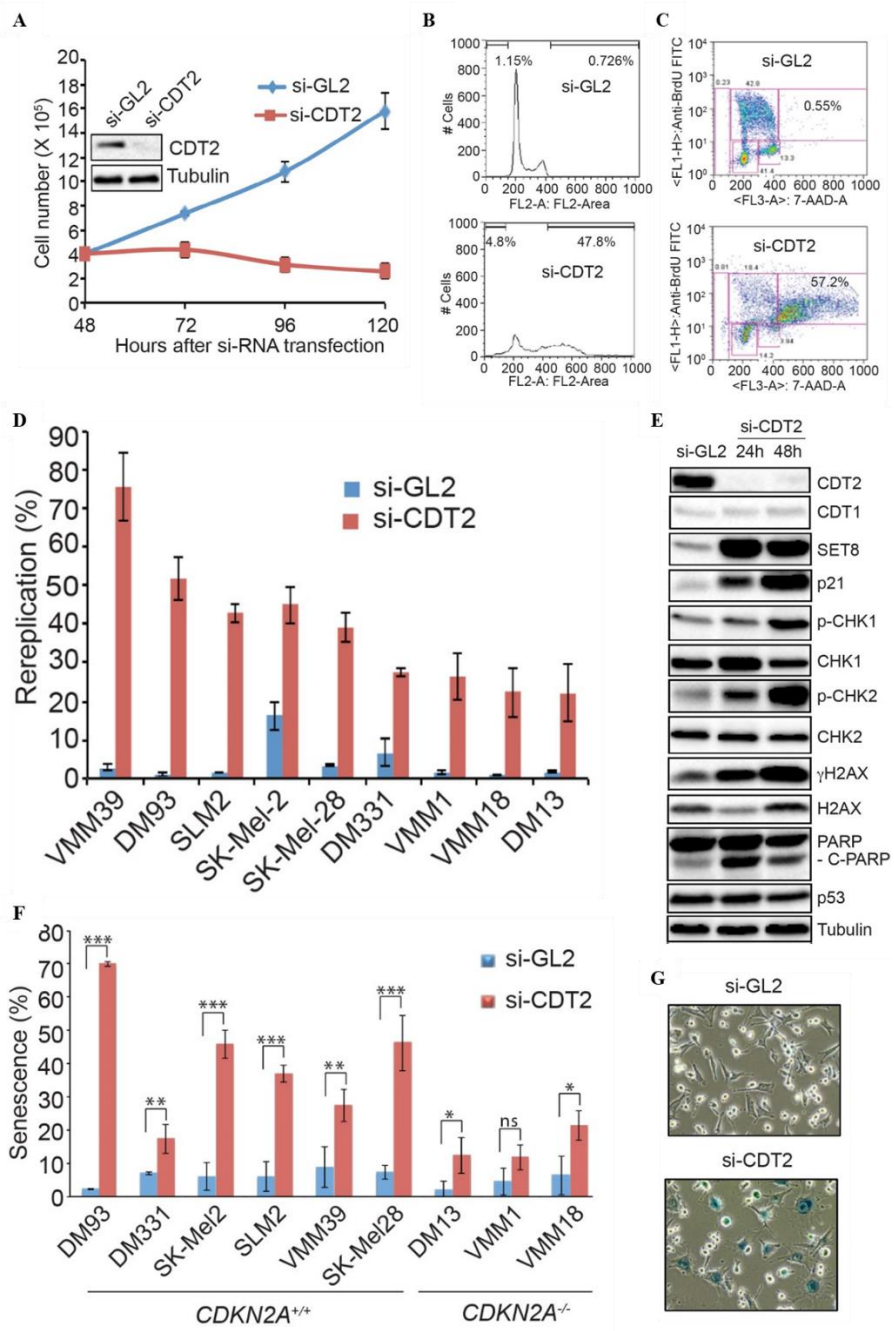
A
si-GL2
si-CDT2
CDT2
Tubulin
Cell number (X 10⁵)
Hours after si-RNA transfection
B
1.15%
0.726%
si-GL2
4.8%
47.8%
si-CDT2
Cells
FL2-A: FL2-Area
C
si-GL2
0.55%
si-CDT2
57.2%
<FL1-H>:Anti-BrdU FITC
<FL3-A>: 7-AAD-A
D
si-GL2
si-CDT2
Rereplication (%)
VMM39
DM93
SLM2
SK-Mel-2
SK-Mel-28
DM331
VMM1
VMM18
DM13
E
si-CDT2
si-GL2 24h 48h
CDT2
CDT1
SET8
p21
p-CHK1
CHK1
p-CHK2
CHK2
γH2AX
H2AX
PARP
- C-PARP
p53
Tubulin
F
si-GL2
si-CDT2
Senescence (%)
DM93
DM331
SK-Mel2
SLM2
VMM39
SK-Mel28
DM13
VMM1
VMM18
ns
CDKN2A+/+
CDKN2A-/-
G
si-GL2
si-CDT2

Figure 2.2: CDT2 Is Required for Melanoma Cell Proliferation and Its Depletion Results in Rereplication and Senescence

A. Growth curve showing the impact of deletion of CDT2 by siRNA on the proliferation rate of DM93 melanoma cells. Immunoblot showing the expression level of CDT2 post knockdown (inset)

B. Flow cytometry profile showing the cell cycle distribution in DM93 cells after transfection with siGl2 (control) and siCDT2. Propedium iodide (PI) used as a marker for DNA content (FL2 - x-axis).

C. Flow cytometry profile of DM93 cells showing BrdU incorporation post transfection with siGl2 (control) or siCDT2. Cells were pulsed with BrdU one hour before harvesting and then stained with BrdU antibody and 7-AAD (DNA marker).

D. Histogram showing the impact of CDT2 knockdown on the rereplication induction in a panel of melanoma cells. Rereplication analyzed 72 hours post transfection with siRNA and quantified with flow cytometry (PI staining).

E. Immunoblotting showing the expression level of various proteins at 24 or 48 hours post transfection with siCDT2.

F-G. Histogram (**F**) showing the impact of CDT2 knockdown on the percentage of cells undergoing senescence in a panel of melanoma cells. Senescence was quantified using β-gal staining as shown in the DM93 representative images in G.

Results in A, D, F represent the average of 3 independent experiments +/- SD. P-values were calculated using Student's *t*-test.

3.3. Rereplication and Senescence induced after CDT2 Inactivation in Melanoma Require p21 and SET8

$CRL4^{CDT2}$ is an important barrier to excessive origin relicensing leading to DNA rereplication (Abbas and Dutta 2011). We tested if the observed rereplication and senescence induced in melanoma cells is dependent on the $CRL4^{CDT2}$ substrates. siRNA-mediated depletion of CDT1, p21, or SET8 in two melanoma cells lines (DM93 and VMM39) significantly inhibited the rereplication and senescence induced after CDT2 depletion. While the knockdown of p21 or SET8 did not significantly impair cell cycle distribution, CDT1 depletion increases the G1 population suggesting its role in S-phase entry (Fig. 2.3A-B, and data not shown). Therefore CDT1, p21, and SET8 are all required for rereplication and senescence induced after CDT2 depletion.

DNA Rereplication observed in mammalian cells and in other higher eukaryotes, such as zebrafish and *C. elegans*, in many cases has been attributed to failure to degrade CDT1 by SCF^{SKP2} and/or $CRL4^{CDT2}$ (Abbas and Dutta 2011; Abbas, Keaton, and Dutta 2013). Consistent with the literature, ectopic expression of CDT1 induced rereplication in melanoma cells. However, we observed that the overexpression of SCF^{SKP2}-resistant CDT1 mutant ($CDT1^{\Delta CY}$) induced more robust rereplication than the overexpression of wild type CDT1 (wt-CDT1) or $CRL4^{CDT2}$-resistant CDT1 mutant ($CDT1^{\Delta PIP}$) in melanoma (Fig. 2.3C). Consistently, the depletion of the APC ubiquitin ligase inhibitor EMI1, which results in the stabilization of Cyclin A (required for SCF^{SKP2} mediated degradation of CDT1) and the CDT1 inhibitor geminin, induced rereplication in melanoma cells. Geminin depletion induced rereplication in U2OS and in Cal27 head and neck squamous cell carcinoma cells but failed to do so in DM93 and VMM39 melanoma cells (Fig. 2.3D-E).

These results suggest that CDT1 is regulated in melanoma cells primarily by the Cyclin A-dependent SCF^{SKP2}-mediated proteolysis.

In addition, we tested if the stabilization of the other two $CRL4^{CDT2}$ substrates (p21 and SET8) is sufficient to induce rereplication and senescence in melanoma. Ectopic expression of both wild type p21 and SET8 did not induce rereplication or senescence in melanoma cells (Fig. 2.3F-G). However, stable overexpression of the or $CRL4^{CDT2}$-resistant non-degradable SET8 ($SET8^{\Delta PIP}$), and not the catalytically inactive protein ($SET8^{\Delta PIP\text{-}CD}$) resulted in robust rereplication and senescence in DM93 and VMM39 (Fig. 2.3F-G). On the other hand, overexpression of stable p21 ($p21^{\Delta PIP}$) was sufficient to induce senescence, but not rereplication, and was associated with an intra-S-phase growth arrest in both DM93 and VMM39 cells. Therefore, deregulated SET8 expression is required and sufficient to promote rereplication and senescence in melanoma cells after CDT2 inactivation.

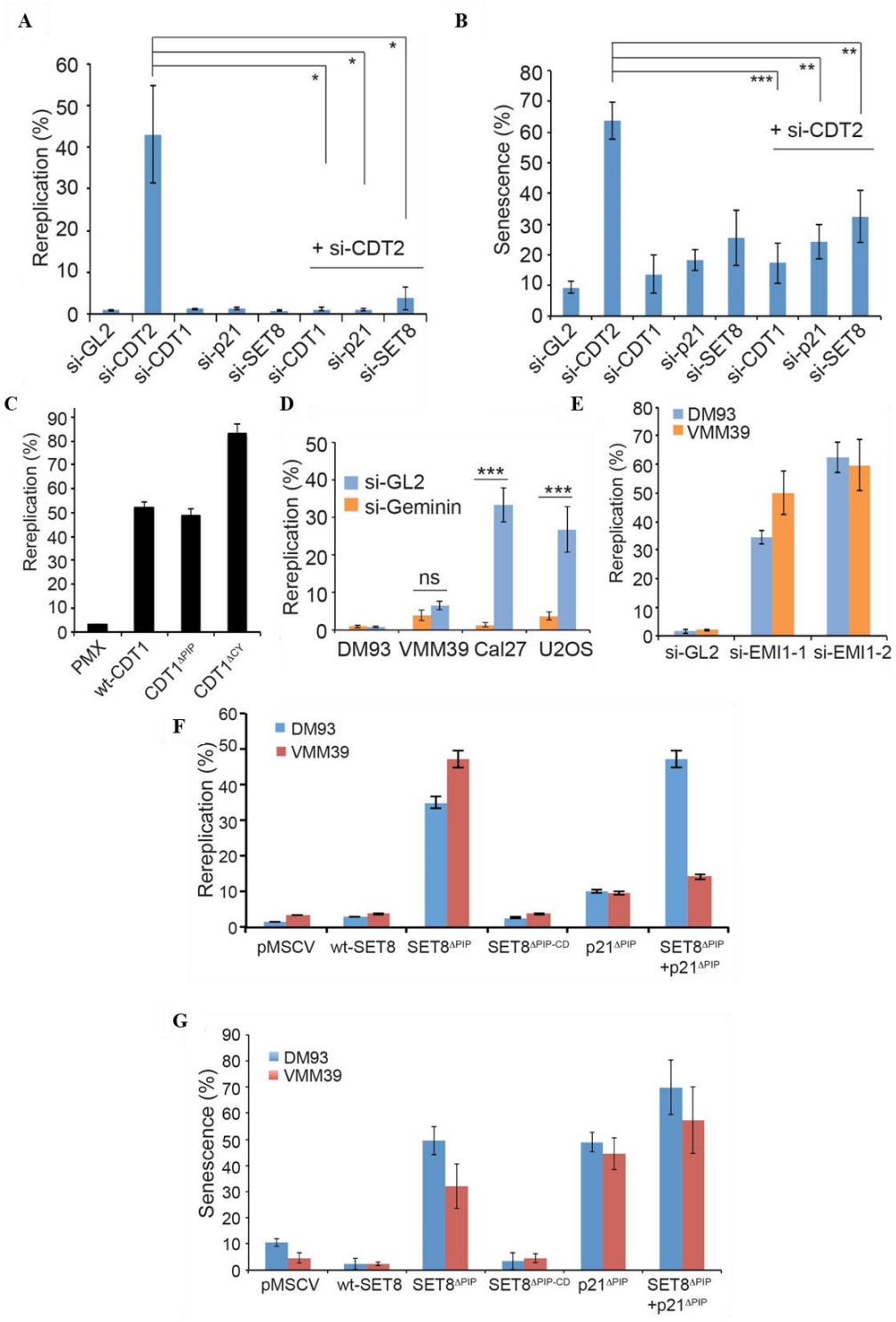
A
Rereplication (%)
si-GL2
si-CDT2
si-CDT1
si-p21
si-SET8
si-CDT1
si-p21
si-SET8
+ si-CDT2
B
Senescence (%)
+ si-CDT2
C
Rereplication (%)
PMX
wt-CDT1
CDT1ΔPIP
CDT1ΔCY
D
Rereplication (%)
si-GL2
si-Geminin
ns
DM93
VMM39
Cal27
U2OS
E
Rereplication (%)
DM93
VMM39
si-GL2
si-EMI1-1
si-EMI1-2
F
Rereplication (%)
DM93
VMM39
pMSCV
wt-SET8
SET8ΔPIP
SET8ΔPIP-CD
p21ΔPIP
SET8ΔPIP +p21ΔPIP
G
Senescence (%)
DM93
VMM39
pMSCV
wt-SET8
SET8ΔPIP
SET8ΔPIP-CD
p21ΔPIP
SET8ΔPIP +p21ΔPIP

Figure 2.3: Rereplication and Senescence induced after CDT2 Inactivation in Melanoma Require p21 and SET8

A. Histogram showing the percentage of rereplication in cells with the indicated siRNA-mediated transfections in DM93. Samples were stained with PI then rereplication was analyzed using flow cytometry.

B. Histogram showing the quantification of senescent DM93 cells detected by β-gal assay after transfection with the indicated siRNAs.

C. Histogram showing the percentage of rereplicating cells following the ectopic expression of the indicated CDT1 proteins compared to the empty vector (PMX) in DM93.

D. Histogram showing the impact of knockdown of Geminin by siRNA on rereplication induction in DM93, VMM39, Cal27 and U2OS.

E. Histogram showing the impact of knockdown of EMI1 using two different siRNAs on rereplication induction in DM93 and VMM39 melanoma cells.

F. Histograms showing the extent of rereplication induced after transduction with retroviruses expressing the indicated proteins in DM93 and VMM39, compared to the empty vector pMSCV.

F. Histograms showing the impact of the ectopic expression of indicated proteins on senescence in DM93 and VMM39, compared to the empty vector pMSCV. Senescence is quantified via β-gal staining.

Results in all histograms represent the average of 3 independent experiments +/- SD. P-values were calculated using Student's *t*-test.

3.4. MLN4924 Suppresses Melanoma Proliferation Through Rereplication and Senescence

The activity of the Cullin-based E3 ubiquitin ligases requires a post translational modification termed Neddylation, which is the covalent attachment of the Cullin protein to the ubiquitin-like moiety NEDD8 (neural precursor cell expressed, developmentally down regulated 8). Neddylation, similar to ubiquitylation, occurs via a three-step enzymatic process (Chen et al. 2015). MLN4924, is s small molecule inhibitor that binds to the Neddylation Activating Enzyme (NAE1) that prevents as a result the activation of all Cullin-based E3 ubiquitin ligases, including $CRL4^{CDT2}$ (Soucy et al. 2009). The use of MLN4924 provides an approach to study the therapeutic potential of inhibiting $CRL4^{CDT2}$ ligase activity in melanoma. Treating DM93 melanoma cells with various doses of MLN4924 resulted in the dose and time-dependent accumulation of CRL substrates including CDT1, CDT2, p21, p27 (Fig. 2.4A-C). SET8 levels were particularly increased at the early time points (3h and 6h) which was associated with the increase in stability of the H4K20 methylations (H4K20me1, H4K20me2, and H4K20me3) which have been shown to contribute to DNA rereplication (Fig. 2.4B-C). (Abbas et al. 2010; Beck et al. 2012).

MLN4924 has been shown to disrupt S-phase and cause the accumulation of DNA damage in various cell lines (Soucy et al. 2009). Consistently, this was observed in our DM93 cells where treatment with MLN4924 led to increased γH2AX and phosphorylation of the checkpoint proteins CHK1 and CHK2, indicating accumulation of DNA damage and cell cycle arrest (in S and G2/M). (Fig. 2.4C and data not shown). Treating DM93 cells with MLN4924 induced a dose and time-dependent increase in rereplication, reaching up

to 68% of cells with >4N DNA content 72hrs post treatment with 1μM (Fig. 2.4D). Rereplication was accompanied with a small increase in the sub G1 population (7%) in DM93 indicative of cell death by apoptosis, which is consistent with the observed accumulation of cleaved PARP from 48h to 96h. (Fig. 2.4C-D).

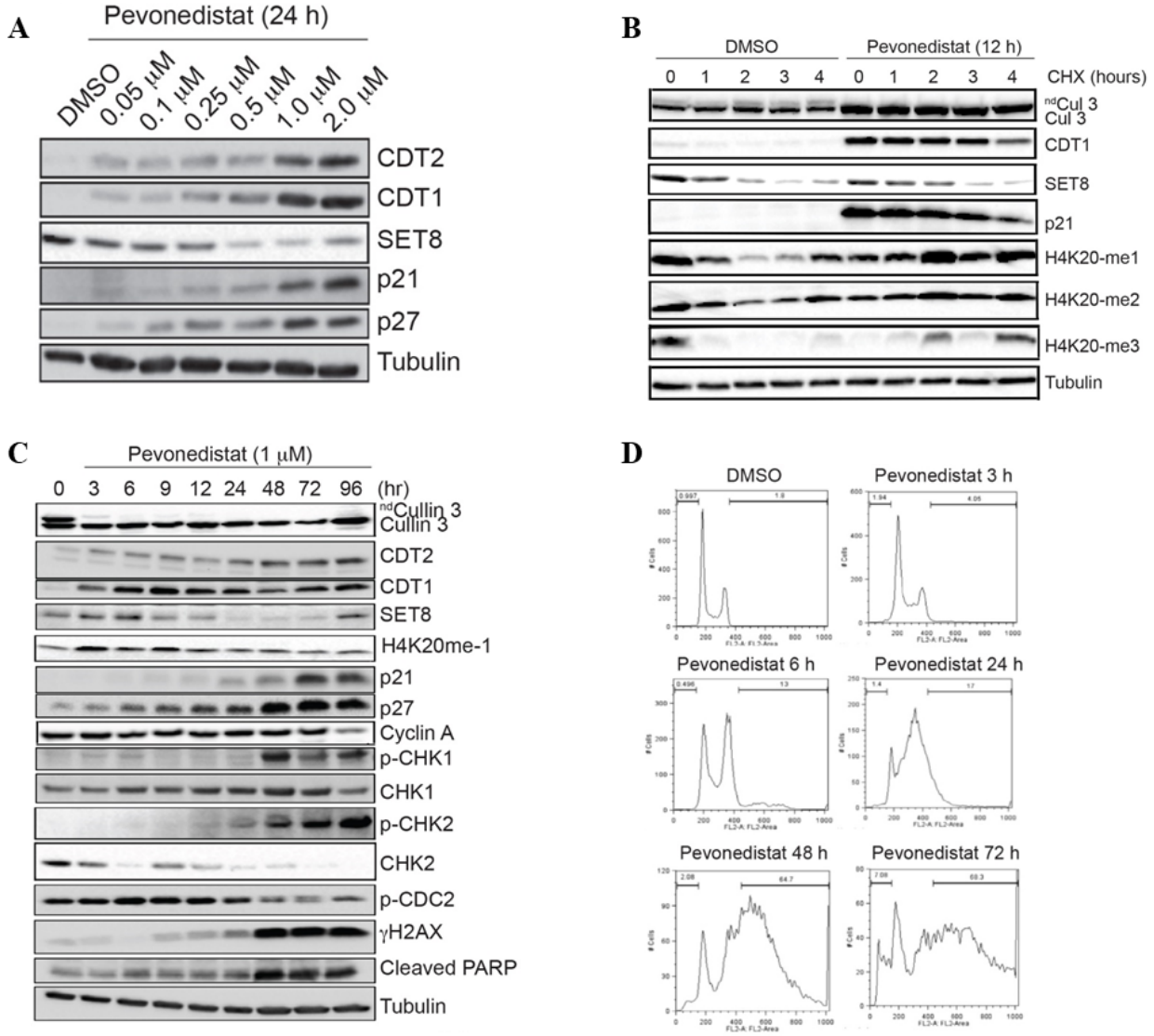

Figure 2.4: MLN4924 Treatment Results in DNA Damage and Rereplication in Melanoma

A. Immunoblot of lysates from DM93 cell treated with MLN4924, or control DMSO, at the indicated doses for 24 hours, then blotted for the indicated proteins. Tubulin is used as a loading control.

B. Immunoblot of lysates extracted from DM93 cells treated with MLN4924, or control DMSO, for 12 hours then exposed to Cycloheximide for the indicated times. CHX used to assess the stability of the indicated proteins with or without MLN4924 treatment.

C. Immunoblot of lysates from DM93 cell treated with 1μM MLN4924, or control DMSO, then harvested at the indicated times. Cell lysates were probed for the indicated proteins. Tubulin is used as a loading control. nd Cullin 3: Neddylated Cullin 3 (upper band).

D. Flow cytometry profiles of cells after treatment with 1μM MLN4924. Cells were harvested at the indicated times following treatment, the samples were stained for PI, and rereplication was analyzed by FACS.

MLN4924 strongly inhibited the proliferation of a panel of nine melanoma cells, as measured by the cell viability MTT assay, with an IC_{50} that ranges from 35nM in VMM39 to 330nM in VMM1 (Fig. 2.5A). In addition to growth inhibition, MLN4924 caused varying degrees of rereplication measured 72h post treatment in the same panel (Fig. 2.5B). Both growth inhibition and the extent of rereplication did not correlate with the BRAF/NRAS mutational status of the melanoma cells tested. The MLN4924-induced rereplication significantly correlates with the basal level of CDT2 expression in these cell lines ($r = 0.745$, $p < 0.01$). However, the latter did not correlate with the MLN4924 IC_{50} (Fig. 2.5C-D). This suggests that increased CDT2 expression may contribute to the MLN4924-induced rereplication. To test this hypothesis, we overexpressed wild type (wt) CDT2 or $CDT2^{R246A}$, a mutant that unable to bind to DDB1 and form the $CRL4^{CDT2}$ complex (Jin et al. 2006) in two melanoma cells (VMM1 and DM13) with relatively low basal levels of CDT2. We observed a statistically significant increase in MLN4924-induced rereplication in the cell lines overexpressing of wt-CDT2, and not $CDT2^{R246A}$, compared to the empty vector control (pMSCV) (Fig. 2.5E). This result demonstrates that the expression and the ubiquitylation activity of CDT2 contribute to the rereplication induced by MLN4924 in melanoma cells.

While MLN4924 induced varying degrees of senescence as early as 48 h post treatment in most melanoma cells tested, it failed to do so in the cell lines with inactivated p16 (CDKN2A) (Fig 2.5E). Similar result was observed in senescence induced after CDT2 depletion in the same panel of melanoma cells (Fig. 2.2F). These results demonstrate that MLN4924 treatment inhibits melanoma cells, irrespective of their BRAF/NRAS

mutational status, through the induction of rereplication that is stimulated with elevated CDT2 expression.

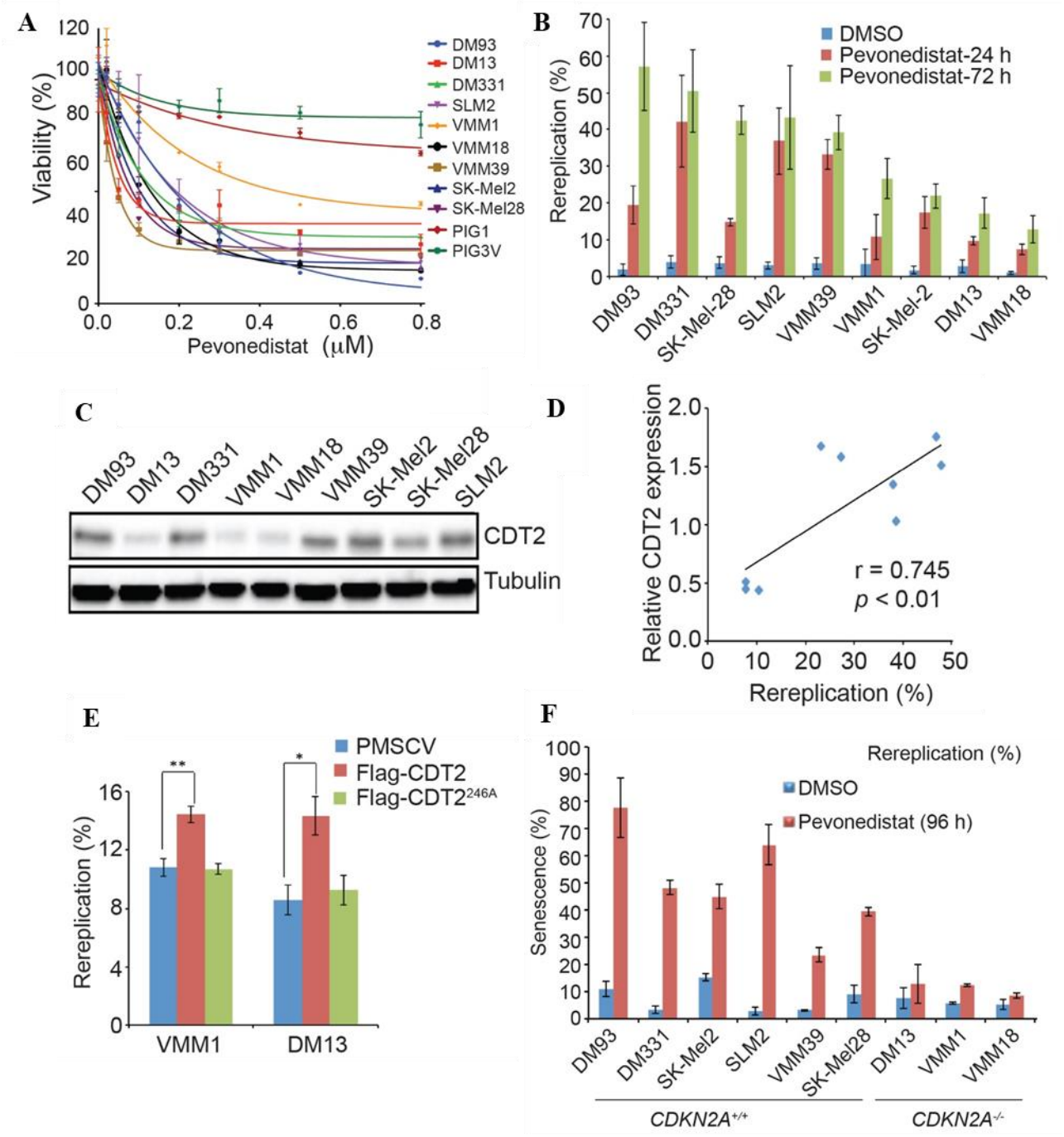
A
Viability (%)
Pevonedistat (μM)
DM93
DM13
DM331
SLM2
VMM1
VMM18
VMM39
SK-Mel2
SK-Mel28
PIG1
PIG3V
B
Rereplication (%)
DMSO
Pevonedistat-24 h
Pevonedistat-72 h
DM93
DM331
SK-Mel-28
SLM2
VMM39
VMM1
SK-Mel-2
DM13
VMM18
C
DM93
DM13
DM331
VMM1
VMM18
VMM39
SK-Mel2
SK-Mel28
SLM2
CDT2
Tubulin
D
Relative CDT2 expression
Rereplication (%)
r = 0.745
p < 0.01
E
PMSCV
Flag-CDT2
Flag-CDT2246A
Rereplication (%)
VMM1
DM13
F
Senescence (%)
Rereplication (%)
DMSO
Pevonedistat (96 h)
DM93
DM331
SK-Mel2
SLM2
VMM39
SK-Mel28
DM13
VMM1
VMM18
CDKN2A+/+
CDKN2A-/-

Figure 2.5: MLN4924 Suppresses Melanoma Proliferation Through Rereplication and Senescence

A. Survival curves showing the cell viability of a panel of melanoma cells and 2 immortalized melanocytes (PIG1 and PIG3V), assessed by an MTT viability assay. Cells were treated with the indicated doses of MLN4924 and the cell viability was calculated as a percent of the control DMSO-treated sample.

B. Histogram showing the extent of rereplication induction in a panel of melanoma cells after treatment with MLN4924 for 24 or 72 hours.

C. Immunoblot showing the base expression of CDT2 in a panel of melanoma cells. Tubulin is used as a loading control.

D. Dot plot showing the correlation between the relative base expression of CDT2, quantified from **C**, and the extent of rereplication induction after 24 hours (shown in **B**.) in a panel of melanoma cells.

E. Histogram showing the impact of the ectopic expression of Flag-CDT2 and Flag-CDT2^{246A}, and pMSCV as an empty vector control, on the percent of rereplication induced after MLN4924 treatment (1μM for 72 hours).

F. Histogram showing the percentage of cells undergoing senescence 96 hours after treatment with 1μM MLN4924. Senescence was quantified using the β-gal assay.

Results in A, B, E, and F represent the average of 3 independent experiments +/- SD. P-values were calculated using Student T-Test.

3.5. Transient Exposure to MLN4924 Irreversibly Inhibited Proliferation and Induced Rereplication and Senescence in Melanoma Cells but Not in Immortalized Melanocytes

To determine the relationship between the growth inhibitory effect of MLN4924 and rereplication induction, we exposed DM93 and VMM39 melanoma cells to 1μM of MLN4924 for increasing periods of time (4, 8, 12, 24 h), then washed the drug and replaced it with fresh media. The proliferation of cells exposed to MLN4924 for 12h and 24h was permanently inhibited and failed to recover even after 5 days of drug removal. On the other hand, cells treated with MLN4924 for only 4 or 8 h were transiently inhibited and proliferation resumed 24 h later (Fig. 2.6A-B). While the transient exposure to MLN4924 for 4 and 8 h failed to stimulate rereplication in melanoma cells, treatment for 12 and 24 h induced significant rereplication (18% and 60% respectively), which gradually decreased at later time points due to the continuous proliferation of a subset of cells that were not affected by the transient drug exposure. (Fig. 2.6C). DM93 cells exposed to MLN4924 continuously or for 12 and 24h maintained relatively high levels of p21, which was destabilized in cells treated for only 8h due to the restoration of cullin neddylation after drug removal (Fig. 2.6A). These results suggest that maintaining the expression of p21 is important for MLN4924-induced rereplication.

Immortalized melanocytes, such as PIG1 and PIG3V, are found to be less susceptible than most melanoma cells tested to MLN4924-induced growth inhibition (IC50 > 500 nM) (Fig. 2.5A). Unlike melanoma cells, 24 h exposure of PIG3V immortalized melanocytes to MLN4924 (1μM) temporarily arrested cells in G1 which eventually recovered and resumed cycling after drug removal. However, continuous exposure to

MLN4924inhibited proliferation without the induction of rereplication or senescence (Fig. 2.6D-E).

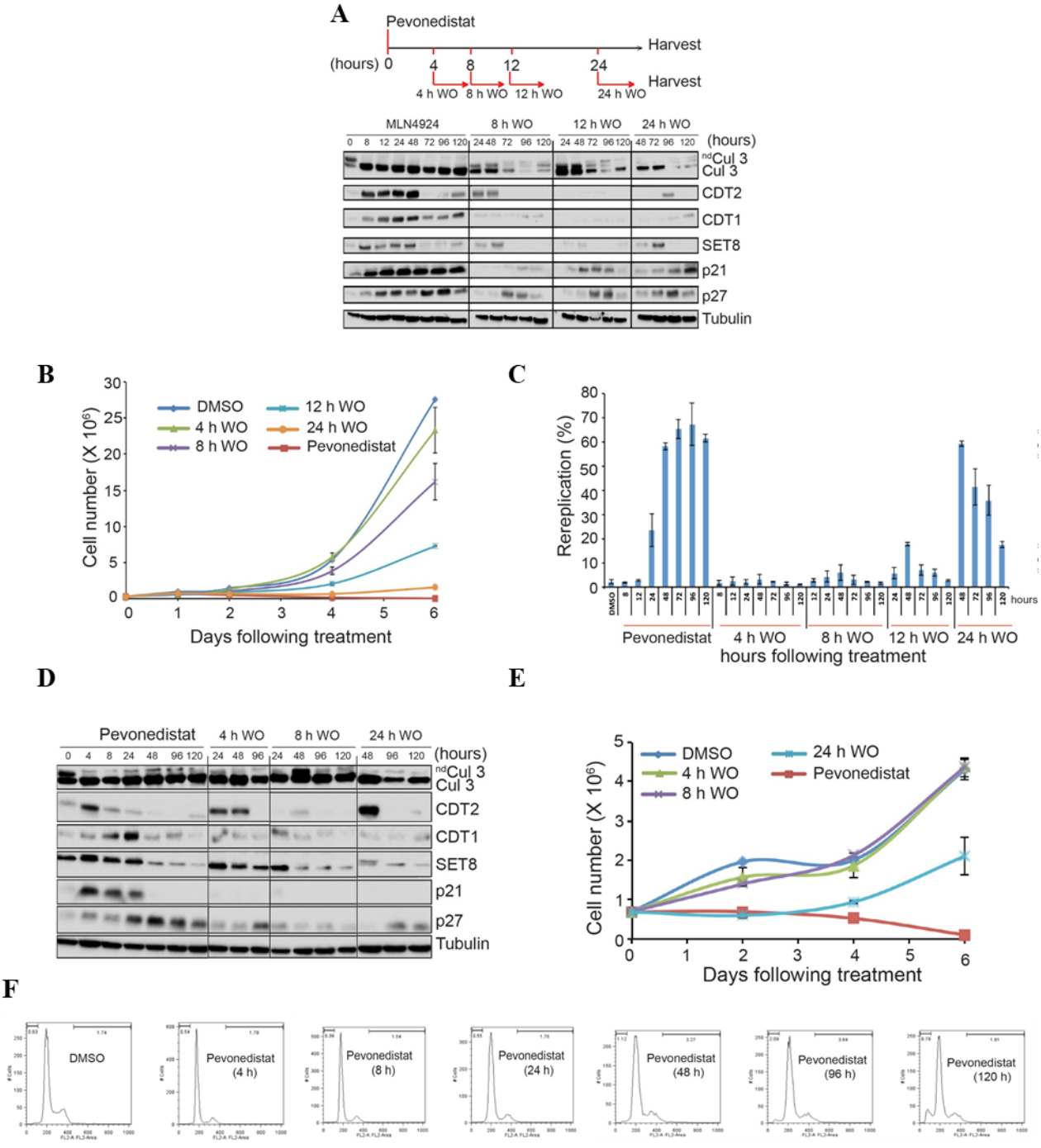

Figure 2.6: Transient Exposure to MLN4924 Irreversibly Inhibited Proliferation and Induced Rereplication and Senescence in Melanoma Cells but Not in Immortalized Melanocytes

A. Immunoblot showing the expression of the indicated protein after transient exposure of DM93 cells to MLN4924. Cells were treated with 1μM MLN4924 either continuously (without washing), or washed 8 h, 12, or 24 hours after the initial treatment. Then cells were harvested at the indicated times (workflow schematic – above). Tublin used as a loading control. nd Cul 3: Neddylated Cullin 3. WO: wash out - the duration of time in which the cells were exposed to MLN4924 before it was replaced with fresh media.

B. Growth curve showing the impact of transient (according to schematic in **A**) or continuous exposure to MLN4924 on DM93 proliferation.

C. Histograms showing the impact of transient or continuous exposure to MLN4924 on rereplication induction in DM93 cells. Cells were harvested at the indicated time and rereplication was determined by PI staining and flow cytometry.

D. Immunoblot showing the expression of the indicated protein after transient exposure of PIG3V immortalized cells to MLN4924. Cells were treated with 1μM MLN4924 either continuously (without washing), or washed 4 h, 8, or 24 hours after the initial treatment. Then lysates were collected at the indicated times. Tublin used as a loading control. nd Cul 3: Neddylated Cullin 3.

E. Growth curve showing the impact of transient or continuous exposure to MLN4924 on PIG3V proliferation.

F. Flow cytometry profiles showing the time dependent impact of MLN4924 on cell cycle distribution and the induction of rereplication on PIG3V immortalized melanocytes.

Results in B, C, E represent the average of 3 independent experiments +/- SD. P-values were calculated using Student T-Test.

3.6. MLN4924-induced Rereplication and Senescence are Dependent on the CRL4^{CDT2}-Mediated Stabilization of p21 and SET8

Previous results indicated that CRL4^{CDT2} ubiquitylation substrates are essential in promoting rereplication induced after CDT2 depletion. Consistently, we showed that transient depletion of CDT1, p21, SET8 by siRNA suppressed MLN4924-induced rereplication and senescence in DM93 (Fig. 2.7A). To further investigate the role these proteins play in the rereplication phenotype, we attempted to delete p21 (*CDKN1A*) or SET8 in melanoma cells using CRISPR/Cas9. Even though we were unable to achieve a complete biallelic deletion in both genes, due to the essential role SET8 play in cell viability (Oda et al. 2010; Schotta et al. 2008), we managed to generate multiple DM93 clones with mono-allelic deletions for p21 or SET8 that exhibited significant reduction in their protein levels (Fig. 2.7B and data not shown). Consistent with our siRNA results, MLN4924-induced rereplication and senescence were significantly reduced in the DM93 clones with hypomorphic deletions of either p21 or SET8 (Fig. 2.7C-D). The observed suppression of rereplication and senescence occurred despite the upregulation of CDT1, suggesting that increased levels of CDT1 are not sufficient to promote rereplication and senescence in cells with reduced levels of p21 or SET8. We have previously shown that the overexpression of CRL4^{CDT2}-resistant SET8 mutant was sufficient to induce rereplication and the melanoma cells with higher CDT2 expression levels exhibited higher extents of MLN4924-induced rereplication (Fig. 2.3F, 2.5C-D). These results altogether further demonstrate that MLN4924-induced rereplication and senescence in melanoma cells are mediated through the CRL4^{CDT2}-dependent stabilization of p21 and SET8.

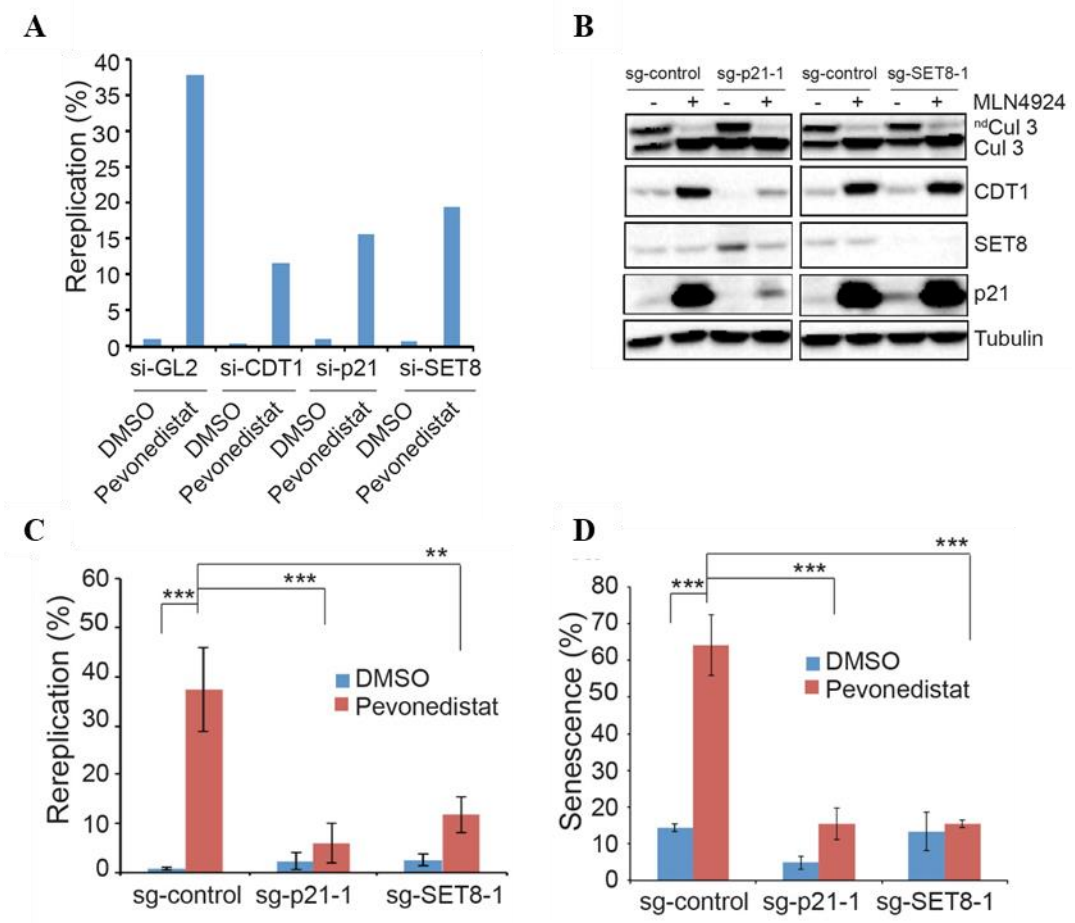
A
Rereplication (%)
si-GL2
si-CDT1
si-p21
si-SET8
DMSO
Pevonedistat
B
sg-control
sg-p21-1
sg-control
sg-SET8-1
MLN4924
ndCul 3
Cul 3
CDT1
SET8
p21
Tubulin
C
Rereplication (%)
DMSO
Pevonedistat
sg-control
sg-p21-1
sg-SET8-1
D
Senescence (%)
DMSO
Pevonedistat
sg-control
sg-p21-1
sg-SET8-1

Figure 2.7: MLN4924-induced Rereplication and Senescence are Dependent on the CRL4CDT2-Mediated Stabilization of p21 and SET8

A. Histogram showing the extent of MLN4924-induced rereplication in DM93 cells depleted of CDT1, p21, or SET8 by siRNA. Gl2 used as a control.

B. Immunoblot showing the expression of the indicated proteins in DM93 cells with hypomorphic expression of p21 or SET8, with or without treatment with 1μM MLN4924.

C-D. Histograms showing the percentage of cells undergoing rereplication (**C**) or senescence (**D**) in the DM93 cells with hypomorphic expression of p21 or SET8.

Results in **C-D** represent the average of 3 independent experiments +/- SD. *P*-values were calculated using Student's *t*-test.

3.7. MLN4924 Suppresses Melanoma Tumor Growth irrespective of BRAF/NRAS Mutational Status, and Its Toxicity is Mediated Through Stabilization of p21 and SET8

To test whether MLN4924 suppresses melanoma growth in *vivo*, we established xenografts of melanoma cell lines such as DM93 ($BRAF^{V600E}$ mutant and NRAS WT), VMM39 (BRAF WT and NRAS/PDGFR activating mutations), or SLM2 (WT for both BRAF and NRAS) in immune-compromised mice and monitored tumor growth. After the tumor reached a minimum volume of 100 mm^3, MLN4924, or DMSO control, were administered daily during the first 5 days of each of two ten-day cycles (Soucy et al. 2009). MLN4924 significantly suppressed tumor growth, compared to the DMSO control, in all three cell lines, but did not result in tumor regression (Fig. 2.8A-D). Slow tumor regrowth was observed in VMM39 and SLM2, but not in DM93 xenografts, after cessation of drug treatment. Analysis of lysates collected from DM93 and VMM39 tumors on Day 25, 10 days after cessation of treatment, showed the inhibition of cullin neddylation, stabilization of cullin substrates such as CDT1 and p21, accumulation of DNA damage and checkpoint activation (Fig. 2.8B). Therefore, MLN4924 inhibits melanoma growth regardless of the mutational status. To further examine if the MLN4924 toxicity *in vivo* is mediated through the $CRL4^{CDT2}$ ligase, we established xenografts from the previous DM93 clones with hypomorphic deletions of p21 or SET8. Consistent with our *in vitro* results, MLN4924 failed to suppress tumor growth in the absence of p21 or SET8, compared to the control (sg-control) (Fig. 2.8E). In summary, MLN4924 suppresses melanoma growth irrespective of the BRAF/NRAS mutational status, and this inhibition requires the expression of p21 or SET8. These results further confirm that MLN4924 exerts its anti-melanoma toxicity through the failure of $CRL4^{CDT2}$ to degrade p21 and SET8.

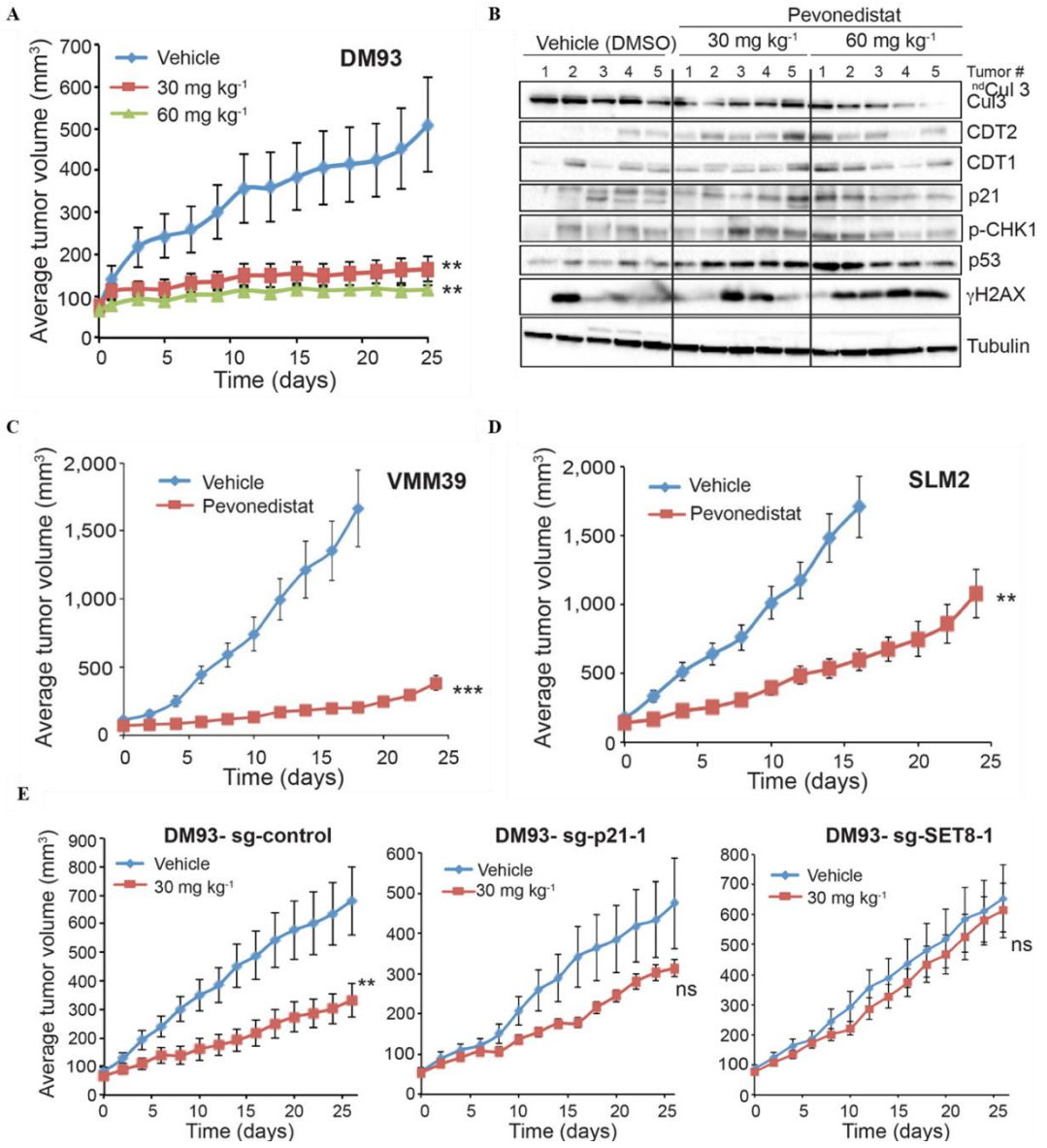
A
DM93
Vehicle
30 mg kg-1
60 mg kg-1
Average tumor volume (mm3)
Time (days)
**
**
B
Vehicle (DMSO)
Pevonedistat
30 mg kg-1
60 mg kg-1
Tumor #
1 2 3 4 5 1 2 3 4 5 1 2 3 4 5
ndCul 3
Cul3
CDT2
CDT1
p21
p-CHK1
p53
γH2AX
Tubulin
C
VMM39
Vehicle
Pevonedistat
Average tumor volume (mm3)
Time (days)
***
D
SLM2
Vehicle
Pevonedistat
Average tumor volume (mm3)
Time (days)
**
E
DM93- sg-control
Vehicle
30 mg kg-1
Average tumor volume (mm3)
Time (days)
**
DM93- sg-p21-1
Vehicle
30 mg kg-1
Time (days)
ns
DM93- sg-SET8-1
Vehicle
30 mg kg-1
Time (days)
ns

Figure 2.8. MLN4924 Suppresses Melanoma Tumor Growth irrespective of BRAF/NRAS Mutational Status, and Its Toxicity is Mediated Through Stabilization of p21 and SET8

A. Graph showing the average volume of DM93 xenografts in nude mice after treatment with MLN4924 (30 or 60mg/kg) according to the treatment schedule indicated in Materials and Methods.

B. Immunoblot of tumor lysates extracted on Day 25 from five randomly selected xenografts of A and probed for the indicated proteins. Tubulin used as a loading control. nd Cul3: Neddylated Cullin 3.

C-D. Graph showing the average volume of VMM39 (**C**) or SLM2 (**D**) tumors in nude mice after treatment with MLN4924 (60 mg/kg) following the regimen indicated in Materials and Methods.

E. Nude mice bearing DM93 tumor xenografts established from DM93 clones with hypomorphic expression of p21 or SET8, in addition to an sg-control. Mice were injected with 30 mg/Kg MLN4924 according to the schedule indicated in the Materials and Methods.

In **A** and **C-E**. Number of animals per group: 12. Graphs show mean tumor volume +/- SEM. *P*-value calculated using Student's *t*-test.

3.8. MLN4924 Synergizes with Vemurafenib to Suppress Melanoma with BRAF Mutations and Is Effective Against Vemurafenib-resistant Tumors

Despite the efficacy and the improved therapeutic outcomes of current anti-melanoma therapies, acquired resistance remains a major clinical challenge. The development of resistance against potent treatments such as the BRAF inhibitor Vemurafenib, which targets BRAF kinases harboring the V600E activating mutation present in more than half of malignant melanomas, significantly reduced the therapeutic efficacy after prolonged treatment in advanced-stage tumors (Alqathama 2020). One of the key strategies to overcome therapeutic resistance is by combination treatment.

We have shown that MLN4924 suppresses melanoma growth *in vitro* and *in vivo* irrespective of the BRAF mutational status. To test whether MLN4924 can synergize with BRAF inhibitors, such as the vemurafenib structural analog PLX4720 (Tsai et al. 2008), we established xenografts of DM331, a BRAF-mutant melanoma cell line that is resistant to vemurafenib. As soon as the tumor volume reaches 150-200mm^3, DM331 xenografts were treated with MLN4924 (60mg/Kg) following a schedule of two cycles of five-day treatment followed by five treatment-free days, while PLX4720 (417mg/Kg) was administered through the diet throughout the period of treatment. The combined administration of both MLN4924 and PLX4720 resulted in a synergistic growth inhibition compared to individual treatments with each drug, both of which suppressed tumor growth to a lesser extent (Fig. 2.9A). To further test whether MLN4924remains effective against tumors that acquired resistance against vemurafenib treatment. We acquired two BRAF-mutant melanoma cell lines, DM331-R and SL-MEL-24-R, extracted *ex vivo* from PLX4720-resistant tumors (Roller et al. 2016). While they remain insensitive to PLX4720,

both cell lines were susceptible to MLN4924-induced inhibition and rereplication *in vitro* (Fig. 2.9B-D). These results show that MLN4924 synergizes with PLX4720 to suppress BRAF melanoma proliferation and is effective against BRAF-resistant tumors.

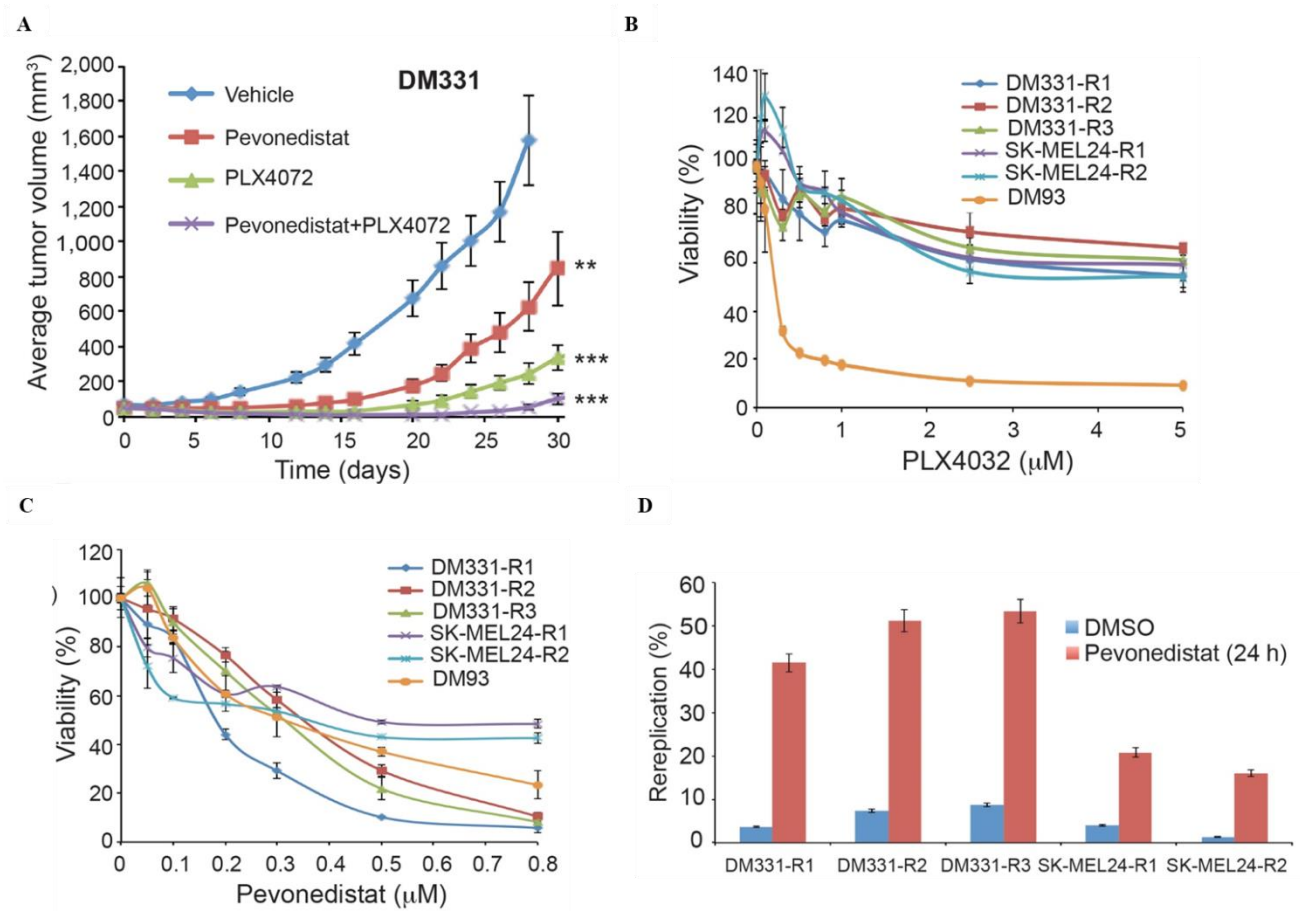

Figure 2.9: MLN4924 Synergizes with Vemurafenib to Suppress Melanoma with BRAF Mutations and Is Effective Against Vemurafenib-resistant Tumors

A. Graph showing the average volume of xenografts from DM331 and were treated with MLN4924 (MLN4924), PLX4072, or a combination according to the schedule indicated in the Materials and Methods. Number of animals per group: 12. Graphs show mean tumor volume +/- SEM. P-value calculated using Student T-Test.

B-C. MTT viability assay to assess sensitivity to PLX4032 (**B**) or MLN4924 (**C**) in DM93 compared with the vemurafenib-resistant ex-vivo cell lines DM331-R (1 to 3) and SK-MEL24-R (1 and 2). Cells were treated with PLX4032 (**B**) or MLN4924 (**C**) at the indicated doses and the viability was calculated as a percent of control DMSO-treated samples.

D. Histogram showing the percent of rereplication in the vemurafenib-resistant ex-vivo cell lines DM331-R (1 to 3) and SK-MEL24-R (1 and 2) in response to MLN4924treatment.

Results represent the average of 3 independent experiments +/- SD. *P*-values were calculated using Student's *t*-test.

4. Discussion:

Multiple studies have shown that The $CRL4^{CDT2}$ substrate receptor CDT2 is overexpressed in various tumors such as gastric and hepatocellular carcinomas, where its expression was associated with poor patient outcome (Kobayashi et al. 2015; Mackintosh et al. 2012; J. Li et al. 2009; Ueki et al. 2008). Consistently, our study demonstrates that CDT2 expression is significantly elevated in patient-derived melanoma samples and correlates with poor overall and disease-free patient survival. CDT2 was found to be elevated in metastatic melanomas compared to primary tumors and its expression does not appear to correlate with BRAF or NRAS activating mutations. The poor prognosis as a result of elevated CDT2 expression could be attributed to the decreased activity of the substrates p21 and SET8, whose degradation upon CDT2 overexpression affect the DNA damage response and cell cycle regulation providing survival advantage to cells with oncogenic properties (Panagopoulos et al. 2020). We also showed that CDT2 expression correlates with MLN4924 toxicity and its ectopic expression render melanoma cells more sensitive to MLN4924-induced rereplication *in vitro*. These results highlight the prognostic significance of CDT2 overexpression in melanoma and its usefulness as a promising clinical biomarker for determining malignant properties independent of classic clinical parameters.

Targeting cullin-based E3 ligase complexes, most notably CRL4s, emerged as a novel anti-cancer strategy due to their critical function in substrate selection, degradation, and a broad regulatory role under physiological and pathological conditions, especially in tumorigenesis. The use of molecular inhibitors, such as sulfonamides and thalidomide

derivatives, as an anti-cancer treatment to target CRL receptors responsible for degrading oncogenic substrates has displayed efficacy against various malignancies including multiple myeloma, lymphoma, colorectal cancer and melanoma (Cheng et al. 2019). In this chapter, we demonstrate the efficacy and the therapeutic potential of inactivating $CRL4^{CDT2}$ E3 ubiquitin ligase in cutaneous melanoma. $CRL4^{CDT2}$ inactivation, via depletion of the substrate adaptor CDT2 or pharmacological inhibition using the neddylation inhibitor MLN4924, suppressed melanoma proliferation *in vitro* and *in vivo* through the induction of robust rereplication and senescence. While oncogenic activating mutations in BRAF or NRAS did not affect the efficacy of MLN4924 in suppressing melanoma *in vitro* and *in vivo*, inactivating mutations in CDKN2A (or p16) appear to be involved in senescence induced after $CRL4^{CDT2}$ inactivation. In addition, MLN4924 synergizes with the BRAF inhibitor vemurafenib in suppressing the growth of melanoma xenografts and remain effective against vemurafenib-resistant tumors *in vitro*. Therefore, our results demonstrate the therapeutic potential of MLN4924 in treating melanoma irrespective of the mutational background, its efficacy as a combination therapy with BRAF inhibitors, and against tumors that relapsed from vemurafenib treatment.

Our results demonstrate that MLN4924 toxicity in melanoma is mediated through the activity of $CRL4^{CDT2}$ and its ability to suppress proliferation and promote rereplication is dependent on the stabilization of its substrates p21 and SET8. This was illustrated in the failure of MLN4924 to induce robust rereplication and suppress melanoma in cell lines with hypomorphic deletions in p21 or SET8. p21 levels were significantly increased in rereplicating cells following $CRL4^{CDT2}$ inactivation, ectopic expression of CDT1,

$SET8^{\Delta PIP}$, or after EMI1 depletion. Even though both substrates are shown to be required for MLN4924-induced toxicity *in vitro* and *in vivo*, only SET8 was both necessary and sufficient to promote rereplication in melanoma. The ability of deregulated SET8 expression to promote rereplication is potentially due to its role in histone H4K20 methylation (Abbas et al. 2010; Tardat et al. 2010). This is supported by the fact that increased dimethylation of H4K20 (H4K20me2), which is caused by both SET8 and the dimethyl transferase SUV4-20H1, was found to enhance ORC1 occupancy at origins of replication and increase MCM loading (Kuo et al. 2012; Brustel et al. 2017). Therefore, the anti-melanoma effect of MLN4924 appears to be mediated primarily through a p21- and SET8-dependent rereplication and senescence. We also found that CDT1 expression was required to promote rereplication induced after $CRL4^{CDT2}$ inactivation. However, unlike p21 and SET8, the observed inhibition of rereplication appears to be secondary to the G1 arrest caused after CDT1 knockdown. Even though ectopic overexpression of CDT1 was sufficient to induce rereplication, its stabilization following MLN4924 treatment (in cells with hypomorphic expressions of p21 or SET8) or post geminin depletion failed to do so in melanoma. However, the inhibition of both geminin and Cyclin A, after depletion of the APC ubiquitin ligase inhibitor EMI1, increased CDT1 levels and induced robust rereplication in melanoma cells. These results suggest that CDT1 is primarily regulated by the Cyclin A-mediated and $CRL1^{SKP2}$-dependent pathway in melanoma cells.

Our work highlights the significance of targeting $CRL4^{CDT2}$-SET8/p21 degradation axis as a therapeutic strategy in treating melanoma. We demonstrate the efficacy of MLN4924, as a single agent or in combination with vemurafenib, in suppressing

melanoma, including tumors that relapsed from BRAF inhibitors, regardless of the classic BRAF or NRAS oncogenic mutations.

5. Materials and Methods:

5.1. Cell Culture and Reagents

VMM39, VMM1, and VMM18 human melanoma cell lines were established from metastatic lesions of patients at the University of Virginia (IRB #5202, by CLS). DM93, DM331, DM13 and SLM2 melanoma cell lines had been established from metastatic lesions by Dr. H.F. Seigler at Duke University (Hogan et al. 2005; Huntington et al. 2004; McGarry and Kirschner 1998; Kittlesen et al. 1998; Molhoek et al. 2008; Slingluff et al. 1993; Yamshchikov et al. 2005; 2001). SK-MEL-2 and SK-MEL-28 melanoma cells were established in Memorial Sloan Kettering Cancer Center and obtained from the American Type Culture Collection (ATCC, Manassas, VA). All melanoma cells were grown in RPMI media supplemented with 10% fetal bovine serum (FBS) and 1% penicillin/streptomycin (P/S). PIG1 and PIG3V melanocytes were described before (Poole et al. 2000) and maintained in Media 254 containing 1% of human melanocyte growth supplement (HMGS), 5% FBS and 1% (P/S). All cells were grown at 37 °C in 5% CO_2. Tissue extraction reagent I was obtained from Invitrogen (Carlsbad, CA). Propidium iodide, 7-AAD and BrdU kit were purchased from BD Biosciences (San Diego, CA). Vector's ImmPRESS polymer kit for TMAs immunostaining was obtained from Vector laboratories (Burlingame, CA). MLN4924 and vemurafenib (PLX4032) were purchased from Active Biochem (Wan Chai, Hong Kong), and were dissolved in DMSO and used at the indicated doses.

5.2. Cell Lysis, SDS-PAGE and Immunoblotting:

Melanoma cells were lysed with RIPA lysis buffer (50 mM Tris, pH 8.0; 150 mM NaCl, 1% NP-40; 0.5% sodium deoxycolate; 0.1% SDS; 1 mM Benzamidin -HCl; 0.5 μg/ml Leupeptin; 0.5 μg/ml Aprotinin; 1 μg/ml pepstatin; 20 mM NaF; 20 mM Na_3VO_4), and equal amounts of protein were electrophoretically separated in a polyacrylamide 8–12% gel (BioRad, Hercules, CA), trans-blotted to a nitrocellulose membrane, and incubated overnight with primary antibodies at 4 °C. The following antibodies were used: anti-p21 (C19), anti-p27 (C19), anti-p53 (DO-1), and anti-tubulin (10D8) were purchased from Santa Cruz (California). Antibodies against SET8, CHK1, CHK2, p-CHK1 (S375), p-CHK2 (T68), H2AX and p-H2AX (γH2AX; T139), and PARP were purchased from Cell Signaling (Danvers, MA). Anti-Cul3 was purchased from Bethyl Laboratories (Montgomery, TX). Anti-CDT1 and anti-CDT2 antibodies were described before (Abbas et al. 2010). The immunoblot signals were detected by enhanced chemiluminescence. For melanoma xenografts, tumors were isolated, washed three times with cold PBS and frozen at − 80 °C until use. Frozen specimens were grinded in a dry-iced mortar and subsequently lysed in 2 × volume of tissue extraction reagent I, supplemented with protease and phosphatase inhibitors as stated above.

Tissue lysates were probed for different proteins by immunoblotting following the procedure described above.

5.3. RNA Interference (siRNA)-Mediated Gene Silencing

si-RNA transfections were performed using lipofectamine RNAimax according to the manufacturer's protocol (Invitrogen, Carlsbad, CA). Cells were seeded at

30% confluency and transfected with the individual siRNAs (10 nM each) in RPMI media supplemented with 10% fetal bovine serum (FBS) and 1% penicillin/streptomycin (P/S). In co-knockdown experiments, DM93 or VMM39 cells were transfected with the individual siRNAs (10 nM each with 10 nM control siGL2-for normalization) or siRNAs targeting CDT1, SET8 or p21 along with siRNA targeting CDT2 (10 nM each – total 20 nM siRNAs). Control cells were transfected with 20 nM si-GL2. Cells were harvested 72 h post-transfection for cell cycle analysis or at 96 h for β-gal staining. The following siRNAs were used (sense strand): si-GL2: 5′-AACGUACGCGGAAUACUUCGA-3′; si-CDT2: 5′-GAAUUAUACUGCUUAUCGA-3′, si-CDT1: 5′-AACGUGGAUGAAGUACCCGAC-3′; si-SET8: 5′-GAUUGAAAGUGGGAAGGAA-3′; si-p21: 5′-AACAUACUGGCCUGGACUG-3′; si-Geminin: 5′-UGCCAACUCUGGAAUCAAA-3′. si-EMI1 were described previously (Machida and Dutta 2007).

5.4. Gene Targeting by CRISPR/Cas9

Single guide-RNAs (sgRNAs) targeting the *DTL* (sg-CDT2-1 and sg-CDT2), *SET8* and *CDKN1A* genes were cloned into pX330 vector containing a human codon-optimized *Sp*Cas9 endonuclease (Addgene #42230) using BbsI restriction enzyme cutting sites, and transfected in the various cell lines. After puromycin selection, cells were seeded to obtain single colonies. Genomic DNA was extracted using 100 mM NaCl, 50 mM Tris-HCl pH 7.0, 5 mM EDTA and 1% SDS. Genotyping was performed using PCR amplification of genomic DNA using the following forward and reverse primer sets, respectively. For CDT2: 5′-TGTTGTGAGAGGCGCAAGCTGC-3′ and 5′-GGTCGGAGGTGGCGTGTGTTTC-3′; for SET8: 5′-

GTCTTTCCCCCACCTCCGCCTG-3′ and 5′-CTTTTTTCGGGGGGCCTGTTTGC-3′; for p21: 5′-TCACCTGAGGTGACACAGCAAAGC-3′ and 5′-GGCCCCGTGGGAAGGTAGAGCTT-3′. Targets of the various sgRNAs are as follows: For *DTL* (*CDT2*): 5′-GCACCGAATTGAAGAGCATC-3′ (for sg-CDT2-1); and 5′-CATTTCTCAGGACGCCAAGC-3′ (for sg-CDT2-2); for *SET8*: 5′-ACGGAGCGCCATGAAGTCCG-3′; for *CDKN1A*: 5′-GCGCCATGTCAGAACCGGCT-3′. Insertions/deletions (Indels) identification was performed using Surveyor Mutation Detection Kit according to the manufacturer's protocol (Integrated DNA Technologies, CA). For sequencing, PCR amplified gene products were cloned into Topo TA Vector using TOPO TA cloning Kit according to the manufacturer's protocol (Invitrogen, CA) and transformed into DH5α. Plasmids were retrieved by the QIAprep Spin Miniprep Kit (Qiagen) and confirmed by sequencing (Eurofins Scientific).

5.5. Cell Proliferation/Viability Assays and Washout Experiments

Proliferation/viability of cultured cells was measured by CellTiter96 Non-radioactive cell proliferation assay (Promega; Madison, WI). Briefly, various wild type and mutant BRAF melanoma cells were seeded in 96 well plates and treated with MLN4924, vemurafenib or the combination MLN4924 and vemurafenib at various concentrations. Control cells were treated with DMSO. 96 h following treatment, cells were stained with the dye solution according to the manufacturer's protocol. Absorbance was recorded at 570 nm and growth curves were established. To test the effect of transient exposure of melanoma cells to MLN4924 on rereplication and growth inhibition, we conducted the washout experiments where melanoma cells or PIG3V melanocytes were treated with 1 μM MLN4924 for

different times (4, 8, 12 and 24 h) before the drug was washed out by washing the cells 2 × with PBS, and adding drug-free fresh growth media to cells. Cells were counted every 24 h by Countess Automated Cell Counter (Invitrogen), and harvested at the indicated times for PI staining and FACS analysis (cell cycle profile) or for immunoblotting.

5.6. Clonogenic Survival Assays

Cell survival following CDT2 depletion or MLN4924 treatment was assessed by clonogenic survival assay, preformed in triplicates. 72 h following transfection with si-GL2 or si-CDT2, cells were trypsinized, counted and seeded in 60 mm dishes. For MLN4924 treatments, cells were counted and seeded in 60 mm dishes and treated 24 h later with various doses of MLN4924 or with DMSO. Cells were cultured for two weeks and were subsequently washed in cold PBS, fixed in cold methanol for 10 min and stained with crystal violet (0.5%) for 10 min. Plates were washed with water, dried and pictures were captured using Imagelab software (BioRad). Quantification of colonies was performed using QuantityOne software (BioRad). Results are represented as mean ± s.e.m. of triplicates normalized to the corresponding DMSO-treated or si-GL2 transfected controls.

5.7. Senescence-Associated β-galactosidase Assays

Senescence was monitored using β-galactosidase (β-gal) staining. Following the various treatments, cells were washed twice with PBS, fixed with 2% formaldehyde/0.2% gluteraldehyde in PBS for 15 min at room temperature, and washed 2 × with PBS. The cells were stained with fresh X-Gal solution (1 mg/ml X-gal, 40 mM $C_6H_8O_7 \cdot H_2O$, 5 mM

$K_3Fe(CN)_6$, 5 mM K4Fe(CN)$_6$·3H_2O, 150 mM NaCl, and 2 mM $MgCl_2$·6H2O in PBS) for 3–12 h at 37 °C in the dark. Cells were washed 3 × in PBS and fixed with 100% methanol for 5 min at room temperature. Bright field blue color images were taken with an AMG EvosXL Core Imager/camera microscope, counting at least 100 cells from at least 3 fields.

5.8. Flow Cytometry Analysis

The effects of MLN4924, vemurafenib and/or silencing of various cell cycle-associated proteins by siRNA on cell cycle distribution and rereplication were assessed by propidium iodide staining and flow cytometry of asynchronous melanoma cultures. Synchronization of cells was not employed to avoid bias and to be able to measure the impact of these perturbations on proliferating cancer cells. Briefly, asynchronous melanoma cell lines were treated with MLN4924 or vemurafenib, or transfected with si-CDT1, si-CDT2, si-SET8, si-p21, si-geminin, si-EMI1 or si-GL2 for a time ranging from 24 to 96 h. Cells were washed with cold PBS, harvested, and fixed in 70% (v/v) ethanol. Cells were subsequently treated with 20 μg of DNase-free RNase and stained with propidium iodide according to instructions of the manufacturer. Samples were analyzed on a FACscan (Becton Dickinson) and G_0-G_1, S, and G_2-M fractions were segmented, and apoptotic (sub-G1 DNA content) and rereplicating (> G2/M DNA content) fractions were determined using FlowJo and ModFit softwares.

5.9. Bromodeoxyuridine (BrdU) Staining and Flow Cytometry

The effects of MLN4924 and/or silencing of cell cycle-associated proteins on cell cycle distribution or rereplication were assessed by flow cytometry according to the

manufacturer's instructions. Different melanoma lines were transfected with si-GL2, si-CDT2, si-CDT1, si-SET8, si-p21 or si-geminin for a time ranging from 24 to 96 h. At the end of treatment, cells were pulsed with BrdU (10 nM) for 1 h in the dark prior to harvesting. Cells were washed with PBS and staining solution before the fixation and permeabilization steps according to the manufacturer's instructions. Cells were subsequently stained with anti-BrdU antibody solution for 20 min at room temperature, washed and stained with 7-AAD solution for 30 min at 4 °C. The cells were re-suspended in 1 ml of staining buffer and kept overnight at 4 °C before analysis. Samples were analyzed on a FACscan (Becton Dickinson), and different phases of the cell cycle were determined using FlowJo and ModFit softwares.

5.10. Staining and Analysis of Melanoma Tissue Microarray (TMA)

Formalin-fixed paraffin-embedded (FFPE) tissue blocks were retrieved from archives of the Department of Pathology, University of Virginia. Use of human tissues was approved by the UVA Institutional Review Board (protocol 10598). Hematoxylin and eosin (H&E) slides from each block were reviewed by a pathologist (JS) to identify tumor areas. TMAs were constructed with 1.0-mm diameter tissue cores from representative tumor areas from the FFPE tissue blocks, transferred into a recipient paraffin block using a semi-automated tissue array instrument (TMArrayer; Pathology Devices). Quadruplicate or triplicate tissue cores were taken from each specimen, resulting in 9 composite TMA blocks containing tissue cores from 18 to 27 specimens each. Control tissues from spleen, liver, placenta, and kidney were included in each TMA block (not shown). Multiple 4 μm sections were cut for H&E and immunohistochemical staining. The human melanoma tissue microarray (TMA)

was evaluated for expression of CDT2 and Ki67 by immunohistochemistry. Details of this TMA have been reported previously (Erdag et al. 2012). These arrays included surgical specimens of human melanoma. Protein expression patterns of CDT2 and Ki67 were assessed in 138 tumor specimens in the TMA. Three nevi were used as a control. Antigen-retrieval step was performed at low pH 0.01% citric acid for 20 min at 100 °C. Endogenous peroxidase was blocked using Vector's Bloxall (SP-6000) for CDT2 detection and 0.3% Hydrogen peroxide for Ki67 detection; for 10 min; prior to serum blocking for 20 min, at room temperature. Incubation with CDT2 primary antibody (Abbas et al. 2008) (1:100 dilution) was performed at room temperature for 30 min. Staining with Ki67 primary antibody (Vector laboratories; 1:50 dilution) was performed overnight at 4 °C. Omitting the primary antibody served as a negative control for the staining. The Secondary antibody (SK-4200 ImmPRESS reagent; 1:500 dilution) was used for 30 min followed by substrate AEC (Vector laboratories) incubation for 20 min, at room temperature as per the kit's instructions. Diaminobenzidine was utilized as the final chromogen and hematoxylin as the nuclear counterstain. Staining frequency of CDT2 and Ki67 were quantified manually by counting the number of positively stained nuclei in an average of three fields per core. The frequency is calculated by dividing the number of positive staining over the total number of cells in the same fields.

Immunohistochemical staining for BRAF mutation (V600E) was performed at the University of North Carolina, using Leica's Bond autostainer (Leica Biosystems, Nussloch, Germany) and the BRAF V600E antibody (Spring Bioscience, clone VE1, dilution 1:400). Mutational status is assessed by the presence or absence of staining in each core. Tumors

with borderline staining and those with discrepant expression in between cores were excluded. The consensus value of the 2–4 representative cores from each tumor/patient sample arrayed was used for scoring and statistical analyses. TMA slides were quantified using Aperio ImageScope V11.2.

5.11. Kaplan-Meier Plot Analysis

Publicly available TCGA data at cBioPortal (Cerami et al. 2012; Gao et al. 2013) was used to plot Kaplan-Meier plots on tumors divided into two groups based on level of CDT2 expressed as a Z-score (Collisson et al. 2014; Taylor et al. 2010; Weinstein et al. 2014).

5.12. Tumor Xenograft Studies

Animals were housed and handled in accordance with the guidelines of the Animal Care and Use Committee (ACUC) of the University of Virginia. The effect of MLN4924 on melanoma growth was tested in flank xenograft models. Foxn1^{nu} (20–25 g body weight, 4–5 weeks old females) athymic nude immune-deficient mice (Harlan laboratories) were used in this study. MLN4924 was dissolved in sterile 10% DMSO containing PBS (stock 1 mM) and stored in − 20 °C until use. 2×10^6 of DM93, VMM39, SLM2, DM331 or SK-MEL-24 melanoma cells were implanted in both flanks of immune-deficient mice (n = 12 mice per group) and tumor growth was monitored until reaching an average volume of 150–200 mm^3. Mice were randomized into groups for treatment. Animals were administered 0.2 mL MLN4924 solution (30 or 60 mg/kg body weight as indicated) intraperitoneally on a schedule of two cycles of five-day treatment followed by five treatment-free days, for a total of 3 weeks, or more as indicated. Control animals were treated with an equal volume

of sterile vehicle (10% DMSO in PBS). Where indicated, mice received control rodent diet, or diet with 417 mg/kg PLX4720 (Research Diets, Inc. New Brunswick, NJ). Tumors were measured with an electronic caliper every other day for 3 weeks post-drug injection. Animal weight was recorded once a week to detect any weight loss due to the toxicity of drug treatment or tumor burden. At the end of treatment, animals were euthanized and tumors harvested for further processing. The results shown are mean tumor volumes at the indicated time ± s.e.m.; *$p < 0.05$, **$p < 0.01$, ***$p < 0.001$.

5.13. Statistical Analysis

All experiments were performed in triplicates. Numerical data were expressed as mean ± standard deviation (SD). Where applicable, data are presented as the mean ± s.e.m. Two group comparisons were analyzed by two-sided Student's *t*-test. *P*-values were determined for all analyses and $p < 0.05$ was considered significant. Synergy was determined using the Bliss model of independence (BLISS 1939; Fitzgerald et al. 2006). For correlations, a Spearman correlation was used and *p*-values < 0.05 were considered statistically significant.

6. References:

Abbas, Tarek, and Anindya Dutta. 2011. “CRL4Cdt2: Master Coordinator of Cell Cycle Progression and Genome Stability.” *Cell Cycle*. Taylor and Francis Inc. https://doi.org/10.4161/cc.10.2.14530.

Abbas, Tarek, Mignon A. Keaton, and Anindya Dutta. 2013. “Genomic Instability in Cancer.” *Cold Spring Harbor Perspectives in Biology* 5 (3): a012914.

https://doi.org/10.1101/cshperspect.a012914.

Abbas, Tarek, Etsuko Shibata, Jonghoon Park, Sudhakar Jha, Neerja Karnani, and Anindya Dutta. 2010. "CRL4Cdt2 Regulates Cell Proliferation and Histone Gene Expression by Targeting PR-Set7/Set8 for Degradation." *Molecular Cell* 40 (1): 9–21. https://doi.org/10.1016/j.molcel.2010.09.014.

Abbas, Tarek, Uma Sivaprasad, Kenta Terai, Virginia Amador, Michele Pagano, and Anindya Dutta. 2008. "PCNA-Dependent Regulation of P21 Ubiquitylation and Degradation via the CRL4Cdt2 Ubiquitin Ligase Complex." *Genes and Development* 22 (18): 2496–2506. https://doi.org/10.1101/gad.1676108.

Alqathama, Aljawharah. 2020. "BRAF in Malignant Melanoma Progression and Metastasis: Potentials and Challenges." *American Journal of Cancer Research* 10 (4): 1103.

Arias, Emily E., and Johannes C. Walter. 2006. "PCNA Functions as a Molecular Platform to Trigger Cdt1 Destruction and Prevent Re-Replication." *Nature Cell Biology* 8 (1): 84–90. https://doi.org/10.1038/ncb1346.

Beck, David B., Adam Burton, Hisanobu Oda, Céline Ziegler-Birling, Maria Elena Torres-Padilla, and Danny Reinberg. 2012. "The Role of PR-Set7 in Replication Licensing Depends on Suv4-20h." *Genes and Development* 26 (23): 2580–89. https://doi.org/10.1101/gad.195636.112.

BLISS, C. I. 1939. "THE TOXICITY OF POISONS APPLIED JOINTLY1." *Annals of Applied Biology* 26 (3): 585–615. https://doi.org/10.1111/j.1744-

7348.1939.tb06990.x.

Brustel, Julien, Nina Kirstein, Fanny Izard, Charlotte Grimaud, Paulina Prorok, Christelle Cayrou, Gunnar Schotta, et al. 2017. “Histone H4K20 Tri-methylation at Late-firing Origins Ensures Timely Heterochromatin Replication.” *The EMBO Journal* 36 (18): 2726–41. https://doi.org/10.15252/embj.201796541.

Bui, Duyen T., and Joachim J. Li. 2019. “DNA Rereplication Is Susceptible to Nucleotide-Level Mutagenesis.” *Genetics* 212 (2): 445–60. https://doi.org/10.1534/genetics.119.302194.

“Cancer Facts and Figures.” 2020. *American Cancer Society*. https://www.cancer.org/content/dam/cancer-org/research/cancer-facts-and-statistics/annual-cancer-facts-and-figures/2020/cancer-facts-and-figures-2020.pdf.

Cerami, Ethan, Jianjiong Gao, Ugur Dogrusoz, Benjamin E. Gross, Selcuk Onur Sumer, Bülent Arman Aksoy, Anders Jacobsen, et al. 2012. “The CBio Cancer Genomics Portal: An Open Platform for Exploring Multidimensional Cancer Genomics Data.” *Cancer Discovery* 2 (5): 401–4. https://doi.org/10.1158/2159-8290.CD-12-0095.

Chen, Zhi, Jie Sui, Fan Zhang, and Caiguo Zhang. 2015. “Cullin Family Proteins and Tumorigenesis: Genetic Association and Molecular Mechanisms.” *Journal of Cancer*. Ivyspring International Publisher. https://doi.org/10.7150/jca.11076.

Cheng, Ji, Jianping Guo, Brian J. North, Kaixiong Tao, Pengbo Zhou, and Wenyi Wei. 2019. “The Emerging Role for Cullin 4 Family of E3 Ligases in Tumorigenesis.” *Biochimica et Biophysica Acta - Reviews on Cancer*. Elsevier B.V.

https://doi.org/10.1016/j.bbcan.2018.11.007.

Collisson, Eric A., Joshua D. Campbell, Angela N. Brooks, Alice H. Berger, William Lee, Juliann Chmielecki, David G. Beer, et al. 2014. “Comprehensive Molecular Profiling of Lung Adenocarcinoma: The Cancer Genome Atlas Research Network.” *Nature* 511 (7511): 543–50. https://doi.org/10.1038/nature13385.

Davies, M. A., and Y. Samuels. 2010. “Analysis of the Genome to Personalize Therapy for Melanoma.” *Oncogene*. Nature Publishing Group. https://doi.org/10.1038/onc.2010.323.

Erdag, Gulsun, Jochen T. Schaefer, Mark E. Smolkin, Donna H. Deacon, Sofia M. Shea, Lynn T. Dengel, James W. Patterson, and Craig L. Slingluff. 2012. “Immunotype and Immunohistologic Characteristics of Tumor-Infiltrating Immune Cells Are Associated with Clinical Outcome in Metastatic Melanoma.” *Cancer Research* 72 (5): 1070–80. https://doi.org/10.1158/0008-5472.CAN-11-3218.

Fitzgerald, Jonathan B., Birgit Schoeberl, Ulrik B. Nielsen, and Peter K. Sorger. 2006. “Systems Biology and Combination Therapy in the Quest for Clinical Efficacy.” *Nature Chemical Biology*. Nature Publishing Group. https://doi.org/10.1038/nchembio817.

Gaillard, Hélène, Tatiana García-Muse, and Andrés Aguilera. 2015. “Replication Stress and Cancer.” *Nature Reviews Cancer*. Nature Publishing Group. https://doi.org/10.1038/nrc3916.

Gao, Jianjiong, Bülent Arman Aksoy, Ugur Dogrusoz, Gideon Dresdner, Benjamin Gross,

S. Onur Sumer, Yichao Sun, et al. 2013. “Integrative Analysis of Complex Cancer Genomics and Clinical Profiles Using the CBioPortal.” *Science Signaling* 6 (269): pl1–pl1. https://doi.org/10.1126/scisignal.2004088.

Garbe, Claus, and Thomas K. Eigentler. 2018. “Vemurafenib.” In *Recent Results in Cancer Research*, 211:77–89. Springer New York LLC. https://doi.org/10.1007/978-3-319-91442-8_6.

Glickman, Michael H., and Aaron Ciechanover. 2002. “The Ubiquitin-Proteasome Proteolytic Pathway: Destruction for the Sake of Construction.” *Physiological Reviews*. American Physiological Society. https://doi.org/10.1152/physrev.00027.2001.

Godbersen, J. Claire, Leigh Ann Humphries, Olga V. Danilova, Peter E. Kebbekus, Jennifer R. Brown, Alan Eastman, and Alexey V. Danilov. 2014. “The Nedd8-Activating Enzyme Inhibitor MLN4924 Thwarts Microenvironment- Driven NF-KB Activation and Induces Apoptosis in Chronic Lymphocytic Leukemia B Cells.” *Clinical Cancer Research* 20 (6): 1576–89. https://doi.org/10.1158/1078-0432.CCR-13-0987.

Goldinger, Simone M., Carla Murer, Pascale Stieger, and Reinhard Dummer. 2013. “Targeted Therapy in Melanoma - the Role of BRAF, RAS and KIT Mutations.” In *European Journal of Cancer, Supplement*, 11:92–96. https://doi.org/10.1016/j.ejcsup.2013.07.011.

Gu, Yanyan, Jonathan L. Kaufman, Leon Bernal, Claire Torre, Shannon M. Matulis, R.

Donald Harvey, Jing Chen, Shi Yong Sun, Lawrence H. Boise, and Sagar Lonial. 2014. “MLN4924, an NAE Inhibitor, Suppresses AKT and MTOR Signaling via Upregulation of REDD1 in Human Myeloma Cells.” *Blood* 123 (21): 3269–76. https://doi.org/10.1182/blood-2013-08-521914.

Hogan, Kevin T., Jennifer N. Sutton, Kyo U. Chu, Jennifer A.C. Busby, Jeffrey Shabanowitz, Donald F. Hunt, and Craig L. Slingluff. 2005. “Use of Selected Reaction Monitoring Mass Spectrometry for the Detection of Specific MHC Class I Peptide Antigens on A3 Supertype Family Members.” *Cancer Immunology, Immunotherapy* 54 (4): 359–71. https://doi.org/10.1007/s00262-004-0592-y.

Huntington, Jonathan T., Janiel M. Shields, Channing J. Der, Colby A. Wyatt, Ulrike Benbow, Craig L. Slingluff, and Constance E. Brinckerhoff. 2004. “Overexpression of Collagenase 1 (MMP-1) Is Mediated by the ERK Pathway in Invasive Melanoma Cells. Role of BRAF Mutation and Fibroblast Growth Factor Signaling.” *Journal of Biological Chemistry* 279 (32): 33168–76. https://doi.org/10.1074/jbc.M405102200.

Jin, Jianping, Emily E. Arias, Jing Chen, J. Wade Harper, and Johannes C. Walter. 2006. “A Family of Diverse Cul4-Ddb1-Interacting Proteins Includes Cdt2, Which Is Required for S Phase Destruction of the Replication Factor Cdt1.” *Molecular Cell* 23 (5): 709–21. https://doi.org/10.1016/j.molcel.2006.08.010.

Kittlesen, D J, L W Thompson, P H Gulden, J C Skipper, T A Colella, J Shabanowitz, D F Hunt, V H Engelhard, C L Slingluff, and J A Shabanowitz. 1998. “Human Melanoma Patients Recognize an HLA-A1-Restricted CTL Epitope from Tyrosinase Containing

Two Cysteine Residues: Implications for Tumor Vaccine Development." *Journal of Immunology (Baltimore, Md. : 1950)* 160 (5): 2099–2106. http://www.ncbi.nlm.nih.gov/pubmed/9498746.

Kobayashi, Hiroki, Shuhei Komatsu, Daisuke Ichikawa, Tsutomu Kawaguchi, Shoji Hirajima, Mahito Miyamae, Wataru Okajima, et al. 2015. "Overexpression of Denticleless E3 Ubiquitin Protein Ligase Homolog (DTL) Is Related to Poor Outcome in Gastric Carcinoma." *Oncotarget* 6 (34): 36615–24. https://doi.org/10.18632/oncotarget.5620.

Kuo, Alex J., Jikui Song, Peggie Cheung, Satoko Ishibe-Murakami, Sayumi Yamazoe, James K. Chen, Dinshaw J. Patel, and Or Gozani. 2012. "The BAH Domain of ORC1 Links H4K20me2 to DNA Replication Licensing and Meier-Gorlin Syndrome." *Nature* 484 (7392): 115–19. https://doi.org/10.1038/nature10956.

Li, Hua, Mingjia Tan, Lijun Jia, Dongping Wei, Yongchao Zhao, Guoan Chen, Jie Xu, et al. 2014. "Inactivation of SAG/RBX2 E3 Ubiquitin Ligase Suppresses KrasG12D-Driven Lung Tumorigenesis." *Journal of Clinical Investigation* 124 (2): 835–46. https://doi.org/10.1172/JCI70297.

Li, J., E. K.O. Ng, Y. P. Ng, C. Y.P. Wong, J. Yu, H. Jin, V. Y.Y. Cheng, et al. 2009. "Identification of Retinoic Acid-Regulated Nuclear Matrix-Associated Protein as a Novel Regulator of Gastric Cancer." *British Journal of Cancer* 101 (4): 691–98. https://doi.org/10.1038/sj.bjc.6605202.

Li, Lihui, Mingsong Wang, Guangyang Yu, Ping Chen, Hui Li, Dongping Wei, Ji Zhu, et

al. 2014. “Overactivated Neddylation Pathway as a Therapeutic Target in Lung Cancer.” https://doi.org/10.1093/jnci/dju083.

Lin, Jie Jessie, Michael A. Milhollen, Peter G. Smith, Usha Narayanan, and Anindya Dutta. 2010. “NEDD8-Targeting Drug MLN4924 Elicits DNA Rereplication by Stabilizing Cdt1 in S Phase, Triggering Checkpoint Activation, Apoptosis, and Senescence in Cancer Cells.” *Cancer Research* 70 (24): 10310–20. https://doi.org/10.1158/0008-5472.CAN-10-2062.

Liontos, Michalis, Marilena Koutsami, Maria Sideridou, Konstantinos Evangelou, Dimitris Kletsas, Brynn Levy, Athanassios Kotsinas, et al. 2007. “Deregulated Overexpression of HCdt1 and HCdc6 Promotes Malignant Behavior.” *Cancer Research* 67 (22): 10899–909. https://doi.org/10.1158/0008-5472.CAN-07-2837.

Machida, Yuichi J., and Anindya Dutta. 2007. “The APC/C Inhibitor, Emi1, Is Essential for Prevention of Rereplication.” *Genes and Development* 21 (2): 184–94. https://doi.org/10.1101/gad.1495007.

Mackintosh, C., J. L. Ordóñez, D. J. García-Domínguez, V. Sevillano, A. Llombart-Bosch, K. Szuhai, K. Scotlandi, et al. 2012. “1q Gain and CDT2 Overexpression Underlie an Aggressive and Highly Proliferative Form of Ewing Sarcoma.” *Oncogene* 31 (10): 1287–98. https://doi.org/10.1038/onc.2011.317.

McGarry, Thomas J., and Marc W. Kirschner. 1998. “Geminin, an Inhibitor of DNA Replication, Is Degraded during Mitosis.” *Cell* 93 (6): 1043–53. https://doi.org/10.1016/S0092-8674(00)81209-X.

Merlet, J., J. Burger, J. E. Gomes, and L. Pintard. 2009. “Regulation of Cullin-RING E3 Ubiquitin-Ligases by Neddylation and Dimerization.” *Cellular and Molecular Life Sciences*. https://doi.org/10.1007/s00018-009-8712-7.

Micco, Raffaella Di, Marzia Fumagalli, Angelo Cicalese, Sara Piccinin, Patrizia Gasparini, Chiara Luise, Catherine Schurra, et al. 2006. “Oncogene-Induced Senescence Is a DNA Damage Response Triggered by DNA Hyper-Replication.” *Nature* 444 (7119): 638–42. https://doi.org/10.1038/nature05327.

Milhollen, Michael A., Usha Narayanan, Teresa A. Soucy, Petter O. Veiby, Peter G. Smith, and Benjamin Amidon. 2011. “Inhibition of NEDD8-Activating Enzyme Induces Rereplication and Apoptosis in Human Tumor Cells Consistent with Deregulating CDT1 Turnover.” *Cancer Research* 71 (8): 3042–51. https://doi.org/10.1158/0008-5472.CAN-10-2122.

Milhollen, Michael A., Tary Traore, Jennifer Adams-Duffy, Michael P. Thomas, Allison J. Berger, Lenny Dang, Lawrence R. Dick, et al. 2010. “MLN4924, a NEDD8-Activating Enzyme Inhibitor, Is Active in Diffuse Large B-Cell Lymphoma Models: Rationale for Treatment of NF-KB-Dependent Lymphoma.” *Blood* 116 (9): 1515–23. https://doi.org/10.1182/blood-2010-03-272567.

Miller, Kimberly D., Leticia Nogueira, Angela B. Mariotto, Julia H. Rowland, K. Robin Yabroff, Catherine M. Alfano, Ahmedin Jemal, Joan L. Kramer, and Rebecca L. Siegel. 2019. “Cancer Treatment and Survivorship Statistics, 2019.” *CA: A Cancer Journal for Clinicians* 69 (5): 363–85. https://doi.org/10.3322/caac.21565.

Molhoek, Kerrington R., Heinrich Griesemann, Jianfen Shu, Jeffrey E. Gershenwald, David L. Brautigan, and Craig L. Slingluff. 2008. “Human Melanoma Cytolysis by Combined Inhibition of Mammalian Target of Rapamycin and Vascular Endothelial Growth Factor/Vascular Endothelial Growth Factor Receptor-2.” *Cancer Research* 68 (11): 4392–97. https://doi.org/10.1158/0008-5472.CAN-07-5844.

Moretti, Silvia, Adelina Spallanzani, Alessandra Chiarugi, Massimo Fabiani, and Cinzia Pinzi. 2001. “Correlation of Ki-67 Expression in Cutaneous Primary Melanoma with Prognosis in a Prospective Study: Different Correlation According to Thickness.” *Journal of the American Academy of Dermatology* 44 (2): 188–92. https://doi.org/10.1067/mjd.2001.110067.

Oda, Hisanobu, Michael R. Hübner, David B. Beck, Michiel Vermeulen, Jerard Hurwitz, David L. Spector, and Danny Reinberg. 2010. “Regulation of the Histone H4 Monomethylase PR-Set7 by CRL4Cdt2-Mediated PCNA-Dependent Degradation during DNA Damage.” *Molecular Cell* 40 (3): 364–76. https://doi.org/10.1016/j.molcel.2010.10.011.

Panagopoulos, Andreas, Stavros Taraviras, Hideo Nishitani, and Zoi Lygerou. 2020. “CRL4Cdt2: Coupling Genome Stability to Ubiquitination.” *Trends in Cell Biology*. Elsevier Ltd. https://doi.org/10.1016/j.tcb.2020.01.005.

PDQ Adult Treatment Editorial Board. 2002. *Melanoma Treatment (PDQ®): Health Professional Version*. *PDQ Cancer Information Summaries*. National Cancer Institute (US). http://www.ncbi.nlm.nih.gov/pubmed/26389469.

Poole, I. Caroline Le, Raymond E. Boissy, Rangaprasao Sarangarajan, Jing Chen, Judith J. Forristal, Pranav Sheth, Wiete Westerhof, George Babcock, Pranab K. Das, and Catharine B. Saelinger. 2000. "PIG3V, an Immortalized Human Vitiligo Melanocyte Cell Line, Expresses Dilated Endoplasmic Reticulum." *In Vitro Cellular & Developmental Biology - Animal 2000 36:5* 36 (5): 309–19. https://doi.org/10.1290/1071-2690(2000)036<0309:PAIHVM>2.0.CO;2.

Roller, Devin G., Brian Capaldo, Stefan Bekiranov, Aaron J. Mackey, Mark R. Conaway, Emanuel F. Petricoin, Daniel Gioeli, and Michael J. Weber. 2016. "Combinatorial Drug Screening and Molecular Profiling Reveal Diverse Mechanisms of Intrinsic and Adaptive Resistance to BRAF Inhibition in V600E BRAF Mutant Melanomas." *Oncotarget* 7 (3): 2734–53. https://doi.org/10.18632/oncotarget.6548.

Schotta, Gunnar, Roopsha Sengupta, Stefan Kubicek, Stephen Malin, Monika Kauer, Elsa Callén, Arkady Celeste, et al. 2008. "A Chromatin-Wide Transition to H4K20 Monomethylation Impairs Genome Integrity and Programmed DNA Rearrangements in the Mouse." *Genes and Development* 22 (15): 2048–61. https://doi.org/10.1101/gad.476008.

Senga, Takeshi, Umasundari Sivaprasad, Wenge Zhu, Jong Park Jong, Emily E. Arias, Johannes C. Walter, and Anindya Dutta. 2006. "PCNA Is a Cofactor for CDT1 Degradation by CUL4/DDB1-Mediated N-Terminal Ubiquitination." *Journal of Biological Chemistry* 281 (10): 6246–52. https://doi.org/10.1074/jbc.M512705200.

Slingluff, C L, A L Cox, R A Henderson, D F Hunt, and V H Engelhard. 1993.

"Recognition of Human Melanoma Cells by HLA-A2.1-Restricted Cytotoxic T Lymphocytes Is Mediated by at Least Six Shared Peptide Epitopes." *The Journal of Immunology* 150 (7): 2955–63.

Solus, Jason F., and Stefan Kraft. 2013. "Ras, Raf, and MAP Kinase in Melanoma." *Advances in Anatomic Pathology*. https://doi.org/10.1097/PAP.0b013e3182976c94.

Soucy, Teresa A., Peter G. Smith, Michael A. Milhollen, Allison J. Berger, James M. Gavin, Sharmila Adhikari, James E. Brownell, et al. 2009. "An Inhibitor of NEDD8-Activating Enzyme as a New Approach to Treat Cancer." *Nature* 458 (7239): 732–36. https://doi.org/10.1038/nature07884.

Talantov, Dmitri, Abhijit Mazumder, Jack X. Yu, Thomas Briggs, Yuqiu Jiang, John Backus, David Atkins, and Yixin Wang. 2005. "Novel Genes Associated with Malignant Melanoma but Not Benign Melanocytic Lesions." *Clinical Cancer Research* 11 (20): 7234–42. https://doi.org/10.1158/1078-0432.CCR-05-0683.

Tardat, Mathieu, Julien Brustel, Olivier Kirsh, Christine Lefevbre, Mary Callanan, Claude Sardet, and Eric Julien. 2010. "The Histone H4 Lys 20 Methyltransferase PR-Set7 Regulates Replication Origins in Mammalian Cells." *Nature Cell Biology* 12 (11): 1086–93. https://doi.org/10.1038/ncb2113.

Taylor, Barry S., Nikolaus Schultz, Haley Hieronymus, Anuradha Gopalan, Yonghong Xiao, Brett S. Carver, Vivek K. Arora, et al. 2010. "Integrative Genomic Profiling of Human Prostate Cancer." *Cancer Cell* 18 (1): 11–22. https://doi.org/10.1016/j.ccr.2010.05.026.

Truong, Lan N., and Xiaohua Wu. 2011. “Prevention of DNA Re-Replication in Eukaryotic Cells.” *Journal of Molecular Cell Biology* 3 (1): 13–22. https://doi.org/10.1093/JMCB/MJQ052.

Tsai, James, John T. Lee, Weiru Wang, Jiazhong Zhang, Hanna Cho, Shumeye Mamo, Ryan Bremer, et al. 2008. “Discovery of a Selective Inhibitor of Oncogenic B-Raf Kinase with Potent Antimelanoma Activity.” *Proceedings of the National Academy of Sciences of the United States of America* 105 (8): 3041–46. https://doi.org/10.1073/pnas.0711741105.

Tu, Zhigang, Katherine M. Aird, Benjamin G. Bitler, Jasmine P. Nicodemus, Neil Beeharry, Bing Xia, Tim J. Yen, and Rugang Zhang. 2011. “Oncogenic Ras Regulates BRIP1 Expression to Induce Dissociation of BRCA1 from Chromatin, Inhibit DNA Repair, and Promote Senescence.” *Developmental Cell* 21 (6): 1077–91. https://doi.org/10.1016/j.devcel.2011.10.010.

Ueki, T., T. Nishidate, J. H. Park, M. L. Lin, A. Shimo, K. Hirata, Y. Nakamura, and T. Katagiri. 2008. “Involvement of Elevated Expression of Multiple Cell-Cycle Regulator, DTL/RAMP (Denticleless/RA-Regulated Nuclear Matrix Associated Protein), in the Growth of Breast Cancer Cells.” *Oncogene* 27 (43): 5672–83. https://doi.org/10.1038/onc.2008.186.

Weinstein, John N., Rehan Akbani, Bradley M. Broom, Wenyi Wang, Roeland G.W. Verhaak, David McConkey, Seth Lerner, et al. 2014. “Comprehensive Molecular Characterization of Urothelial Bladder Carcinoma.” *Nature* 507 (7492): 315–22.

https://doi.org/10.1038/nature12965.

Yamshchikov, Galina, Lee Thompson, William G. Ross, Holly Galavotti, William Aquila, Donna Deacon, Jennifer Caldwell, James W. Patterson, Donald F. Hunt, and Craig L. Slingluff. 2001. “Analysis of a Natural Immune Response against Tumor Antigens in a Melanoma Survivor: Lessons Applicable to Clinical Trial Evaluations.” *Clinical Cancer Research* 7 (3): 909s-916s.

Yamshchikov, Galina V., David W. Mullins, Chien-Chung Chang, Takeshi Ogino, Lee Thompson, Jennifer Presley, Holly Galavotti, et al. 2005. “Sequential Immune Escape and Shifting of T Cell Responses in a Long-Term Survivor of Melanoma.” *The Journal of Immunology* 174 (11): 6863–71. https://doi.org/10.4049/jimmunol.174.11.6863.

VIII.

Chapter III:

The Neddylation Inhibitor MLN4924 Sensitizes Head and Neck Squamous Cell Carcinoma to Radiation Therapy

1. Abstract

The $CRL4^{CDT2}$ E3 ubiquitin ligase plays a crucial role in preserving genomic integrity and proper cell cycle progression. Through the timely ubiquitylation and proteolysis its substrates during S-phase, $CRL4^{CDT2}$ acts as a barrier against deregulated origin licensing, or rereplication, which is a cytotoxic phenomenon that results from the accumulation of aberrant replication intermediates and leads to DNA damage, chromosomal breakage, apoptosis, and even tumorigenesis. We demonstrate that CDT2, the substrate adaptor of the $CRL4^{CDT2}$ E3 ligase, is overexpressed in head and neck squamous cell carcinoma (HNSCC) and its expression is essential for cellular growth. Depletion of CDT2 suppresses proliferation and induces robust rereplication in human papilloma virus (HPV)-negative HNSCCs. We demonstrate that the treatment with MLN4924, a neddylation inhibitor that inhibits the activity of all Cullin-based E3 ligases including $CRL4^{CDT2}$, suppresses proliferation of HNSCC cells through the induction of robust rereplication *in vitro*. MLN4924 also suppresses HNSCC tumor growth in animal models. Importantly, we show that MLN4924 enhances the sensitivity of HNSCCs to ionizing radiation in vitro and in vivo. Rereplication induction as a result of $CRL4^{CDT2}$ inactivation or CDT1 activation was sufficient to confer radio-sensitivity in HNSCCs *in vitro*. These results highlight the efficacy of MLN4924 as a radio-sensitizing agent in HNSCC and that rereplication is a promising anti-tumor therapeutic strategy for radio-sensitization.

2. Introduction:

2.1. Head and Neck Squamous Cell Carcinoma (HNSCC): Current Therapies and Challenges:

Head and Neck Squamous Cell Carcinoma (HNSCC) represent the malignancy developed from the squamous epithelium to the upper aerodigestive track with tumors occurring in the larynx, pharynx, and oral cavity (Alterio et al. 2019; Arenz et al. 2014). While tobacco and alcohol consumption remain the most important risk factors for developing HNSCC, increasing evidence link HNSCC to infections with high-risk types of human papillomaviruses (HPVs), particularly HPV-16. HPV-positive HNSCCs express two viral oncogenes E6 and E7 that interact p53 and pRb promoting transformation of epithelial cells (Arenz et al. 2014). Metastatic or recurrent HNSCCs, irrespective of their HPV status, remain a clinical challenge, and despite five decades of advances in chemotherapy and radiation therapy, prognosis and treatment has not significantly improved (Sim, Leidner, and Bell 2019). The median overall survival rate is between 6 and 13 months for second and first-line chemotherapy respectively for patients with recurrent metastasis. Platinum doublet chemotherapy is the current standard of care, and the limited options of second-line therapeutics have a response rate of less than 13% and are associated with significant side effects. Most patients whose HNSCC tumors regress after chemotherapy do not experience a significant increase in longevity and most of them will succumb back to malignancy (Sim, Leidner, and Bell 2019).

Recent advent in immunotherapy, such as the approval of the anti-PD1 antibodies as a second line therapy for platinum-resistant recurrent metastatic HNSCC, demonstrate a

small but promising improvement in the response rate (to up to 20%) and patient overall survival (Ferris et al. 2016; Seiwert et al. 2016; Sim, Leidner, and Bell 2019). Radiotherapy, which is used in almost half of all cancer patients, remains one of the main treatments with curative-intent in HNSCC, and is often administered as an adjuvant therapy following surgery for HNSCC patients (Mladenov et al. 2013). Many HNSCC patients, however, experience unsatisfactory clinical outcome from radiation, where 50% of them experience localized recurrence within 3 years (Ferlay et al. 2015). For advanced stage HNSCC, current chemoradiation therapy, such as the delivery of 70 Gy over 6 to 7 weeks, is extremely intense and considered highly toxic to patients (Sim, Leidner, and Bell 2019). Even though radiotherapy is regarded as a crucial and promising treatment option for HNCC, a significant work remains to be done to develop new therapeutic approaches and effective novel radiosensitizers to increase local tumor control, decrease radiation-induced toxicity, and improve the response rate in HNSCC patients.

2.2. The protective role of $CRL4^{CDT2}$ against aberrant DNA replication:

Ubiquitin mediated proteolysis via the 26S proteasome is a tightly regulated process that oversees proper protein turnover and maintain genomic integrity and protein homeostasis (Glickman and Ciechanover 2002). The cullin RING E3 ubiquitin ligase ($CRL4^{CDT2}$) plays a pivotal role in ensuring proper DNA replication and cell cycle progression by the timely ubiquitylation and degradation of positive regulators of the initiation of DNA replication during S-phase (Abbas and Dutta 2011; Abbas, Keaton, and Dutta 2013). $CRL4^{CDT2}$ substrates include the licensing factor CDT1, the CDK inhibitor p21, and the monomethyl transferase SET8, all of which are essential for proper origin

licensing and DNA replication (Senga et al. 2006; Arias and Walter 2006; Abbas, Keaton, and Dutta 2013; Abbas and Dutta 2011). Failure to properly degrade $CRL4^{CDT2}$ substrates can lead to multiple rounds of erroneous replication re-initiation during the same cell division cycle which results in rereplication. The consequences of rereplication can be disastrous to the cell and results in various forms of genomic instabilities such as DNA breaks, collapsed replication forks, chromosomal breakage, senescence, apoptosis, and even tumorigenesis (Liontos et al. 2007; Bui and Li 2019; Truong and Wu 2011; Abbas, Keaton, and Dutta 2013).

Excessive origin licensing leading to robust rereplication can be triggered by the deregulation of the expression of licensing factors through the genetic inactivation of $CRL4^{CDT2}$ (by depletion of CDT2 by siRNA), CDT1 activation (by ectopic overexpression of CDT1 or knockdown of its inhibitor Geminin), activation of the APC/C^{CDC20} E3 ligase (by the knockdown of its inhibitor EMI1), or expression of catalytically-active non-degradable SET8 (Abbas, Keaton, and Dutta 2013; Jin et al. 2006; Benamar et al. 2016; Abbas and Dutta 2011). Rereplication can also be induced using the small molecule inhibitor MLN4924 (pevonedistat), which inhibits neddylation, a ubiquitination-like post translational modification required for the activity of Cullin-based E3 ligases including $CRL4^{CDT2}$ (Soucy et al. 2009; Merlet et al. 2009). The toxicity exhibited by MLN4924, which is in multiple ongoing clinical trials, in many cancer systems *in vitro* and *in vivo* and its efficacy against recurrent tumors, such as vemurafenib-resistant melanoma, renders this inhibitor an attractive anti-cancer therapeutic strategy in HNSCC (Soucy et al. 2009; Lin et al. 2010; Benamar et al. 2016). In this Chapter, we show that CDT2 is overexpressed in

HNSCC and its knockdown results in robust rereplication and suppression of cell proliferation. We also demonstrate that the induction of rereplication through $CRL4^{CDT2}$ inactivation or treatment with MLN4924 radio-sensitizes HNSCC in vitro and in mouse models of HNSCC.

3. Results & Discussion:

3.1. CDT2 Expression is elevated in HNSCC:

We have previously shown in Chapter II that CDT2 expression is elevated in melanoma, and other human malignancies including breast cancer, human gastric cancer, Ewing carcinoma, and aggressive hepatocellular carcinoma (J. Li et al. 2009; Benamar et al. 2016; Ueki et al. 2008; Pan et al. 2006; Mackintosh et al. 2012). Examining a publicly available database that analyzed the RNA expression profile from various head and neck tissues, we found that CDT2 expression was elevated in nasopharyngeal and oropharyngeal carcinomas (5.5- and 4.5-fold) compared to nasopharynx and cervix uteri/oral cavity respectively (Fig. 3.1A-B) (Pyeon et al. 2007; Ginos et al. 2004; Sengupta et al. 2006; Peng et al. 2011). Using the datasets described above, we found that CDT2 expression is also elevated in additional HNSCC including oral cavity, tonsillar, and floor of the mouth carcinomas (Data not shown). Unlike melanoma and gastric cancer, after examining two RNA-seq datasets available at The Cancer Genome Atlas (TCGA), we were unable to find a statistically significant correlation between CDT2 mRNA expression and the overall or disease-free patient survival (Fig. 3.1C-D). Therefore, CDT2 is overexpressed in HNSCC and its elevated expression is not predictive of patient outcome.

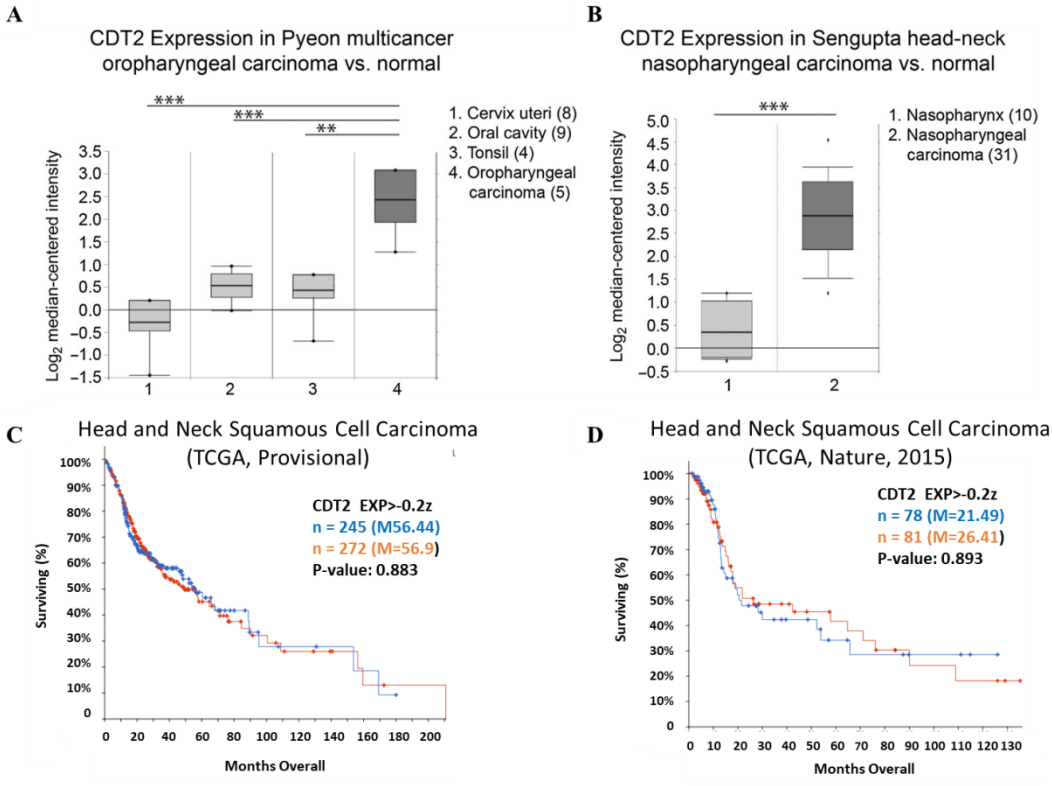
A
CDT2 Expression in Pyeon multicancer oropharyngeal carcinoma vs. normal
***
***
**
1. Cervix uteri (8)
2. Oral cavity (9)
3. Tonsil (4)
4. Oropharyngeal carcinoma (5)
Log2 median-centered intensity
B
CDT2 Expression in Sengupta head-neck nasopharyngeal carcinoma vs. normal
***
1. Nasopharynx (10)
2. Nasopharyngeal carcinoma (31)
Log2 median-centered intensity
C
Head and Neck Squamous Cell Carcinoma (TCGA, Provisional)
CDT2 EXP>-0.2z
n = 245 (M56.44)
n = 272 (M=56.9)
P-value: 0.883
Surviving (%)
Months Overall
D
Head and Neck Squamous Cell Carcinoma (TCGA, Nature, 2015)
CDT2 EXP>-0.2z
n = 78 (M=21.49)
n = 81 (M=26.41)
P-value: 0.893
Surviving (%)
Months Overall

Figure 3.1: CDT2 Expression is elevated in HNSCC and does not correlate with patient outcome

A-B. Box plot showing the mRNA expression of CDT2 in (**A**) oropharyngeal carcinoma compared to benign cervix uteri, oral cavity, and tonsil, and in (**B**) Nasopharyngeal carcinoma compared to nasopharynx. Data collected from publicly available Oncomine databases (Pyeon et al. 2007; Ginos et al. 2004; Sengupta et al. 2006; Peng et al. 2011)

C-D. Survival curves showing the lack of correlation between HNSCC patient outcome and CDT2 expression stratified by CDT2 mean expression. **C** and **D** represent two separate datasets. M: median survival (months), N= sample size (number of patients), EXP: mRNA expression of CDT2 cutoff.

Error bars represent three independent experiments +/- SD.
P-values are calculated using student t-test. * = $p < 0.05$; ** = $p < 0.01$. *** = $p < 0.001$; ns, not significant.

3.2. CDT2 is essential for HNSCC cell proliferation and prevention of rereplication.

CDT2, the substrate adaptor of the $CRL4^{CDT2}$ E3 ligase, is required to maintain proper S-phase progression (Abbas, Keaton, and Dutta 2013; Jin et al. 2006). We have previously demonstrated that CDT2 is required for the proper growth of melanoma cells. To test whether CDT2 is essential in HNSCC, we depleted CDT2 by siRNA in two HPV-negative HNSCC cell lines: Cal27 and FaDu. Both cell lines contain some of the most common mutations in HNSCC such as p53, p16, and NOTCH2/3 receptors (Stransky et al. 2011; Agrawal et al. 2011; Nichols et al. 2012). Depletion of CDT2 by siRNA significantly suppressed cell proliferation and colony formation in both Cal27 and FaDu (Fig 3.2A-B). This growth suppression was accompanied with a stabilization of the $CRL4^{CDT2}$ substrates p21 and SET8, but not CDT1 (Fig 3.2C). The absence of CDT1 stabilization post $CRL4^{CDT2}$ inactivation could be due to the activity of SCF^{SKP2} E3 ligase (Liu et al. 2004; X. Li et al. 2003; Nishitani et al. 2006). Inhibition of proliferation in CDT2-depleted cells was also accompanied with the expected increase in DNA damage (γH2AX) and checkpoint markers (phosphorylation of CHK1 and CHK2) consistent with the role CDT2 plays in genome preservation (Fig 3.2C).

Flow cytometry analysis with Propidium Iodide (PI) staining shows that depletion of CDT2 in Cal27 and FaDu induced robust rereplication in both cell lines (55.7% and 43.9% respectively) (Fig. 3.2D). Neither senescence (β-galactosidase assay) nor significant apoptosis (percentage of sub G1 or cleaved PARP) was detected after CDT2 depletion in both cell lines (Data not shown). The absence of senescence could be explained by the fact that both cell lines lack of p16 expression, which has been shown to be associated with rereplication-induced senescence (Benamar et al. 2016). These results demonstrate that CDT2 is essential for HNSCC proliferation and the prevention of erroneous DNA rereplication.

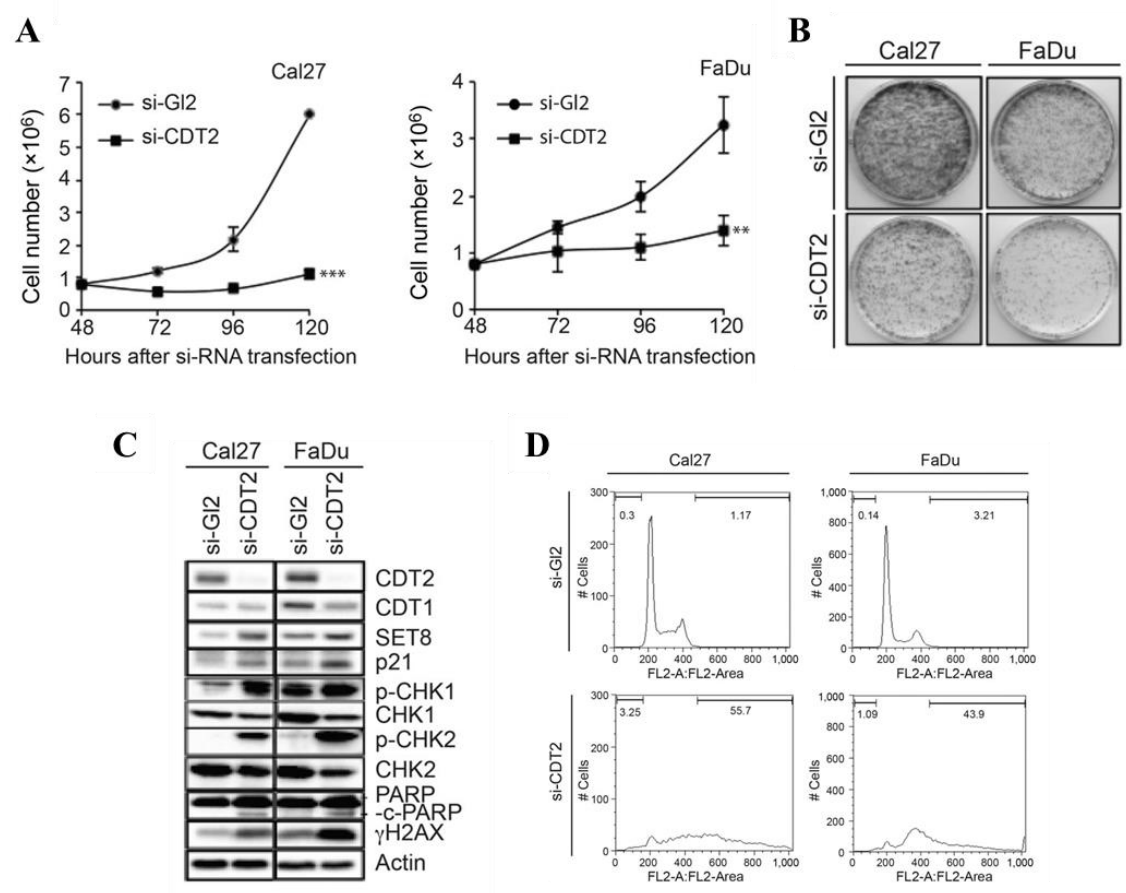

Figure 3.2: CDT2 is essential for HNSCC cell proliferation and prevention of rereplication.

A. Growth curve showing the impact of silencing CDT2 by siRNA on cell proliferation of Cal27 and FaDu. Counting starts at 48 hours post transfection.

B. Representative images of colony formation assay of Cal27 and FaDu after transfection with siGl2 (control) or siCDT2.

C. Immunoblot showing the protein expression levels pf the indicated markers 48 hours after silencing CDT2 by siRNA in Cal27 and FaDu.

D. Flow cytometry profiles of Cal27 and FaDu transfected with siCDT2 or siGl2 (control) then stained with PI 72 hours post transfection.

Error bars represent three independent experiments +/- SD.
P values are calculated using student's *t*-test. * = $p < 0.05$; ** = $p < 0.01$. *** = $p < 0.001$; ns, not significant.

3.3. MLN4924 promotes rereplication in HNSCC suppressing cell proliferation

$CRL4^{CDT2}$ plays a pivotal role in preserving genomic integrity by preventing excessive origin relicensing that leads to rereplication (Abbas and Dutta 2011). All cullin-based E3 ligases, including $CRL4^{CDT2}$, require a post translational modification termed neddylation for their activation. MLN4924 is a small molecular inhibitor that interrupts the neddylation process by binding to the Neddylation Activating Enzyme 1 (NAE1), which as a result prevents the activation of all cullin-based E3 ligases (Soucy et al. 2009). We have shown in Chapter II that MLN4924 induces rereplication in melanoma and various cancer cells, and its growth suppression and rereplication toxicity are dependent on the stabilization of the $CRL4^{CDT2}$ substrates SET8 and p21 (Benamar et al. 2016; Soucy, Smith, and Rolfe 2009). We tested if MLN4924 can suppress HNSCC growth through the induction of rereplication and senescence. Similar to CDT2 depletion, treatment with MLN4924 suppressed cell proliferation and colony formation in Cal27 and FaDu in a dose- and time-dependent manner (Fig 3.3A-B). While both cell lines Cal27 and FaDu underwent significant rereplication as early as 24 hours (and reached 61% and 60.4% respectively 72 hours post 80nmol/L), we observed less than 10% of sub G1 population, indicative of apoptotic cells, in Cal27 whereas little to no apoptosis was detected in FaDu 72 hours after treatment (Fig 3.3C-D). Inhibition of cullin neddylation was observed in both cell lines as early as 3 hours after treatment. CDT1 and SET8 were rapidly stabilized after treatment with 100 nM MLN4924but returned to their steady state levels by 24 hours, unlike p21 which persisted longer (Fig. 3.3E-F). Similar to CDT2 depletion, MLN4924 resulted in an increase in DNA damage (γH2AX) and the activation of cell cycle

checkpoints (increase in the phosphorylation of CHK1 and CHK2) as early as 24 hours (Fig. 3.3E-F).

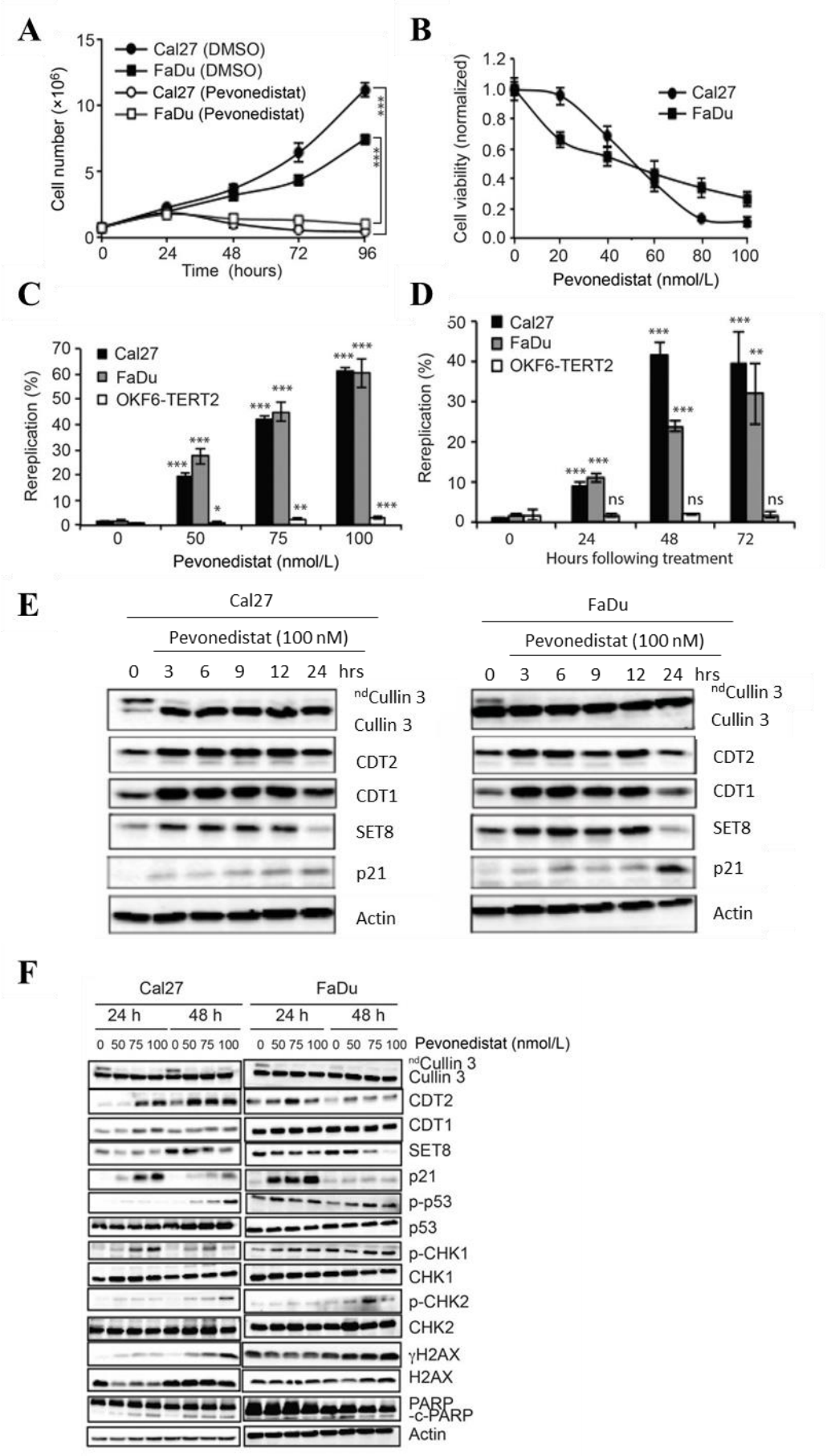
A
Cal27 (DMSO)
FaDu (DMSO)
Cal27 (Pevonedistat)
FaDu (Pevonedistat)
Cell number (×10⁶)
Time (hours)
B
Cal27
FaDu
Cell viability (normalized)
Pevonedistat (nmol/L)
C
Cal27
FaDu
OKF6-TERT2
Rereplication (%)
Pevonedistat (nmol/L)
D
Cal27
FaDu
OKF6-TERT2
Rereplication (%)
Hours following treatment
E
Cal27
Pevonedistat (100 nM)
0 3 6 9 12 24 hrs
FaDu
Pevonedistat (100 nM)
0 3 6 9 12 24 hrs
ndCullin 3
Cullin 3
CDT2
CDT1
SET8
p21
Actin
F
Cal27
FaDu
24 h
48 h
0 50 75 100 0 50 75 100 0 50 75 100 0 50 75 100 Pevonedistat (nmol/L)
ndCullin 3
Cullin 3
CDT2
CDT1
SET8
p21
p-p53
p53
p-CHK1
CHK1
p-CHK2
CHK2
γH2AX
H2AX
PARP
-c-PARP
Actin

Figure 3.3: MLN4924 promotes rereplication in HNSCC suppressing cell proliferation.

A-B. Growth curve showing the impact of MLN4924 treatment on cell proliferation (**A**) and colony formation (**B**) of Cal27 and FaDu cell lines. **A**. MLN4924 administered on Day 0 at (80 nmol/L). **B**. MLN4924 administered at the indicated doses for 12 days before staining.

C-D. Histogram showing the dose dependent (**C**) and time dependent (**D**) increase in rereplication induction in Cal27, FaDu, and immortalized keratinocytes.

E-F. Immunoblots of protein lysates extracted from Cal27 and FaDu at the indicated times and doses. Actin: loading control. nd Cullin: Neddylated cullins.

Error bars represent three independent experiments +/- SD.
P values are calculated using student's *t*-test. * = $p < 0.05$; ** = $p < 0.01$. *** = $p < 0.001$; ns, not significant.

3.4. MLN4924 sensitizes HNSCC cells to IR *in vitro and in vivo*

HNCSS tumors symptoms are known to emerge very late, therefore they are often diagnosed at an advanced stage further complicating the course of treatment (Kotowski et al. 2011). With HPV-negative HNSCC tumors are notoriously known for the low response to radiotherapy, it is critical to identify additional radiosensitizers that increase radiation efficacy in HPV-negatives, and decrease the adverse side effect that results from the need to administer high radiation doses (Kimple et al. 2013; Arenz et al. 2014; Kotowski et al. 2011). Given their sensitivity to MLN4924, we sought to examine if the neddylation inhibitor can sensitize HPV-negative cells (Cal27 and FaDu) to radiation. Using clonogenic survival assays, we confirmed that both Cal27 and FaDu are very resistant to ionizing radiation *in vitro*, demonstrated by their relatively high surviving fraction even at 9 Gy. Then pretreatment of both cell lines with MLN4924 before irradiation shows a statistically significant dose-dependent enhancement in toxicity (Fig 3.4A-B). The sensitivity enhancement ratio (SER), measured at 10% survival following MLN4924 treatment in Cal27 (80nmol/L) and FaDu (60nmol/L) was 2.99 and 1.49 respectively (Fig 3.4A-B). Additional HPV-negative HNSCCs, such as UNC7 and SCC25, were also radio-sensitized by MLN4924 treatment 24 hours before irradiation (Data not shown). These results demonstrate that treatment with MLN4924 was sufficient to radio-sensitize radioresistant HPV-negative HNSCC cell lines *in vitro*

MLN4924 has been shown to sensitize breast cancer cells to radiation via a radiation-induced p21-mediated G2/M arrest (Yang et al. 2012). Similarly, MLN4924 radio-sensitized colorectal cancer cells, which was attributed to the radiation-induced p27-

mediated G2/M arrest (Wan et al. 2016). In addition to G2/M arrest, radio-sensitization by MLN4924 in pancreatic cancer was also attributed to rereplication and the induction of apoptosis (Wei et al. 2012). To examine the mechanism that underlies the MLN4924-induced radio-sensitivity in HNSCC, we found that exposure to IR (2 or 4 Gy) significantly enhanced the rereplication induced after MLN4924 treatment, compared to individual treatments with IR or the drug (Fig. 4D-E). While 40nmol/L of MLN4924 induced 16.8% and 21.6% rereplication in Cal27 and FaDu, exposure to 2Gy 24 hours post drug treatment enhanced the rereplication extent to 32.9% and 42.2% respectively (Fig. 3.4C and data not shown). Biochemical analysis of protein expression from Cal27 lysates did not show a considerable upregulation of p21 in the treatment combination compared to MLN4924 or radiation alone, but it did a small but reproducible increase in γH2AX, suggesting the accumulation of DNA damage (Fig. 3.4D). These results suggest that radiation-induced disruption of cell cycle progression and genomic instability is further enhanced after exposure to MLN4924, this synergistic lethality is manifested in the increase of MLN4924-induced DNA rereplication *in vitro*.

To examine if the observed radio-sensitivity can be achieved *in vivo*, we established xenografts of Cal27 cell line in immune-compromised mice and monitored the tumor growth. As soon as the tumor reaches a minimum volume of 100 mm^3, we created four randomized group of 8 mice each. First group was treated with MLN4924 (20 mg/Kg) on a schedule of two cycles of 5 IP injections daily separated by 5 days of no treatment. The second group received localized radiation (1 Gy) on a daily basis. The third group received both treatments following the indicated schedules, while the fourth control group

was treated with DMSO. Consistent with our in vitro data, while each individual treatment inhibited tumor growth, the combined treatment resulted in a more significant suppression than each treatment alone (Fig. 3.4E). It is important to note that despite the efficacy of each treatment, neither MLN4924, radiation, or the combination results in tumor regression, at least up until the experiment was terminated at 32 days post the initial treatment. These results demonstrate that MLN4924 enhances radiation sensitivity in HNSCC *in vitro* and *in vivo*.

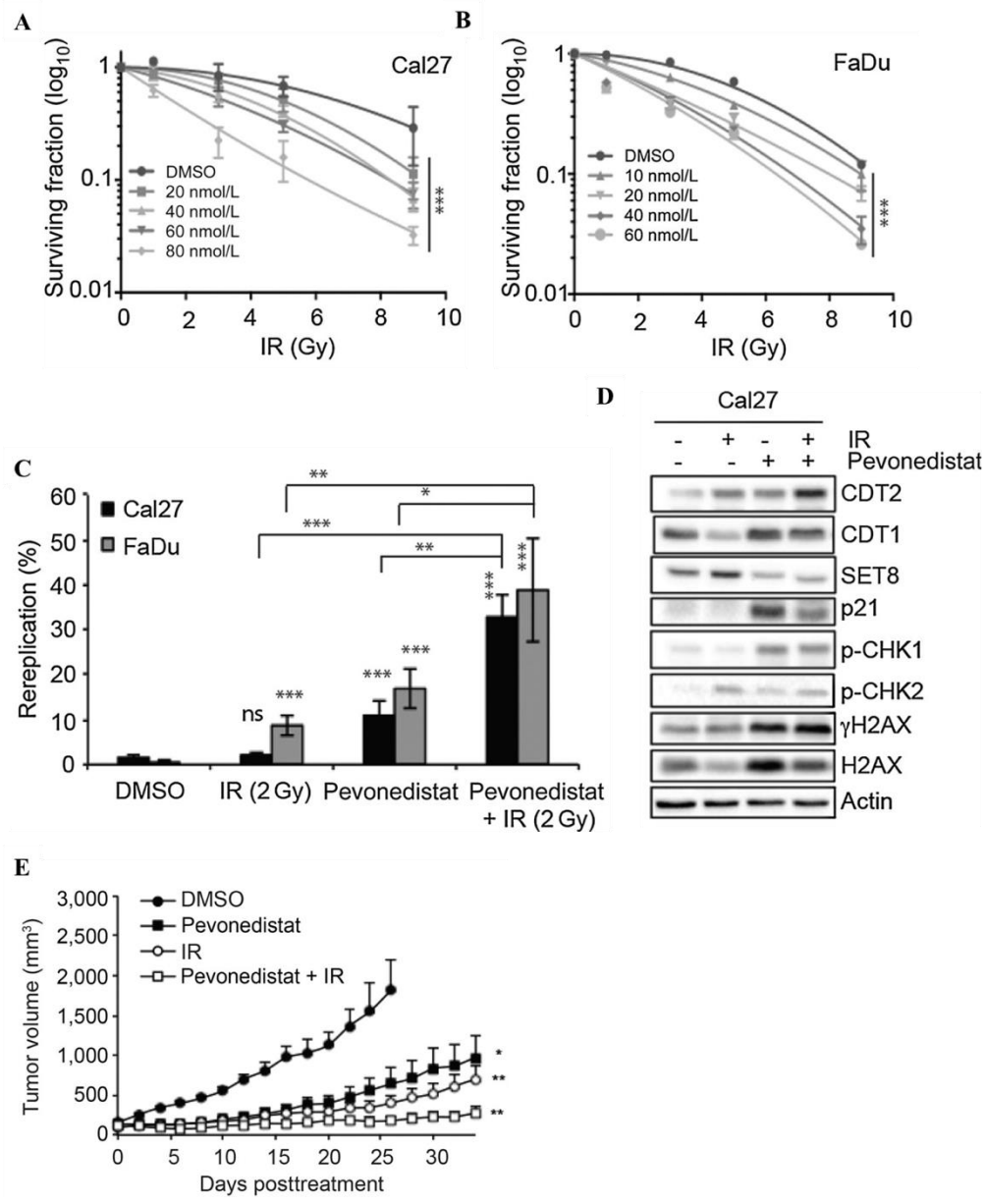
A
Cal27
Surviving fraction (log10)
DMSO
20 nmol/L
40 nmol/L
60 nmol/L
80 nmol/L
***
IR (Gy)
B
FaDu
DMSO
10 nmol/L
20 nmol/L
40 nmol/L
60 nmol/L
***
IR (Gy)
C
Cal27
FaDu
Rereplication (%)
**
*
***
**
***
***
***
***
ns
***
DMSO
IR (2 Gy)
Pevonedistat
Pevonedistat + IR (2 Gy)
D
Cal27
IR
Pevonedistat
CDT2
CDT1
SET8
p21
p-CHK1
p-CHK2
γH2AX
H2AX
Actin
E
Tumor volume (mm3)
DMSO
Pevonedistat
IR
Pevonedistat + IR
*
**
**
Days posttreatment

Figure 3.4: MLN4924 sensitizes HNSCC cells to IR in vitro and in vivo

A-B. Graph showing the dose dependent effect of the combination of MLN4924 and ionizing radiation at the indicated doses on colony formation in Cal27 (**A**) and FaDu (**B**). MLN4924 was administered 24 hours before irradiation.

C. Histogram showing the extent of rereplication in cells treated with MLN4924 (80 nmol/L) and/or irradiation (2Gy) in Cal27 and FaDu. MLN4924 was administered 24 hours before IR exposure.

D. Immunoblotting analysis of protein extract of Cal27 cells treated with IR (2Gy) and MLN4924 (80 nmol/L).

E. Graph showing tumor growth in response to the indicated treatments MLN4924 (20mg/Kg) and IR (1 Gy) following the treatment schedule detailed in the Materials and Methods. Mean tumor volumes ± SEM are shown. $n = 8$ mice per group.

Error bars represent three independent experiments +/- SD.
P-values are calculated using student's *t*-test. * = $p < 0.05$; ** = $p < 0.01$. *** = $p < 0.001$; ns, not significant.

3.5. Induction of rereplication is sufficient to confer radiation sensitivity in HNSCC

We have shown that exposure to ionizing radiation enhances MLN4924-induced rereplication in both Cal27 and FaDu. To further examine if rereplication is the primary mechanism of MLN4924-enhanced radiation sensitivity and is sufficient to confer radio-sensitivity in HNSCC, we irradiated Cal27 and FaDu cells 72 hours after inactivation of $CRL4^{CDT2}$ by si-CDT2 and assessed the clonogenic survival. As expected, silencing CDT2 enhanced radiation sensitivity in Cal27, and to a lesser extent in FaDu (Fig. 3.5A). siCDT2-induced rereplication was significantly enhanced (SER = 1.34) in the combined treatment in both cell lines (Fig. 3.5D). In addition, DNA damage (γH2AX) and checkpoint activation (phosphorylation of CHK1 and CHK2) were enhanced in the combined treatment (Fig. 3.5G). These results demonstrate that rereplication induced after $CRL4^{CDT2}$ inactivation, by CDT2 depletion or MLN4924 treatment) is sufficient to confer radio-sensitivity in HNSCCs.

Given that $CRL4^{CDT2}$ is a pivotal in preserving genomic instability by acting as a barrier against rereplication, we asked if rereplication can still confer radio-sensitivity in HNSCC cells with intact $CRL4^{CDT2}$ activity. To address that, we induced rereplication by silencing either the CDT1 inhibitor geminin or the APC/C ubiquitin ligase inhibitor EMI1. The depletion of each factor individually has been shown to be sufficient to induce robust rereplication in many cancer cells. Silencing of either Geminin or EMI1 prior to IR exposure greatly enhanced radiation sensitivity in Cal27 and FaDu (Fig. 3.5B-C). Similar to what we observed after $CRL4^{CDT2}$ inactivation, depletion of geminin or EMI1 greatly enhanced the rereplication induction in the combination treatment, as well as increasing

DNA damage and checkpoint activation (Fig. 3.5E-F, H-I). These results altogether demonstrate that exposure to low doses of ionizing radiation greatly enhances rereplication induction by various agents, and rereplication is sufficient to confer radio-sensitivity in HNSCC.

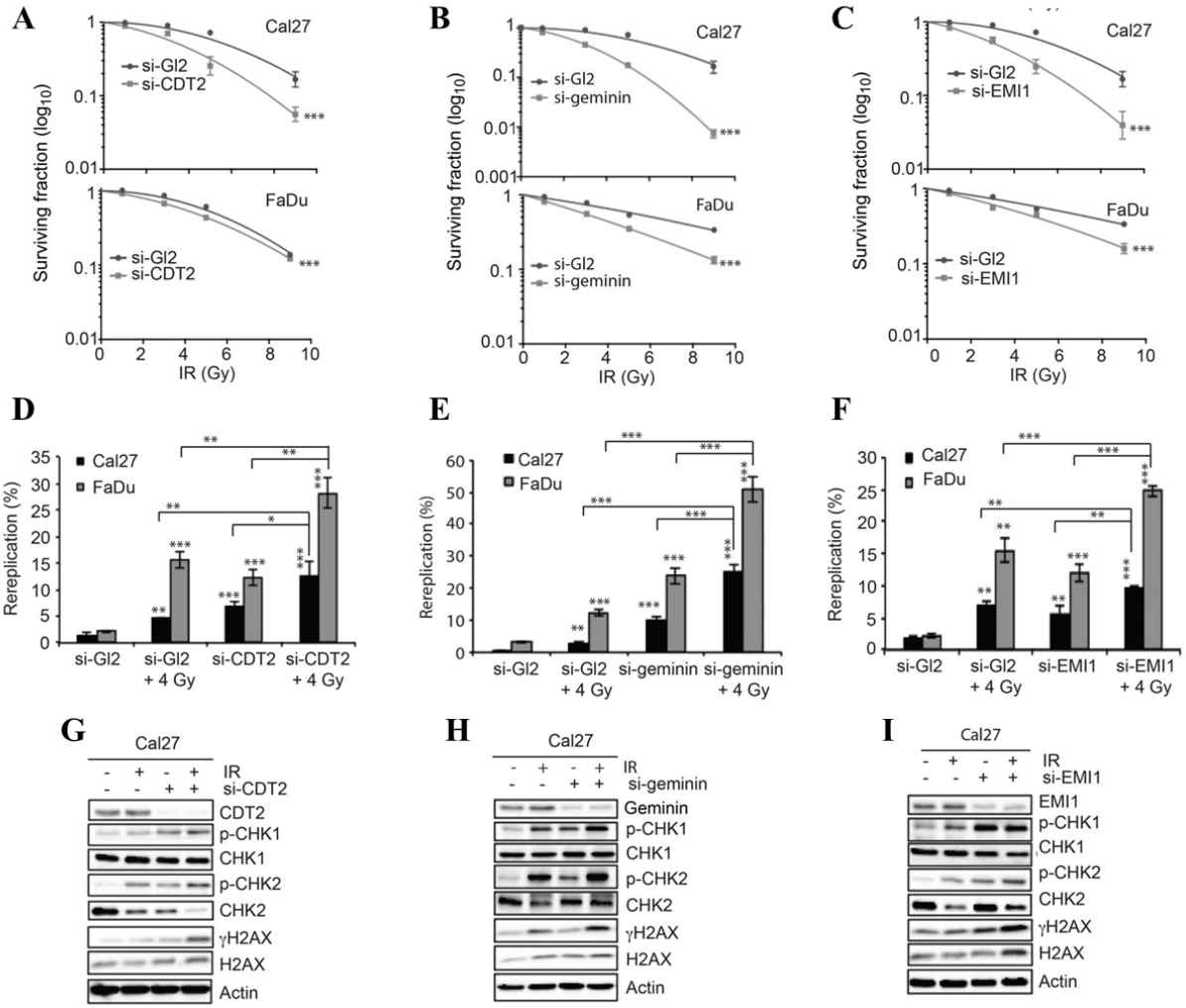
A
Cal27
si-Gl2
si-CDT2
FaDu
Surviving fraction (log10)
IR (Gy)
B
Cal27
si-Gl2
si-geminin
FaDu
C
Cal27
si-Gl2
si-EMI1
FaDu
D
Cal27
FaDu
Rereplication (%)
si-Gl2
si-Gl2 + 4 Gy
si-CDT2
si-CDT2 + 4 Gy
E
si-geminin
si-geminin + 4 Gy
F
si-EMI1
si-EMI1 + 4 Gy
G
Cal27
IR
si-CDT2
CDT2
p-CHK1
CHK1
p-CHK2
CHK2
γH2AX
H2AX
Actin
H
si-geminin
Geminin
I
si-EMI1
EMI1

Figure 3.5: Induction of rereplication is sufficient to confer radiation sensitivity in HNSCC

A-C. Survival curves showing the impact of transient silencing of the indicated proteins on the sensitivity to irradiation from a clonogenic assay on Cal27 and FaDu. Cells were exposed to IR 48 hours after transfection with siCDT2 (A), siGeminin (B), or siEMI1 (C).

D-E. Histograms showing the impact of transient silencing of the indicated proteins rereplication induction. Cells were irradiated at 4Gy 48 hours post transfection with siCDT2 (D), siGeminin (E), or siEMI1 (F), then harvested 48 hours later, stained with PI then analyzed by flow cytometry.

G-H. Immunoblot of Cal27 lysate extracted 6 hours after irradiation with 4 Gy, which was done 48 hours post transfection with siCDT2 (G), siGeminin (H), or siEMI1 (I). Actin used as a loading control.

Error bars represent three independent experiments +/- SD.
P-values are calculated using student's *t*-test. * = $p < 0.05$; ** = $p < 0.01$. *** = $p < 0.001$; ns, not significant.

4. Materials and Methods:

4.1. Tissue culture and reagents

Cal27, FaDu, and SCC25 HNSCC cells were obtained from the ATCC in 2012. UNC7 cells were provided by Dr. Wendell Yarbrough (Vanderbilt University, Nashville, TN) in 2013. Cells were grown in DMEM/Ham's nutrient mixture F12 supplemented with 10% FBS and 1% penicillin/streptomycin. OKF6-TERT2 cells were purchased from Dr. James Rhienwald at Harvard Medical School (Department of Dermatology, Boston, MA) in 2013 and were cultured in GIBCO keratinocyte serum-free medium, supplemented with 25 μg/mL BPE, 0.4 mmol/L $CaCl_2$, 0.2 ng/mL EGF, and 1% penicillin/streptomycin. All cell lines were maintained under 37°C in 5% CO_2 and were regularly tested for mycoplasma contamination using MycoAlert (Lonza). Cells were authenticated on the basis of growth and morphologic characteristics as well as by DNA fingerprinting (University of Arizona, Tucson, AZ). MLN4924 was purchased from Active Biochem and was dissolved in 10% DMSO in sterile PBS. Propidium iodide, 7-AAD, and BrdU Kit were purchased from BD Biosciences. Antibodies against p21 (C19), p53 (DO-1), geminin (FL-209), and actin (I-19) were purchased from Santa Cruz Biotechnology. Antibodies against SET8, CHK1, CHK2, γH2AX, p-CHK1 (S375), p-CHK2 (T68), p-p53 (S15), and PARP were purchased from Cell Signaling Technology. Anti-Cul3 antibody was purchased from Bethyl Laboratories. Anti-EMI1 antibody was purchased from Life Technologies. Anti-CDT1 and anti-CDT2 antibodies were described before (Abbas et al. 2010).

4.2. Cell lysis, SDS-PAGE, and immunoblotting

HNSCC cells were lysed using RIPA lysis buffer (50 mmol/L Tris, pH 8.0, 150 mmol/L NaCl, 1% NP-40, 0.5% sodium deoxycolate, 0.1% SDS, 1 mmol/L benzamidine-HCl, 0.5 μg/mL leupeptin, 0.5 μg/mL aprotinin, 1 μg/mL pepstatin, 20 mmol/L NaF, 20 mmol/L Na_3VO_4). Equal amounts of protein were electrophoretically separated in a polyacrylamide 8% to 12% gel (Bio-Rad), transblotted to a nitrocellulose membrane, and incubated with primary antibodies for 1 hour at room temperature or overnight at 4°C. The immunoblot signals were detected by enhanced chemiluminescence (EMD Millipore).

4.3. siRNA-mediated gene silencing

Transfections of different siRNAs (10 nmol/L) were performed using lipofectamine RNAimax according to the manufacturer's protocol (Invitrogen). The following siRNAs (sense strands) were used: si-GL2: 5′-AACGUACGCGGAAUACUUCGA-3′; si-CDT2: 5′-GAAUUAUACUGCUUAUCGA-3′; si-geminin: 5′-UGCCAACUCUGGAAUCAAA-3′. si-EMI1: 5′-CGAAGUGUCUCUGUAAUUA-3′.

4.4. Cell proliferation and clonogenic survival assays

HNSCC cells were transfected with siRNA (48 hours prior to first count) or treated with MLN4924 (24 hours prior to first count). Cells (8×10^5) were seeded in 60-mm plates, and cell proliferation was determined by staining with trypan blue and counting by Countess Automated Cell Counter (Invitrogen). Depending on the cell growth rate, cell counts were recorded either every 24 or 48 hours, and growth curves were established. The effect of MLN4924 treatment or transient silencing of CDT2, geminin, or EMI1 on cell proliferation or on radiation sensitivity was tested using clonogenic survival assays. Cells

were transfected with the appropriate siRNA 48 hours prior to seeding. Cells were then counted using Countess Automated Cell Counter and were seeded at 15,000 cells per plate in 60-mm dishes. Twenty-four hours after seeding, cells were irradiated with various doses and were cultured for 7 to 10 days. Once colonies reached the appropriate size (>50 cells each), they were washed twice with cold PBS, fixed in cold 100% methanol for 10 minutes, and stained with crystal violet (0.5%) for 10 minutes. The plates were washed, dried, and imaged using Image Lab software (Bio-Rad). QuantityOne software (Bio-Rad) was used to quantify the number of colonies, and survival curves were established on the basis of the linear quadratic model, using the formula $S = e^{-\alpha D-\beta D2}$, where S represents the surviving fraction and D the dose of irradiation. Results are represented as mean ± SD of three independent experiments normalized to the corresponding nonirradiated plates for each group. When the effect of MLN4924 on cell radio-sensitivity was tested, cells were seeded at 15,000 cells per 60-mm plate and allowed to adhere for 4 to 6 hours. MLN4924 was then added upon cell adherence at varying concentrations, and cells were irradiated the following day. The duration of the experiment and the stopping procedure were as described above.

4.5. Flow cytometry analysis

The effect of MLN4924 treatment or CDT2, geminin, or EMI1 knockdown on the cell cycle (and induction of DNA rereplication) was assessed by flow cytometry with propidium iodide (PI) staining. Cells were harvested at 72 or 96 hours posttreatment with MLN4924 or post-transfection, respectively. Cells were collected, washed with PBS, and resuspended in ethanol (75%). Cells were subsequently treated with 20 μg of DNase-free

RNase and stained with PI following the manufacturer's protocol. FACScan (Becton Dickinson) was used to analyze the samples, and G_0–G_1, S, and G_2–M fractions were segmented. Subsequent analysis using FlowJo and ModFit softwares was used to determine apoptotic and rereplicating fractions. Where indicated, Cal27 and FaDu cells were treated with MLN4924 for 48 hours and pulsed with bromodeoxyuridine (BrdU; 10 nmol/L) for 1 hour in the dark prior to harvesting. Cells were washed with PBS and staining solution before fixation and permeabilization steps according to the manufacturer's protocol. Cells were subsequently stained with anti-BrdU antibody solution for 20 minutes at room temperature, washed, and stained with 7-AAD for 30 minutes at 4°C. Cells were resuspended in 1 mL of staining buffer and stored at 4°C overnight before analysis. Sampled were analyzed on a FACScan (Becton Dickinson), and different fractions of BrdU-positive cells were determined using FlowJo and ModFit softwares.

4.6. In vivo xenograft mice experiments

The animal studies were conducted in accordance with the guidelines established by the University of Virginia Animal Care and Use Committee. The effect of MLN4924 on tumor growth was tested in a flank HNSCC xenograft model. Four- to 5-week-old Foxn1^{nu} athymic female nude immunodeficient mice (20–25 g bodyweight; Harlan Laboratories) were used in this study. MLN4924 was prepared in 10% DMSO containing PBS and filtered before use. Cal27 cells (5×10^6; suspended in 200 μL sterile PBS) were inoculated subcutaneously in both flanks of nude mice (8 mice/group). When the tumor size reached 100 mm^3 (10 days post-inoculation), mice were randomized and were treated

with MLN4924 (20 mg/kg) or with control vehicle (DMSO), administered intraperitoneally on a regimen of 5 days on/5 days off for 2 cycles. Tumors from a third group of mice were exposed to 1 Gy IR daily, 5 days per week for 3 weeks, and a fourth group of mice received both MLN4924 and IR treatments. Tumor irradiation was performed at the University of Virginia X-Ray facility, and only the tumors on both flanks were irradiated while the rest of animal body was shielded. For combination treatment, MLN4924 was given 2 hours prior to radiation exposure with the same schedule as for the individual treatments. Mice were weighed once a week during the entire course of the experiment, and no significant effect of either treatment was observed. Tumor growth was monitored every other day using an electronic caliper, for 3 weeks posttreatment, and average of tumor volumes were calculated using the formula $[L \times W^2)/2]$. The results are represented as the mean tumor volumes ± SEM, and $P < 0.05$ was considered statistically significant.

4.7. Kaplan–Meier plot analysis

The Cancer Genome Atlas data, publicly available at cBioPortal (Gao et al. 2013; Cerami et al. 2012), were used to plot Kaplan–Meier plots on tumors divided into two groups based on CDT2 expression as a *z*-score (Weinstein et al. 2014; Collisson et al. 2014).

4.8. Statistical analysis

All experiments were performed in triplicates and results with $P < 0.05$ were considered statistically significant. All quantitative differences were analyzed by Student's *t*-test.

Synergy was determined using the Bliss model of independence (BLISS 1939; Fitzgerald et al. 2006).

5. References:

Abbas, Tarek, and Anindya Dutta. 2011. “CRL4Cdt2: Master Coordinator of Cell Cycle Progression and Genome Stability.” *Cell Cycle*. Taylor and Francis Inc. https://doi.org/10.4161/cc.10.2.14530.

Abbas, Tarek, Mignon A. Keaton, and Anindya Dutta. 2013. “Genomic Instability in Cancer.” *Cold Spring Harbor Perspectives in Biology* 5 (3): a012914. https://doi.org/10.1101/cshperspect.a012914.

Abbas, Tarek, Etsuko Shibata, Jonghoon Park, Sudhakar Jha, Neerja Karnani, and Anindya Dutta. 2010. “CRL4Cdt2 Regulates Cell Proliferation and Histone Gene Expression by Targeting PR-Set7/Set8 for Degradation.” *Molecular Cell* 40 (1): 9–21. https://doi.org/10.1016/j.molcel.2010.09.014.

Agrawal, Nishant, Mitchell J. Frederick, Curtis R. Pickering, Chetan Bettegowda, Kyle Chang, Ryan J. Li, Carole Fakhry, et al. 2011. “Exome Sequencing of Head and Neck Squamous Cell Carcinoma Reveals Inactivating Mutations in NOTCH1.” *Science* 333 (6046): 1154–57. https://doi.org/10.1126/science.1206923.

Alterio, Daniela, Giulia Marvaso, Annamaria Ferrari, Stefania Volpe, Roberto Orecchia, and Barbara Alicja Jereczek-Fossa. 2019. “Modern Radiotherapy for Head and Neck Cancer.” *Seminars in Oncology*. W.B. Saunders. https://doi.org/10.1053/j.seminoncol.2019.07.002.

Arenz, Andrea, Frank Ziemann, Christina Mayer, Andrea Wittig, Kirstin Dreffke, Stefanie Preising, Steffen Wagner, Jens Peter Klussmann, Rita Engenhart-Cabillic, and Claus

Wittekindt. 2014. “Increased Radiosensitivity of HPV-Positive Head and Neck Cancer Cell Lines Due to Cell Cycle Dysregulation and Induction of Apoptosis.” *Strahlentherapie Und Onkologie* 190 (9): 839–46. https://doi.org/10.1007/s00066-014-0605-5.

Arias, Emily E., and Johannes C. Walter. 2006. “PCNA Functions as a Molecular Platform to Trigger Cdt1 Destruction and Prevent Re-Replication.” *Nature Cell Biology* 8 (1): 84–90. https://doi.org/10.1038/ncb1346.

Benamar, Mouadh, Fadila Guessous, Kangping Du, Patrick Corbett, Joseph Obeid, Daniel Gioeli, Craig L. Slingluff, and Tarek Abbas. 2016. “Inactivation of the CRL4-CDT2-SET8/P21 Ubiquitylation and Degradation Axis Underlies the Therapeutic Efficacy of Pevonedistat in Melanoma.” *EBioMedicine* 10 (August): 85–100. https://doi.org/10.1016/j.ebiom.2016.06.023.

BLISS, C. I. 1939. “THE TOXICITY OF POISONS APPLIED JOINTLY1.” *Annals of Applied Biology* 26 (3): 585–615. https://doi.org/10.1111/j.1744-7348.1939.tb06990.x.

Bui, Duyen T., and Joachim J. Li. 2019. “DNA Rereplication Is Susceptible to Nucleotide-Level Mutagenesis.” *Genetics* 212 (2): 445–60. https://doi.org/10.1534/genetics.119.302194.

Cerami, Ethan, Jianjiong Gao, Ugur Dogrusoz, Benjamin E. Gross, Selcuk Onur Sumer, Bülent Arman Aksoy, Anders Jacobsen, et al. 2012. “The CBio Cancer Genomics Portal: An Open Platform for Exploring Multidimensional Cancer Genomics Data.”

Cancer Discovery 2 (5): 401–4. https://doi.org/10.1158/2159-8290.CD-12-0095.

Collisson, Eric A., Joshua D. Campbell, Angela N. Brooks, Alice H. Berger, William Lee, Juliann Chmielecki, David G. Beer, et al. 2014. "Comprehensive Molecular Profiling of Lung Adenocarcinoma: The Cancer Genome Atlas Research Network." *Nature* 511 (7511): 543–50. https://doi.org/10.1038/nature13385.

Ferlay, Jacques, Isabelle Soerjomataram, Rajesh Dikshit, Sultan Eser, Colin Mathers, Marise Rebelo, Donald Maxwell Parkin, David Forman, and Freddie Bray. 2015. "Cancer Incidence and Mortality Worldwide: Sources, Methods and Major Patterns in GLOBOCAN 2012." *International Journal of Cancer* 136 (5): E359–86. https://doi.org/10.1002/ijc.29210.

Ferris, Robert L., George Blumenschein, Jerome Fayette, Joel Guigay, A. Dimitrios Colevas, Lisa Licitra, Kevin Harrington, et al. 2016. "Nivolumab for Recurrent Squamous-Cell Carcinoma of the Head and Neck." *New England Journal of Medicine* 375 (19): 1856–67. https://doi.org/10.1056/NEJMoa1602252.

Fitzgerald, Jonathan B., Birgit Schoeberl, Ulrik B. Nielsen, and Peter K. Sorger. 2006. "Systems Biology and Combination Therapy in the Quest for Clinical Efficacy." *Nature Chemical Biology*. Nature Publishing Group. https://doi.org/10.1038/nchembio817.

Gao, Jianjiong, Bülent Arman Aksoy, Ugur Dogrusoz, Gideon Dresdner, Benjamin Gross, S. Onur Sumer, Yichao Sun, et al. 2013. "Integrative Analysis of Complex Cancer Genomics and Clinical Profiles Using the CBioPortal." *Science Signaling* 6 (269):

pl1–pl1. https://doi.org/10.1126/scisignal.2004088.

Ginos, Matthew A., Grier P. Page, Bryan S. Michalowicz, Ketan J. Patel, Sonja E. Volker, Stefan E. Pambuccian, Frank G. Ondrey, George L. Adams, and Patrick M. Gaffney. 2004. "Identification of a Gene Expression Signature Associated with Recurrent Disease in Squamous Cell Carcinoma of the Head and Neck." *Cancer Research* 64 (1): 55–63. https://doi.org/10.1158/0008-5472.CAN-03-2144.

Glickman, Michael H., and Aaron Ciechanover. 2002. "The Ubiquitin-Proteasome Proteolytic Pathway: Destruction for the Sake of Construction." *Physiological Reviews*. American Physiological Society. https://doi.org/10.1152/physrev.00027.2001.

Jin, Jianping, Emily E. Arias, Jing Chen, J. Wade Harper, and Johannes C. Walter. 2006. "A Family of Diverse Cul4-Ddb1-Interacting Proteins Includes Cdt2, Which Is Required for S Phase Destruction of the Replication Factor Cdt1." *Molecular Cell* 23 (5): 709–21. https://doi.org/10.1016/j.molcel.2006.08.010.

Kimple, Randall J., Molly A. Smith, Grace C. Blitzer, Alexandra D. Torres, Joshua A. Martin, Robert Z. Yang, Chimera R. Peet, et al. 2013. "Enhanced Radiation Sensitivity in HPV-Positive Head and Neck Cancer." *Cancer Research* 73 (15): 4791–4800. https://doi.org/10.1158/0008-5472.CAN-13-0587.

Kotowski, Ulana, Gregor Heiduschka, Markus Brunner, Cornelia Czembirek, Christina Eder-Czembirek, Rainer Schmidt, Tammer Fahim, and Dietmar Thurnher. 2011. "Radiosensitization of Head and Neck Cancer Cells by the Phytochemical Agent

Sulforaphane." *Strahlenther Onkol* 187: 575–80. https://doi.org/10.1007/s00066-011-2218-6.

Li, J., E. K.O. Ng, Y. P. Ng, C. Y.P. Wong, J. Yu, H. Jin, V. Y.Y. Cheng, et al. 2009. "Identification of Retinoic Acid-Regulated Nuclear Matrix-Associated Protein as a Novel Regulator of Gastric Cancer." *British Journal of Cancer* 101 (4): 691–98. https://doi.org/10.1038/sj.bjc.6605202.

Li, Xianghong, Qiping Zhao, Rong Liao, Peiqing Sun, and Xiaohua Wu. 2003. "The SCFSkp2 Ubiquitin Ligase Complex Interacts with the Human Replication Licensing Factor Cdt1 and Regulates Cdt1 Degradation." *Journal of Biological Chemistry* 278 (33): 30854–58. https://doi.org/10.1074/jbc.C300251200.

Lin, Jie Jessie, Michael A. Milhollen, Peter G. Smith, Usha Narayanan, and Anindya Dutta. 2010. "NEDD8-Targeting Drug MLN4924 Elicits DNA Rereplication by Stabilizing Cdt1 in S Phase, Triggering Checkpoint Activation, Apoptosis, and Senescence in Cancer Cells." *Cancer Research* 70 (24): 10310–20. https://doi.org/10.1158/0008-5472.CAN-10-2062.

Liontos, Michalis, Marilena Koutsami, Maria Sideridou, Konstantinos Evangelou, Dimitris Kletsas, Brynn Levy, Athanassios Kotsinas, et al. 2007. "Deregulated Overexpression of HCdt1 and HCdc6 Promotes Malignant Behavior." *Cancer Research* 67 (22): 10899–909. https://doi.org/10.1158/0008-5472.CAN-07-2837.

Liu, Enbo, Xianghong Li, Feng Yan, Qiping Zhao, and Xiaohua Wu. 2004. "Cyclin-Dependent Kinases Phosphorylate Human Cdt1 and Induce Its Degradation." *Journal*

of Biological Chemistry 279 (17): 17283–88. https://doi.org/10.1074/jbc.C300549200.

Mackintosh, C., J. L. Ordóñez, D. J. García-Domínguez, V. Sevillano, A. Llombart-Bosch, K. Szuhai, K. Scotlandi, et al. 2012. "1q Gain and CDT2 Overexpression Underlie an Aggressive and Highly Proliferative Form of Ewing Sarcoma." *Oncogene* 31 (10): 1287–98. https://doi.org/10.1038/onc.2011.317.

Merlet, J., J. Burger, J. E. Gomes, and L. Pintard. 2009. "Regulation of Cullin-RING E3 Ubiquitin-Ligases by Neddylation and Dimerization." *Cellular and Molecular Life Sciences*. https://doi.org/10.1007/s00018-009-8712-7.

Mladenov, Emil, Simon Magin, Aashish Soni, and George Iliakis. 2013. "DNA Double-Strand Break Repair as Determinant of Cellular Radiosensitivity to Killing and Target in Radiation Therapy." *Frontiers in Oncology* 3 (May): 113. https://doi.org/10.3389/fonc.2013.00113.

Nichols, Anthony C., John Yoo, David A. Palma, Kevin Fung, Jason H. Franklin, James Koropatnick, Joe S. Mymryk, Nizar N. Batada, and John W. Barrett. 2012. "Frequent Mutations in TP53 and CDKN2A Found by Next-Generation Sequencing of Head and Neck Cancer Cell Lines." *Archives of Otolaryngology - Head and Neck Surgery* 138 (8): 732–39. https://doi.org/10.1001/archoto.2012.1558.

Nishitani, Hideo, Nozomi Sugimoto, Vassilis Roukos, Yohsuke Nakanishi, Masafumi Saijo, Chikashi Obuse, Toshiki Tsurimoto, et al. 2006. "Two E3 Ubiquitin Ligases, SCF-Skp2 and DDB1-Cul4, Target Human Cdt1 for Proteolysis." *The EMBO Journal* 25 (5): 1126–36. https://doi.org/10.1038/sj.emboj.7601002.

Pan, Hung Wei, Han Yi E. Chou, Shu Hsiang Liu, Shian Yang Peng, Chao Lien Liu, and Hey Chi Hsu. 2006. "Role of L2DTL, Cell Cycle-Regulated Nuclear and Centrosome Protein, in Aggressive Hepatocellular Carcinoma." *Cell Cycle* 5 (22): 2676–87. https://doi.org/10.4161/cc.5.22.3500.

Peng, Chien Hua, Chun Ta Liao, Shih Chi Peng, Yin Ju Chen, Ann Joy Cheng, Jyh Lyh Juang, Chi Ying Tsai, et al. 2011. "A Novel Molecular Signature Identified by Systems Genetics Approach Predicts Prognosis in Oral Squamous Cell Carcinoma." *PLoS ONE* 6 (8). https://doi.org/10.1371/journal.pone.0023452.

Pyeon, Dohun, Michael A. Newton, Paul F. Lambert, Johan A. Den Boon, Srikumar Sengupta, Carmen J. Marsit, Craig D. Woodworth, et al. 2007. "Fundamental Differences in Cell Cycle Deregulation in Human Papillomavirus-Positive and Human Papillomavirus-Negative Head/Neck and Cervical Cancers." *Cancer Research* 67 (10): 4605–19. https://doi.org/10.1158/0008-5472.CAN-06-3619.

Seiwert, Tanguy Y., Barbara Burtness, Ranee Mehra, Jared Weiss, Raanan Berger, Joseph Paul Eder, Karl Heath, et al. 2016. "Safety and Clinical Activity of Pembrolizumab for Treatment of Recurrent or Metastatic Squamous Cell Carcinoma of the Head and Neck (KEYNOTE-012): An Open-Label, Multicentre, Phase 1b Trial." *The Lancet Oncology* 17 (7): 956–65. https://doi.org/10.1016/S1470-2045(16)30066-3.

Senga, Takeshi, Umasundari Sivaprasad, Wenge Zhu, Jong Park Jong, Emily E. Arias, Johannes C. Walter, and Anindya Dutta. 2006. "PCNA Is a Cofactor for CDT1 Degradation by CUL4/DDB1-Mediated N-Terminal Ubiquitination." *Journal of*

Biological Chemistry 281 (10): 6246–52. https://doi.org/10.1074/jbc.M512705200.

Sengupta, Srikumar, Johan A. Den Boon, I. How Chen, Michael A. Newton, David B. Dahl, Meng Chen, Yu Juen Cheng, et al. 2006. "Genome-Wide Expression Profiling Reveals EBV-Associated Inhibition of MHC Class I Expression in Nasopharynaeal Carcinoma." *Cancer Research* 66 (16): 7999–8006. https://doi.org/10.1158/0008-5472.CAN-05-4399.

Sim, Felix, Rom Leidner, and Richard Bryan Bell. 2019. "Immunotherapy for Head and Neck Cancer." *Oral and Maxillofacial Surgery Clinics of North America*. W.B. Saunders. https://doi.org/10.1016/j.coms.2018.09.002.

Soucy, Teresa A., Peter G. Smith, Michael A. Milhollen, Allison J. Berger, James M. Gavin, Sharmila Adhikari, James E. Brownell, et al. 2009. "An Inhibitor of NEDD8-Activating Enzyme as a New Approach to Treat Cancer." *Nature* 458 (7239): 732–36. https://doi.org/10.1038/nature07884.

Soucy, Teresa A., Peter G. Smith, and Mark Rolfe. 2009. "Targeting NEDD8-Activated Cullin-RING Ligases for the Treatment of Cancer." *Clinical Cancer Research*. American Association for Cancer Research. https://doi.org/10.1158/1078-0432.CCR-09-0343.

Stransky, Nicolas, Ann Marie Egloff, Aaron D. Tward, Aleksandar D. Kostic, Kristian Cibulskis, Andrey Sivachenko, Gregory V. Kryukov, et al. 2011. "The Mutational Landscape of Head and Neck Squamous Cell Carcinoma." *Science* 333 (6046): 1157–60. https://doi.org/10.1126/science.1208130.

Truong, Lan N., and Xiaohua Wu. 2011. “Prevention of DNA Re-Replication in Eukaryotic Cells.” *Journal of Molecular Cell Biology* 3 (1): 13–22. https://doi.org/10.1093/JMCB/MJQ052.

Ueki, T., T. Nishidate, J. H. Park, M. L. Lin, A. Shimo, K. Hirata, Y. Nakamura, and T. Katagiri. 2008. “Involvement of Elevated Expression of Multiple Cell-Cycle Regulator, DTL/RAMP (Denticleless/RA-Regulated Nuclear Matrix Associated Protein), in the Growth of Breast Cancer Cells.” *Oncogene* 27 (43): 5672–83. https://doi.org/10.1038/onc.2008.186.

Wan, Juefeng, Ji Zhu, Guichao Li, and Zhen Zhang. 2016. “Radiosensitization of Human Colorectal Cancer Cells by MLN4924: An Inhibitor of NEDD8-Activating Enzyme.” *Technology in Cancer Research and Treatment* 15 (4): 527–34. https://doi.org/10.1177/1533034615588197.

Wei, Dongping, Hua Li, Jie Yu, Jonathan T Sebolt, Lili Zhao, Theodore S Lawrence, Peter G Smith, Meredith A Morgan, and Yi Sun. 2012. “Radiosensitization of Human Pancreatic Cancer Cells by MLN4924, an Investigational NEDD8-Activating Enzyme Inhibitor.” *Cancer Research* 72 (1): 282–93. https://doi.org/10.1158/0008-5472.CAN-11-2866.

Weinstein, John N., Rehan Akbani, Bradley M. Broom, Wenyi Wang, Roeland G.W. Verhaak, David McConkey, Seth Lerner, et al. 2014. “Comprehensive Molecular Characterization of Urothelial Bladder Carcinoma.” *Nature* 507 (7492): 315–22. https://doi.org/10.1038/nature12965.

Yang, Dong, Mingjia Tan, Gongxian Wang, and Yi Sun. 2012. “The P21-Dependent Radiosensitization of Human Breast Cancer Cells by MLN4924, an Investigational Inhibitor of NEDD8 Activating Enzyme.” *PLoS ONE* 7 (3). https://doi.org/10.1371/journal.pone.0034079.

IX.

Chapter IV:

Mechanism of Double Strand Break Induced Rereplication in Cancer Cells

1. Abstract

Ionizing radiation (IR) is one of the most commonly prescribed anti-tumor therapeutics employed in the treatment of many human malignancies. IR-induced cytotoxicity is attributed to the generation of severe forms of DNA damage, particularly double-strand breaks (DSBs), leading to chromosomal aberrations that cannot be properly resolved by the DNA repair machinery. In this chapter, we uncovered that exposure to IR, or other DSB-inducing agents, induces rereplication in cancer cells derived from various epithelial origins. We show that DSBs-induced rereplication, or DIRR, correlates with IR-induced toxicity in melanoma cells, suggesting that DIRR could be a major determinant of sensitivity to radiotherapy in cancer cells. We found that DIRR, which is mediated by the DNA replicative polymerases, is independent of canonical ORC1/2-CDT1-mediated origin licensing and is suppressed by an H4K20me2-dependent mechanism. DIRR is enhanced by the failure to recruit 53BP1-RIF1, or its effector Shieldin complex, to DSBs to suppress end resection. In addition, DIRR is suppressed in cells depleted of exonucleases that mediate hyper-resection of broken DSB ends or treated with a pharmacological agent that inhibits strand invasion. In this chapter, we propose that exposure to IR, and other DSB-inducing agents, induces an origin-independent cytotoxic rereplication promoted by unshielded and hyper-resected broken DNA ends that significantly contribute to IR-induced lethality.

2. Introduction:

2.1. Ionizing Radiation Therapy in Cancer:

Ionizing radiation therapy (IR) is a standard of care for the treatment of many human malignancies. At least half of all cancer patients with solid tumors are treated with IR at some point during the course of their disease management (Mladenov et al. 2013). IR uses high energy waves, such as X-rays or gamma-rays, to induces fatal DNA damage as a result of direct ionization of atoms or indirectly through the production of free radicals (Fouad et al. 2019). IR-induced lesions include single strand breaks (SSBs), oxidative base damages, and double strand breaks (DSBs). For instance, a typical clinical X-ray dose of 2 Gy can result in an average of 2,000 SSBs, roughly 4,000 bases damages, but only 40-80 DSBs (Fouad et al. 2019). One of the hallmarks of IR is the induction of "complex or clustered DNA damage," which is the process of causing multiple lesions effecting both DNA strands in close proximity to each other (within one helical turn of the DNA molecule). DSBs, despite its low frequency, represent the simplest and most severe forms of such clustered DNA lesions and is considered the primary contributor to IR-induced cell killing. IR-induced lethality is largely attributed to the generation of chromatid and chromosomal aberrations that are not resolved during mitosis and result from the aberrant joining of DNA double strand breaks (Mladenov et al. 2013; Wang and Lees-Miller 2013; Santivasi and Xia 2014). However, it is now clear that IR exerts other cytotoxic activities, and determining these alternative means of tumor cell killing will provide alternative approaches to improve treatment with IR.

The number of IR-induced DNA lesions is relatively low when compared to the endogenous DNA damage that occurs routinely (50,000 DNA lesions per day) as a result of environmental oxidative stress, such as Reactive Oxygen Species (ROS), or by-products of errors during various biological processes, such as DNA replication and V(D)J recombination (Fouad et al. 2019; Mladenov and Iliakis 2011). Therefore, in order to protect against endogenous and exogenous DNA damage and maintain genomic integrity, cells have evolved highly efficient DNA repair machineries to detect, remove, and faithfully repair DNA lesions. The cellular response that govern the detection and repair of broken DNA ends as a result of internal or external stimulus, such as IR, are termed DNA Damage Response (DDR) and represents an essential cellular component in maintaining genomic instability and the protection against cancer development (Mladenov and Iliakis 2011).

2.2. Rereplication stimulated by low doses of IR:

We have previously shown that deregulated licensing of origins of DNA replication in head and neck squamous cell carcinoma (HNSCC) cells (e.g., following CDT1 activation, silencing of the cullin 4 E3 ubiquitin ligase substrate receptor CDT2, or treatment with the neddylation inhibitor MLN4924) induces rereplication, which was stimulated by low doses of ionizing radiation (IR; 2-4Gy) (Vanderdys et al. 2018). Rereplication, detailed in both Chapter I and II, is a toxic and stochastic process that involves multiple rounds of re-initiation of DNA replication within the same cell cycle. The cell lethality of this phenomenon is due to replication fork stalling and the accumulation of replication intermediates which leads to excessive DNA damage and

apoptosis. Surprisingly, we found that exposure of human cancer cells from various epithelial origins to IR resulted in DNA rereplication, similar to the one observed after deregulated origin licensing (after either genetic or pharmacological inactivation of $CRL4^{CDT2}$). In this chapter, we detail the nature of this IR-induced rereplication, its correlation with IR-induced toxicity, and the role the DNA repair factors play in regulating this phenomenon.

3. Results:

3.1. Ionizing Radiation Induces Rereplication in Cancer Cells

In the previous chapter, we have observed that treatment with low doses of IR (<4Gy) in head and neck squamous cell carcinoma (HNSCC) cells stimulated rereplication induced after MLN4924 treatment or siRNA-mediated depletion of CDT2 or Geminin (Vanderdys et al. 2018). We wondered if what contributed to this stimulation is a form of genomic amplification or a *bona fide* rereplication induced after IR treatment in HNSCC. To address that, we exposed four p53-negative HNSCC cell lines (Cal27, FaDu, SCC25, UNC7) to increasing doses of IR and examined the genomic DNA content by flow cytometry. IR treatment resulted in a dose-dependent increase in the population of cells with more than 4N DNA content, reaching up to 50% in FaDu 48 h post 9Gy treatment, indicative of rereplication (Fig. 4.1A, C). This dose-dependent increase in genomic DNA was not only limited to HNSCC, but was also observed in other cell lines regardless of their epithelial origins or p53 mutational status, including U2OS (human osteosarcoma), HCT116 (human colon cancer), HEK 293T (human embryonic kidney cells), and p53-mutant MDA-MB-231 (breast cancer cells) (Fig. 4.1D-E)

Cell cycle analysis following one-hour pulsing with BrdU confirmed the presence of a significant BrdU-positive population (45%) with more than 4N DNA content in FaDu cells 48 hours post 9Gy treatment (Fig. 4.1B). These results indicate that exposure of various cancer cells to IR leads to active DNA synthesis that results in a significant increase in genomic DNA, indicative of rereplication.

We also observed that IR induced significantly more rereplication in the p53-deficient HCT116 ($p53^{-/-}$) cell line compared to its p53-proficient counterpart HCT116 (p53 WT) in all doses tested (Fig. 4.1E). This result is consistent with the protective role p53 was shown to play in suppressing rereplication induced after deregulated origin licensing (Fig. 4.1F) (Vaziri et al. 2003).

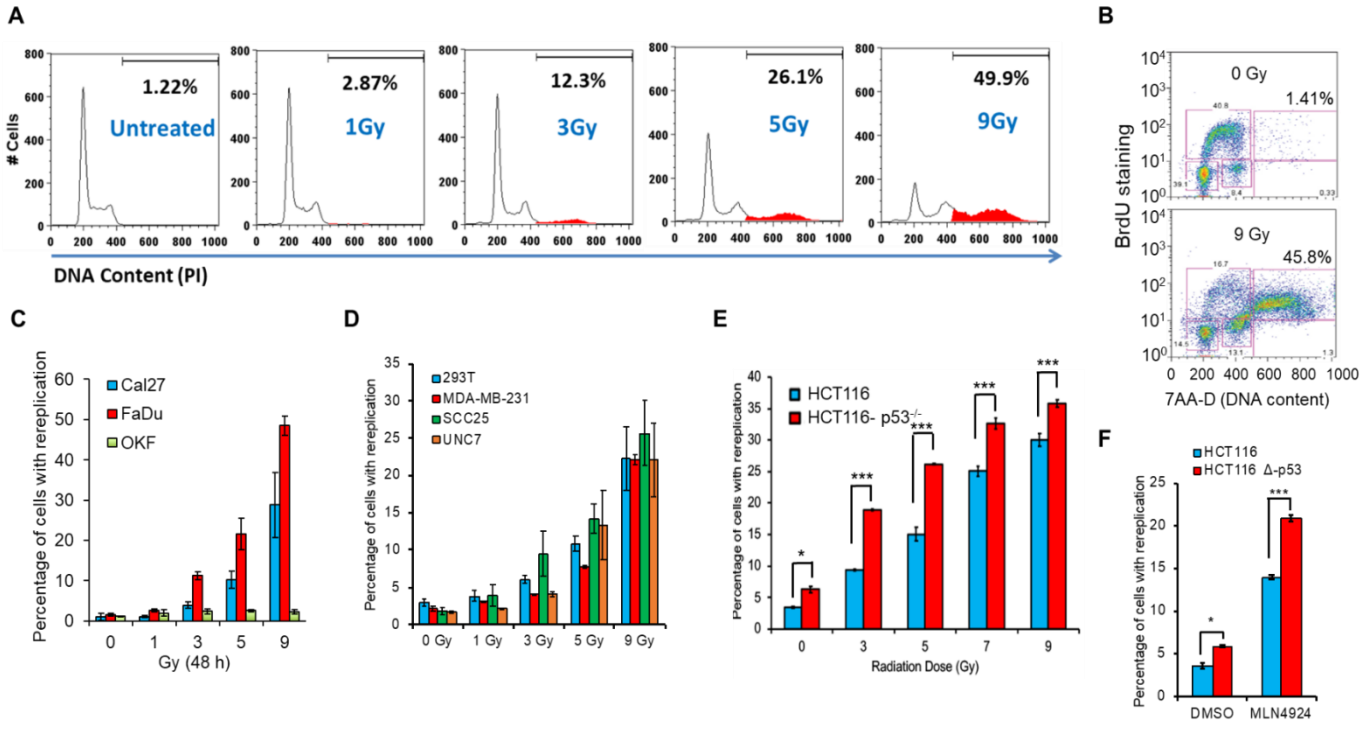

Figure 4.1 Ionizing Radiation result in a dose dependent increase of genomic DNA in cancer cells

A. Flow cytometry profile of FaDu cell line showing the cell cycle distribution after exposure to increasing doses of IR. The red highlighted population represent the cells with more than 4N DNA content. Cells stained with Propidium Iodine (PI).

B. Flow cytometry profile of FaDu cells 48hrs post exposure to 9Gy. Cells were pulsed with BrdU for 1 hour before harvesting, then co-stained with 7-AAD and BrdU antibody.

C. Histogram summarizing the extent of rereplication 48 hours post exposure increasing doses of IR, detected by PI staining and quantified by Flow cytometry (similar to Figure 4.1A), in Cal27, FaDu, and immortalized keratinocytes OKFs.

D. Histogram showing the extent of rereplication 48 hours post exposure increasing doses of IR in 293T, MDA-MB-231, SCC25, UNC7

E-F. Histogram comparing the extent of rereplication in HCT116 (p53 WT) and HCT116 (p53-/-) 72 hours after the exposure to increasing doses of IR **(E)**, or 48 hours after treatment with MLN4924 (0.3 μM) **(F)** .

All the data presented in the histogram represent the average of three independent experiments. Error bars represent SD. P-values: * = $p < 0.05$, ** = $p < 0.01$, *** = $p < 0.001$.

To confirm that the observed increase in genomic DNA is not a result of chromosomal missegregation or failed cytokinesis, we showed that treatment with Nocodazole after exposure to IR did not reduce the percentage of rereplicating cells (Fig. 4.2A-B). This result further demonstrates that the IR-induced increase in genomic DNA occurs in the same cell division cycle and does not require mitotic entry, indicative or rereplication.

In order to further confirm the presence of rereplicating DNA after IR treatment, we used cesium chloride (CsCl) density gradient ultracentrifugation to separate genomic DNA based on density differences caused by the rate of BrdU incorporation during DNA synthesis. This isopycnic centrifugation, first developed by Mathhew Meselson and Franklin Stahl, facilitates the separation of rereplicated DNA, labeled heavy/heavy (H:H) as a result of BrdU incorporation on both strands, from the normal replicated DNA, heavy/light (H:L) and unlabeled DNA (light/light L:L) (Meselson and Stahl 1958; Meselson, Stahl, and Vinograd 1957). U2OS cells were synchronized at the G1/S transition using double thymidine block, then released in the presence of BrdU. 8 hours post release, cells were treated with 9Gy in the presence of nocodazole to prevent cells from slippage onto the next cell division cycle. Genomic DNA was harvested and purified 36 hours post IR treatment, sheared into 0.5-3 kb fragments by sonication, then centrifuged in the presence of 1 g/mL CsCl-TE solution for 66 hours. A considerable H:H fraction, representing 20% of the total DNA, was observed in the IR-treated sample compared to the untreated control, which contained mostly H:L DNA as expected *(Fig. 4.2C-E)*. This result further confirms that the observed IR-induced increase in genomic

DNA is a result of rereplicating cells undergoing more than one round of semi-conservative DNA synthesis in the same cell cycle.

To test whether DNA rereplication utilizes the same replicative machinery employed during normal DNA synthesis during S-phase, we treated asynchronous U2OS cells with the B-family (POL α, δ, and ε) DNA polymerases inhibitor Aphidicolin (2μM) immediately or 24 h post exposure to IR (9Gy). The results show that Aphidicolin treatment significantly inhibited IR-induced rereplication (Fig. 4.2F). Consistently, we observed a decrease in the H:H fractions in the sample treated with Aphidicolin immediately after irradiation when assessed by CsCl density gradient centrifugation (Fig. 4.2G). These results collectively demonstrate that IR induces a dose-dependent *bona fide* rereplication in various cancer cells, irrespective of their epithelial origin, and this aberrant form of DNA replication is mediated by the same replicative DNA polymerases that drive normal DNA synthesis.

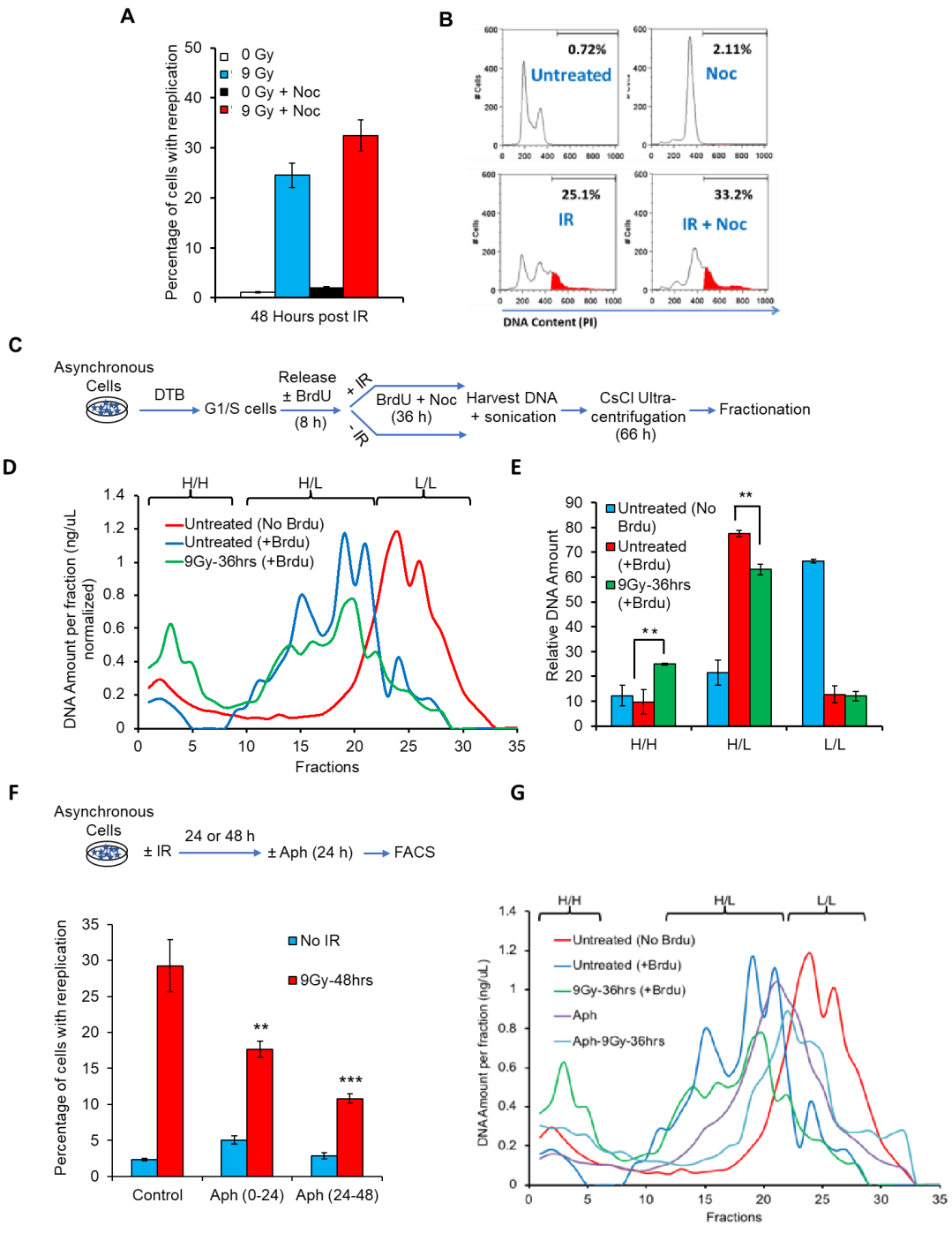
A
Percentage of cells with rereplication
0 Gy
9 Gy
0 Gy + Noc
9 Gy + Noc
48 Hours post IR
B
0.72%
Untreated
2.11%
Noc
25.1%
IR
33.2%
IR + Noc
DNA Content (PI)
C
Asynchronous Cells
DTB
G1/S cells
Release ± BrdU (8 h)
+ IR
- IR
BrdU + Noc (36 h)
Harvest DNA + sonication
CsCl Ultra-centrifugation (66 h)
Fractionation
D
H/H
H/L
L/L
Untreated (No Brdu)
Untreated (+Brdu)
9Gy-36hrs (+Brdu)
DNA Amount per fraction (ng/uL) normalized)
Fractions
E
Untreated (No Brdu)
Untreated (+Brdu)
9Gy-36hrs (+Brdu)
Relative DNA Amount
H/H
H/L
L/L
F
Asynchronous Cells
± IR
24 or 48 h
± Aph (24 h)
FACS
No IR
9Gy-48hrs
Percentage of cells with rereplication
Control
Aph (0-24)
Aph (24-48)
G
H/H
H/L
L/L
Untreated (No Brdu)
Untreated (+Brdu)
9Gy-36hrs (+Brdu)
Aph
Aph-9Gy-36hrs
DNA Amount per fraction (ng/uL)
Fractions

Figure 4.2: Ionizing Radiation Induces Rereplication in Cancer Cells

A-B. The effect of nocodazole block on IR-induced rereplication. A. Histogram showing the extent of rereplication in U2OS cells 48 hours after exposed to 9Gy in the presence or absence of Nocodazole treatment (added 24 hours post irradiation). **B**. Representative flow cytometry profiles of the experiment depicted in A.

C. Experimental workflow of the cesium chloride ultracentrifugation of the BrdU-labeled genomic DNA of U2OS cells to detect IR-induced rereplication.

D-E. Graph showing the relative amount of DNA of each fraction collected after cesium chloride ultracentrifugation (**C**). Heavy (H) represents the DNA labelled with BrdU while Light (L) represent unlabelled DNA. The average area under the curve of three independent experiments is represented in histogram shown in **E**.

F. Histogram showing the extent of rereplication in U2OS cells 48 hours after exposed to 9Gy in the presence or absence of Aphidicolin treatment, added either immediately or 24 hours post irradiation, as depicted in the workflow (above).

G. Graph showing the relative amount of DNA of each fraction collected after cesium chloride ultracentrifugation using the same experimental workflow as in **C**, with or without the additional treatment of Aphidicolin (added at the time of irradiation).

3.2. IR Induces Rereplication through DSBs in Cancer Cells

Exposure to IR can result in a wide range of severe biological changes to the cell and cause various DNA damage lesions including single strand breaks (SSBs), double strand breaks (DSBs), oxidative damage, DNA-protein crosslinks, and clustered DNA lesions. Despite the multitude of lesions caused by IR, complex DSBs represent the most severe due to its relatively low reparability that poses a serious threat to genomic integrity and cell survival. (Fouad et al. 2019; Mladenov and Iliakis 2011). Since DSBs are regarded as the primary contributor to IR-induced lethality, we examined if the IR-induced rereplication is mediated through DSBs. To test this hypothesis, we first demonstrated that treatment with other DSB-inducing agents, such as the topoisomerase II inhibitor etoposide (1 μg ml^{-1}) and doxorubicin (0.1 μM), and not non-DSB-inducing ultraviolet radiation (100 J/m), resulted in significant rereplication in U2OS cells (Fig. 4.3A). To test whether DSBs, and no other IR-induced DNA damage lesions, are sufficient to promote rereplication in cancer cells, we utilized AsiSI-ER-U2OS cell line that encodes a restriction enzyme fused to an estrogen receptor ligand-binding domain. Treatment with 4-Hydroxytamoxifen (4-OHT) promotes the nuclear localization of the enzyme complex which delivers approximately 150 DSBs per nucleus (Iacovoni et al. 2010; Massip et al. 2010; Zhou et al. 2014). Treatment with 300nM of 4-OHT induced rereplication (35%) in AsiSI-ER-U2OS and not in normal control U2OS cells. Consistent with the previous IR results, this AsiSI-induced rereplication was suppressed in the presence of Aphidicolin (Fig. 4.3B-E). Therefore, these results demonstrate that DSBs are the primary mechanism that mediate rereplication caused by DSBs-inducing agents, including IR. Throughout the rest of the chapter, we will refer to this phenomenon as DSB-Induced Rereplication, or DIRR.

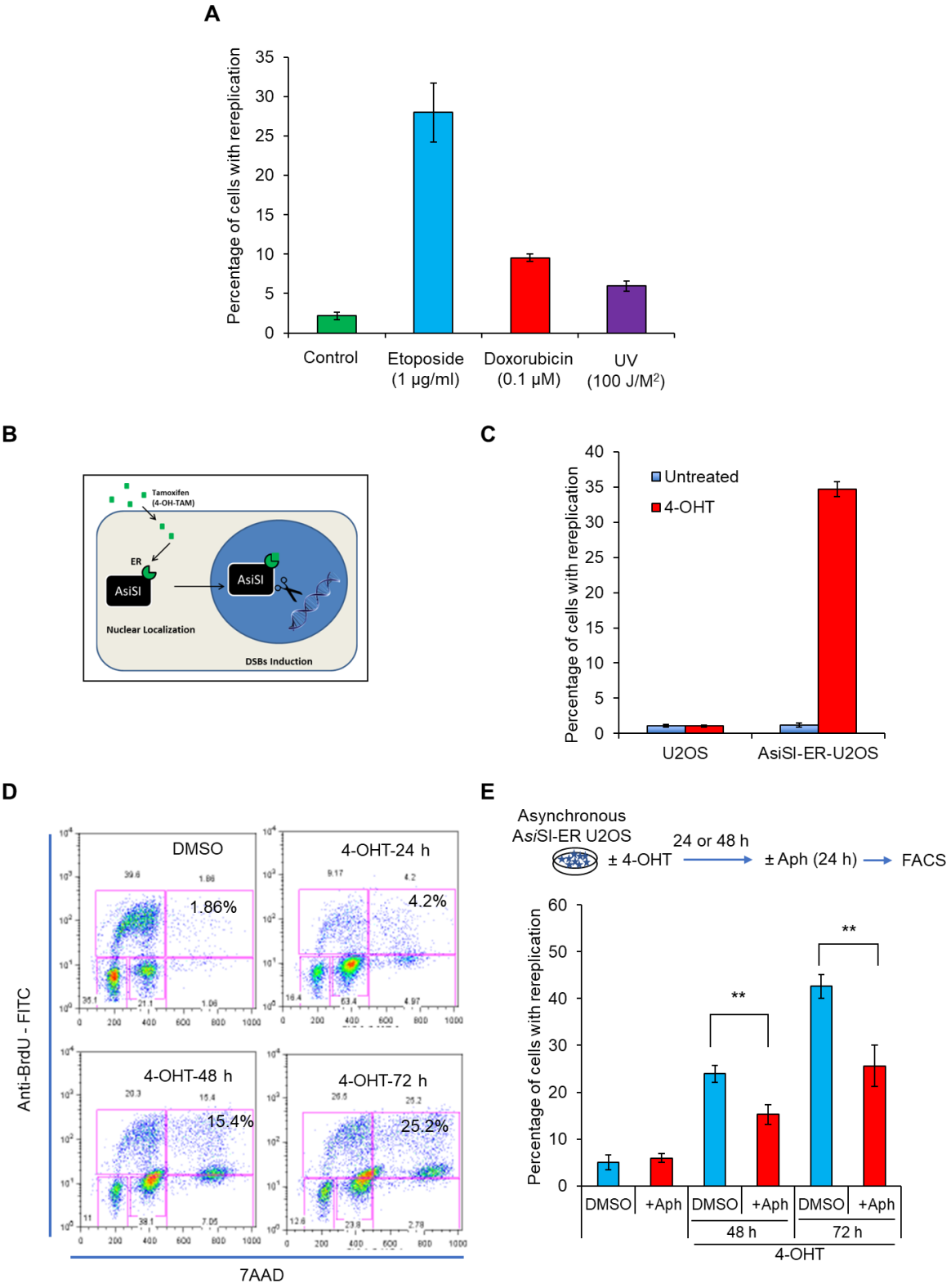
A
Percentage of cells with rereplication
35
30
25
20
15
10
5
0
Control
Etoposide (1 µg/ml)
Doxorubicin (0.1 µM)
UV (100 J/M²)
B
Tamoxifen (4-OH-TAM)
ER
AsiSI
AsiSI
Nuclear Localization
DSBs Induction
C
Percentage of cells with rereplication
Untreated
4-OHT
U2OS
AsiSI-ER-U2OS
D
DMSO
1.86%
4-OHT-24 h
4.2%
4-OHT-48 h
15.4%
4-OHT-72 h
25.2%
Anti-BrdU - FITC
7AAD
E
Asynchronous
AsiSI-ER U2OS
± 4-OHT
24 or 48 h
± Aph (24 h)
FACS
Percentage of cells with rereplication
**
**
DMSO
+Aph
DMSO
+Aph
DMSO
+Aph
48 h
72 h
4-OHT

Figure 4.3: Ionizing Radiation Induces Rereplication through Double Strand Breaks in Cancer Cells

A. Histogram showing the percentage of rereplication in U2OS cells 72 hours after exposure or treatment with etoposide (1 µg/mg), doxorubicin (0.1 µM), or ultraviolet radiation (UV; 100J/m^2)

B. Schematic showing the process of DSB-induction in A*si*SI-ER-U2OS cells upon Tamoxifen (4-OHT) treatment (Iacovoni et al. 2010).

C. Histogram showing the percentage of rereplication after 72 hours after exposure to 4-OHT in A*si*SI-ER-U2OS cells (B) compared to parental control U2OS cells.

D. Representative flow cytometry profiles showing the BrdU incorporation and the extent of rereplication in A*si*SI-ER-U2OS cells treated with 4-OHT after 24, 48, and 72 hours. Cells were pulsed with BrdU for 1 hour prior to harvesting then stained with 7-AAD and anti-BrdU antibody.

E. Histogram showing the extent of rereplication in A*si*SI-ER-U2OS cells 72 hours post treatment with 4-OHT, with or without Aphidicolin treatment added either 24 or 48 hours post 4-OHT. Workflow of the experiment depicted above the histogram.

3.3. IR-induced Rereplication correlates with IR-induced cytotoxicity in cancer cells

To test if the IR-induced rereplication contributes to cancer cell sensitivity to radiation, we exposed a panel of 13 melanoma cell lines with varying mutational background as well as PIG3V immortalized melanocyte to 9 Gy and assessed the extent of rereplication 48 and 72 h post treatment. While the rereplication population in PIG3V melanocytes was less than 5%, most melanoma cells underwent significant but varying extents of rereplication (7% to 30%), which does not appear to correlate with the proliferation rate of these cells (Fig. 4.4A-B). Interestingly, we observed that the extent of rereplication, both after 48 h or 72 h, induced in this panel of melanoma cells strongly correlates with the sensitivity to IR measured by a clonogenic survival assay after exposure to increasing doses of radiation (Fig. 4.4C-D). Similar results were obtained when we irradiated a panel of 11 breast cancer cells, where the resulting rereplication also correlated with sensitivity to irradiation assessed by clonogenic survival (Fig. 4.4E, data not shown). However, we were unable to assess the radiation sensitivity in the entire breast cancer panel due to the inability of several cell lines to form colonies in culture. These results suggest that IR-induced rereplication represents a major determinant of sensitivity to radiotherapy in cancer cells.

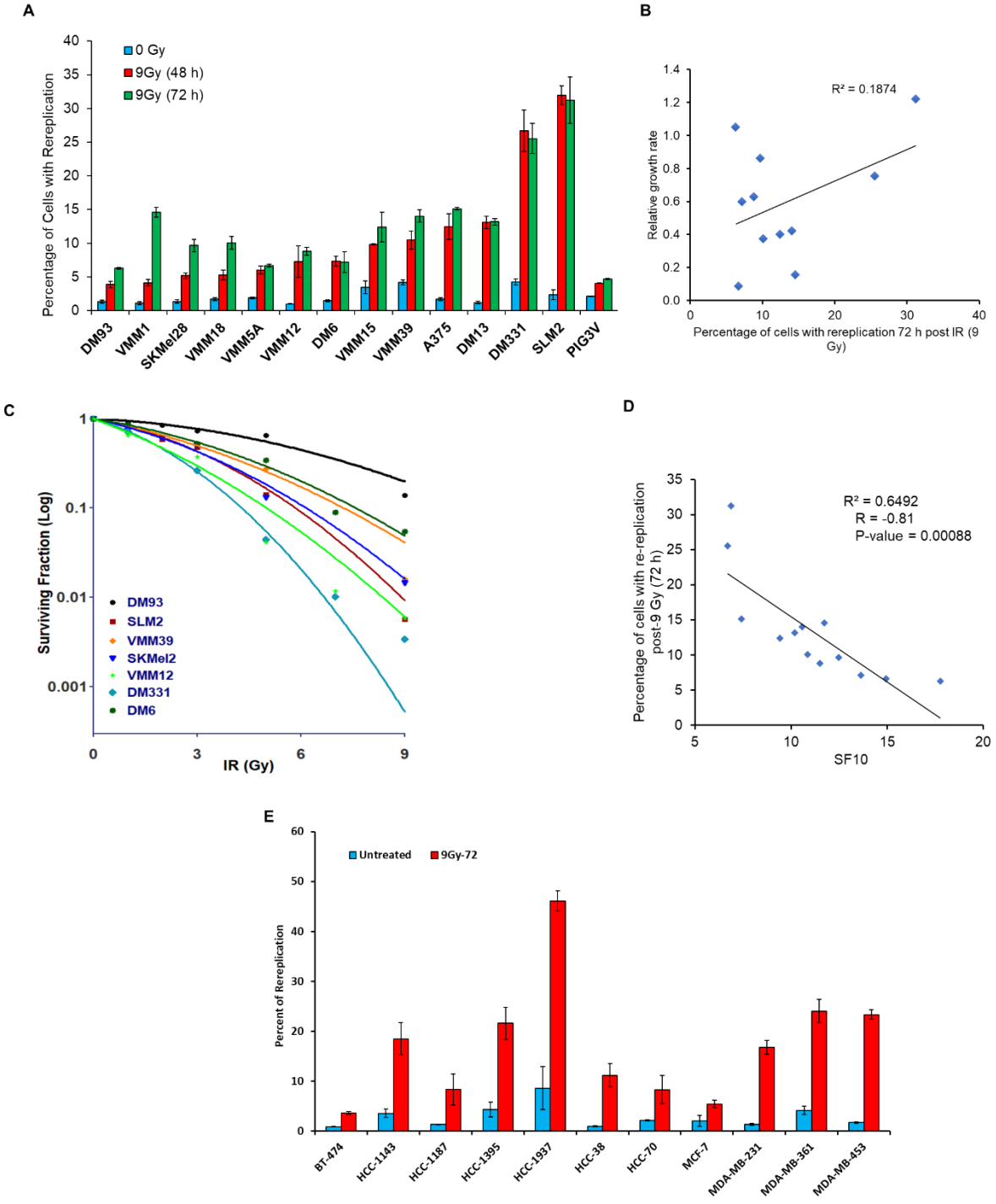
A
Percentage of Cells with Rereplication
0 Gy
9Gy (48 h)
9Gy (72 h)
DM93
VMM1
SKMel28
VMM18
VMM5A
VMM12
DM6
VMM15
VMM39
A375
DM13
DM331
SLM2
PIG3V
B
Relative growth rate
R² = 0.1874
Percentage of cells with rereplication 72 h post IR (9 Gy)
C
Surviving Fraction (Log)
DM93
SLM2
VMM39
SKMel2
VMM12
DM331
DM6
IR (Gy)
D
Percentage of cells with re-replication post-9 Gy (72 h)
R² = 0.6492
R = -0.81
P-value = 0.00088
SF10
E
Percent of Rereplication
Untreated
9Gy-72
BT-474
HCC-1143
HCC-1187
HCC-1395
HCC-1937
HCC-38
HCC-70
MCF-7
MDA-MB-231
MDA-MB-361
MDA-MB-453

Figure 4.4: IR-induced Rereplication correlates with IR-induced cytotoxicity in cancer cells

A. Histogram showing the percentage of rereplication induction in a panel of melanoma cells, including an immortalized melanocyte (PIG3V), 48 and 72 hours post exposure to 9 Gy.

B. Plot showing the correlation between the doubling time of melanoma cells and the extent of rereplication 72 hours post irradiation (quantified in A).

C. Plot showing the clonogenic survival of various melanoma cell lines in response to increasing doses of ionizing radiation. Colonies were counted two weeks post treatment.

D. Plot showing the correlation between the clonogenic survival of melanoma cells, represented by the surviving fraction (SF10 – dose needed to achieve 90% killing) and the extent of rereplication 72 hours post irradiation (quantified in A).

E. Histogram showing the percentage of rereplication induction in a panel of breast cancer cell lines 72 hours post exposure to 9 Gy.

3.4. DIRR does not require origin licensing and is suppressed by the histone methyltransferases SET8 and SUV4-20H1

The cell cycle profiles of rereplicating cells post IR treatment resemble those of rereplication induced following the inactivation of the E3 ubiquitin ligase $CRL4^{CDT2}$ caused by genetic depletion of its substrate adaptor CDT2, or pharmacological inhibition using the neddylation inhibitor MLN4924 (pevonedistat). $CRL4^{CDT2}$ is a major coordinator of cell cycle progression which plays a critical role in preventing aberrant origin relicensing by promoting the timely ubiquitin-dependent proteolysis of licensing factors, including CDT1 and SET8 (Figure 4.5A) (Abbas and Dutta 2011). As described above, the failure to degrade CDT1 or SET8 in S and G2 phases (e.g. following treatment with MLN4924 or CDT2 depletion) promotes origin re-firing leading to robust rereplication in various cancer cells (Abbas et al. 2010; Benamar et al. 2016; Vanderdys et al. 2018). To examine if DIRR is a consequence of the failure to degrade CDT1 following irradiation, we exposed Cal27 cell line to 4 Gy and observed the CDT1 expression levels by immunoblotting. We found that CDT1 was efficiently degraded following irradiation (Fig. 4.5B). This result indicates that $CRL4^{CDT2}$ activity remains intact following irradiation, and is consistent with the findings that $CRL4^{CDT2}$ is activated in response to DNA damage leading to the rapid degradation of CDT1 (Abbas et al. 2010; 2008; Oda et al. 2010; Jorgensen, Schotta, and Sorensen 2013). In addition, siRNA-mediated knockdown of CDT1, which was shown to prevent rereplication induction after deregulated origin licensing following MLN4924 treatment, failed to suppress IR-induced rereplication (Fig. 4.5C). These findings suggest that IR-induced rereplication DIRR is not a consequence of CDT1-mediated origin re-licensing.

In addition to CDT1, failure to degrade SET8 in S-phase, following $CRL4^{CDT2}$ inactivation or the ectopic expression of $CRL4^{CDT2}$-insensitive but catalytically active mutant $SET8^{\Delta pip}$, was also shown to promote robust rereplication in cancer cells (Benamar et al. 2016; Lin et al. 2010). Similar to CDT1, we found that SET8 is also degraded following irradiation in Cal27 suggesting that DIRR is not a consequence of SET8 stabilization (Fig. 4.5B). SET8 is a mono-methyltransferase responsible for the methylation of the lysine 20 residue of Histone 4 (H4K20). SET8 is an essential gene whose transient depletion results in a genome-wide reduction of H4K20 methylation and subsequent defects in origin licensing (Nishioka et al. 2002; Oda et al. 2009; Limas and Cook 2019). The histone methyl mark H4K20me2, whose mono- and di-methylations are catalyzed by the methyltransferases SET8 and SUV4-20H1 respectively, is involved in the recruitment of the Origin Recognition Complex (ORC) via the bromo adjacent homology (BAH) domain of ORC1 (Tardat et al. 2010; Kuo et al. 2012; Beck et al. 2012). Despite the critical role ORC1/2 are believed to play in origin licensing, we found that depletion of ORC1 or ORC2 in HCT116 cells did not prevent rereplication induction following irradiation (Fig. 4.5D) (Shibata et al. 2016). In addition, siRNA-mediated depletion of SET8, which was shown to prevent rereplication induction following MLN4924 treatment, also failed to suppress IR-induced rereplication (Fig. 4.5C). These results indicate that IR-induced rereplication does not require origin licensing mediated by SET8-dependent recruitment of ORC1/2.

Surprisingly, we found that irradiation following siRNA-mediated SET8 depletion in U2OS stimulated rereplication (Fig. 4.5C). Rereplication was also stimulated in U2OS

cells deleted of SUV4-20H1, where H4K20me2 was reduced, but not with SUV4-20H2 (Fig. 4.5E-F). Deletion of SUV4-20H1 also resulted in the stimulation of IR-induced rereplication in VMM39 melanoma cell line, which barely undergoes rereplication post-irradiation (Fig. 4.5G). These results indicate that H4K20 di-methylation, mediated by both SET8 and SUV4-20H1, is important for suppressing IR-induced rereplication. These results altogether demonstrate that IR-induced rereplication is not a consequence of CDT1/SET8 stabilization, is independent of ORC1/2-CDT1-mediated origin licensing, and is suppressed by an H4K20me2-dependent mechanism.

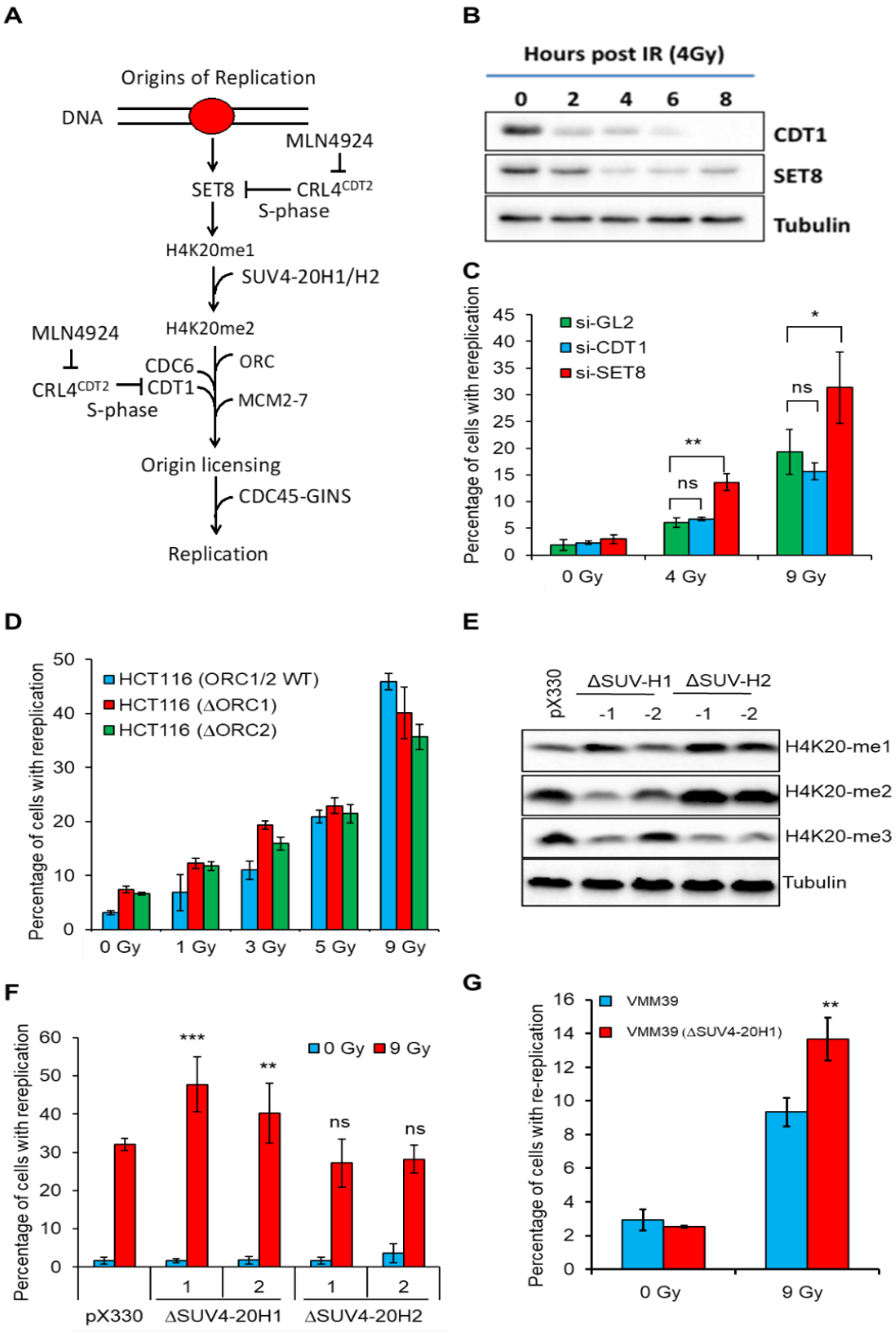
A
Origins of Replication
DNA
MLN4924
SET8
CRL4CDT2
S-phase
H4K20me1
SUV4-20H1/H2
MLN4924
H4K20me2
CDC6
ORC
CRL4CDT2
CDT1
S-phase
MCM2-7
Origin licensing
CDC45-GINS
Replication
B
Hours post IR (4Gy)
0 2 4 6 8
CDT1
SET8
Tubulin
C
Percentage of cells with rereplication
si-GL2
si-CDT1
si-SET8
0 Gy
4 Gy
9 Gy
D
Percentage of cells with rereplication
HCT116 (ORC1/2 WT)
HCT116 (ΔORC1)
HCT116 (ΔORC2)
0 Gy
1 Gy
3 Gy
5 Gy
9 Gy
E
pX330
ΔSUV-H1
ΔSUV-H2
H4K20-me1
H4K20-me2
H4K20-me3
Tubulin
F
Percentage of cells with rereplication
0 Gy
9 Gy
pX330
ΔSUV4-20H1
ΔSUV4-20H2
G
Percentage of cells with re-replication
VMM39
VMM39 (ΔSUV4-20H1)
0 Gy
9 Gy

Figure 4.5. DIRR does not require origin licensing and is suppressed by the histone methyltransferases SET8 and SUV4-20H1

A. Schematic of the key factors involved in origin licensing and the initiation of DNA replication, and their regulation by $CRL4^{CDT2}$ E3 ubiquitin ligase during S-phase to prevent re-firing. The schematic also shows how Pevonedistat (MLN4924) inactivates $CRL4^{CDT2}$ and promotes stabilization of CDT1 and SET8.

B. Western showing the time dependent change in expression levels of CDT1 and SET8 (and Tubulin as a loading control) after exposure to IR (4 Gy) in Cal27 cells.

C. Histogram showing the percentage of rereplication in Cal27 cells depleted from CDT1 or SET8 by siRNA (si-Gl2 as a control). 48 hours post siRNA transfection, the cells were irradiated with 4 or 8 Gy then rereplication was assessed 48 hours post irradiation.

D. Histogram showing the percent of rereplication 72 hours post IR (indicated doses) in HCT116 with deletions in ORC1 or ORC2

E. Immunoblot showing the expression levels of the histone H4K20 methylations (H4K20me1, me2, and me3) in U2OS cells depleted of SUV4-20H1 or SUV4-20H2 (PX330 an empty vector control).

F. Histogram showing the percentage of rereplication 48 hours post 9Gy treatment in U2OS cells depleted of SUV4-20H1 or SUV4-20H2 compared to PX330 empty vector control

G. Histogram showing the percentage of rereplication post 9Gy treatment in VMM39 melanoma cells depleted of SUV4-20H1.

3.5. DIRR is suppressed by 53BP1 recruitment to DSBs to promote NHEJ-mediated repair

We have shown that DSB-induced rereplication appears to be suppressed by an H4K20me2-dependent mechanism. In addition to its role in origin licensing, de novo H4K20 methlyation at DSBs, orchestrated by both SET8 and SUV4-20H1, is known to play an essential, but insufficient, role in the selective binding and recruitment of DSB repair protein p53-binding protein 1 (53BP1) to DSBs to promote nonhomologous end joining repair (NHEJ) (Dulev et al. 2014). This was consistent with our observation that IR-induced 53BP1 foci formation was markedly reduced in cells depleted of SUV4-20H1, but not SUV4-20H2 (Fig. 4.6A-B). The IR-induced rapid recruitment of SET8 and SUV4-20H1 and localization to DNA damage sites is dependent on the DNA-binding subunit Ku70, which cooperates with DNA-PKcs, the catalytic subunit of the nuclear serine-threonine protein kinase (DNAPK), to promote NHEJ-directed repair (Tuzon et al. 2014; Oda et al. 2010; Kong et al. 2009; Dulev et al. 2014; Blackford and Jackson 2017). Based on that, we hypothesize that the DIRR stimulation observed in cells depleted of SET8 or SUV4-20H1 results from defective NHEJ repair.

In order to test if NHEJ plays a role in suppressing DIRR, we first examined the extent of IR-induced rereplication in U2OS and 293T cells lacking the expression of DNA-PKcs. Upon irradiation, we found that rereplication was stimulated both U2OS and 293T cells depleted of DNA-PKcs (Fig. 4.6C and data not shown). In addition, suppression of DNA-PKcs kinase activity following the treatment with the chemical inhibitor NU7441 stimulated DIRR in U2OS and 293T and even in DM93 melanoma cells which does not

undergo significant rereplication post IR (Fig. 4.6D-E, and data not shown). These results indicate that the DNA-PKcs activity is involved in the suppression of DIRR, further suggesting that NHEJ plays an important role in regulating this phenomenon.

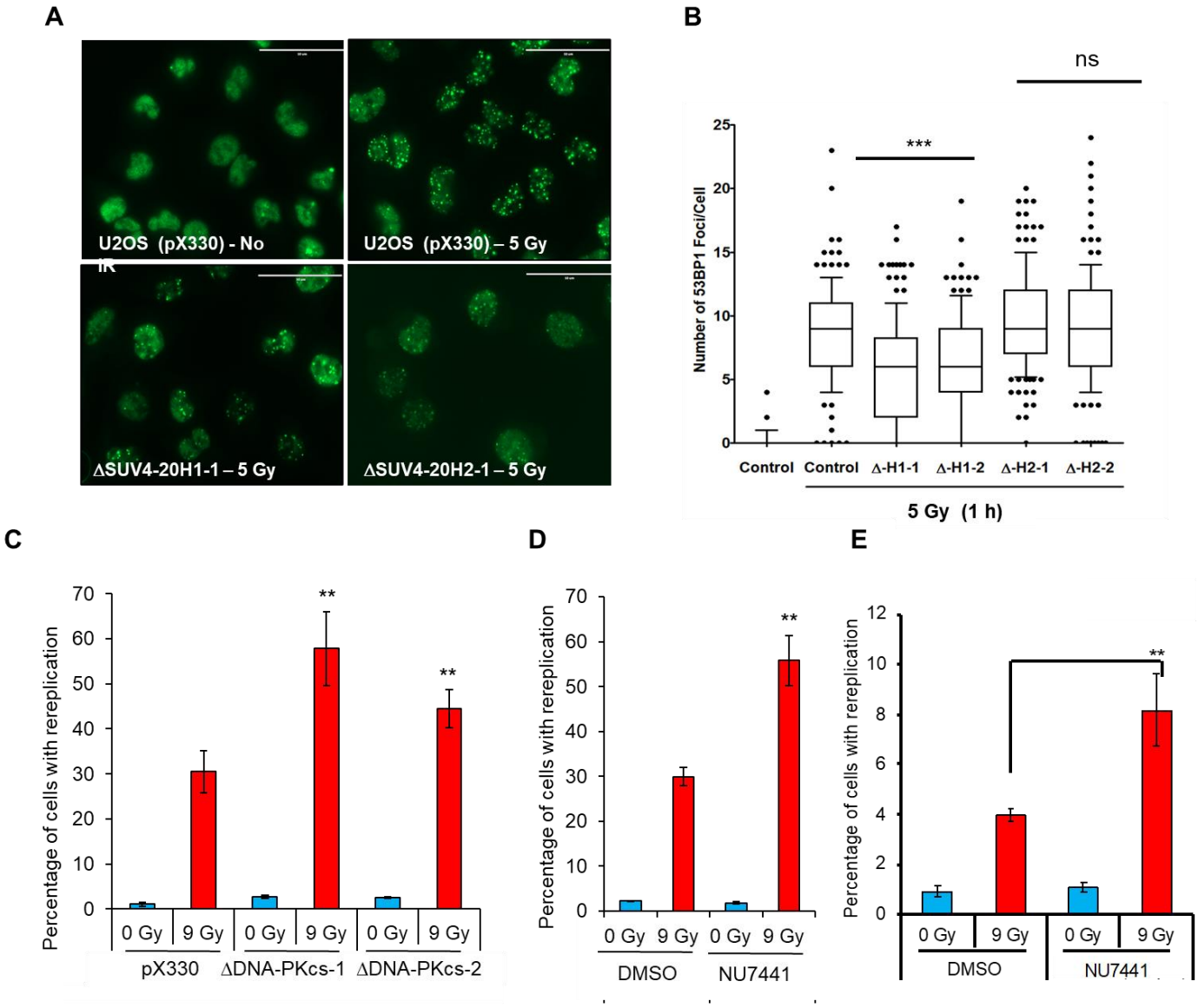

Figure 4.6: Depletion of DNA-PKcs or its pharmacological inhibition suppresses DIRR

A-B. (**A**) Representative immunofluorescence images in U2OS control cells, or cells depleted of SUV4-20H1 or SUV4-20H2 showing 53BP1 foci formation 1 hour after exposure to 5Gy. Quantitation of the number of 53BP1 foci per nucleus in each cell line shown in the box plot in **B**.

C. Histogram showing the extent of rereplication in in two independent U2OS clones depleted of DNA-PKcs 72 hours post exposure to 9Gy.

D-E. Histogram showing the impact of the inhibition of DNA-PKc using the DNA-PKcs inhibitor (NU7441) on rereplication induction 72 hours post irradiation (9Gy) in U2OS (**D**) or DM93 melanoma (**E**). Cells were treated with NU7441 24 hours before exposure to IR.

In the repair of conventional DSBs, 53BP1 is recruited to the damage site, via a host of DNA repair factors and histone marks, to suppress end resection, antagonizing HR and promoting canonical NHEJ (Scully et al. 2019). To examine whether 53BP1 is critical to suppress DIRR, we generated a number of isogenic U2OS and 293T cell lines with CRISPR/Cas9-mediated deletions in 53BP1, its cofactor RIF1, and various DNA repair factors responsible for its recruitment to DSBs, including the ataxia telangiectasia mutated kinase (ATM), the mediator of DNA damage checkpoint proteins 1 (MDC1), and the ubiquitin ligases RNF8 and RNF168 (Panier and Boulton 2013; Scully et al. 2019). We found that deletions in 53BP1, RIF1, and each of the DNA repair factors involved in its recruitment to DSBs (ATM, MDC1, RNF8, or RNF168) stimulated IR-induced rereplication in U2OS and 293T cells (Fig. 4.7A-E). As expected, 53BP1 foci formation following IR exposure was reduced in cells depleted of RIF1, RNF8, or RNF168 (Fig. 4.7F). These results altogether suggest that recruitment of 53BP1 to DSBs is required to suppress IR-induced rereplication.

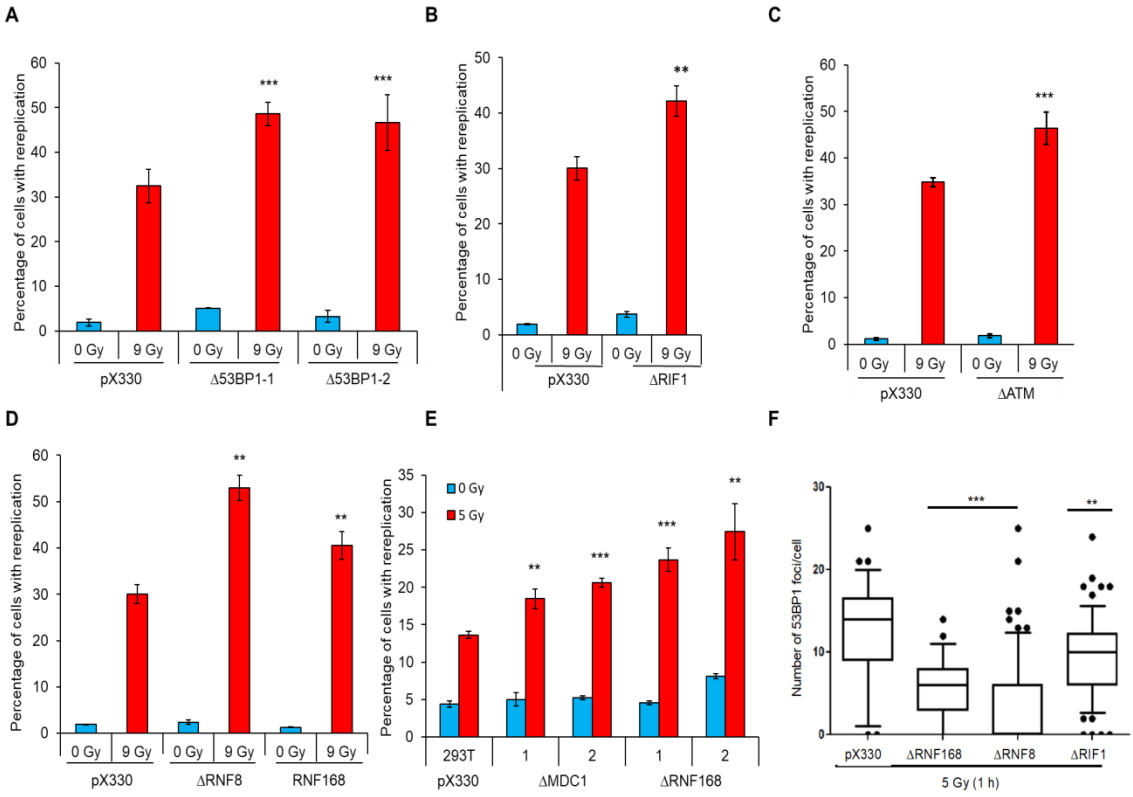
A
B
C
D
E
F
Percentage of cells with rereplication
0 Gy
9 Gy
pX330
Δ53BP1-1
Δ53BP1-2
ΔRIF1
ΔATM
ΔRNF8
RNF168
5 Gy
293T
1
2
ΔMDC1
ΔRNF168
Number of 53BP1 foci/cell
5 Gy (1 h)

Figure 4.7: DIRR is suppressed by 53BP1 recruitment to DSBs promote NHEJ-mediated repair

A. Histogram showing the percentage of rereplication induction 72 hours post IR in control U2OS and two independent clones of U2OS cells depleted in 53BP1.

B-D. Histograms showing the impact of deletions of DNA repair factors on DIRR: RIF1 (**B**), ATM (**C**), RNF8 and RNF168 (**D**) in U2OS cell line compared to a pX330 U2OS control. Rereplication was examined 72 hours post irradiation (9Gy).

E. The percentage of rereplication in 293T cells with sustained deletions in MDC1 or RNF168 (two independent clones for each), compared to 293T pX330 control. Rereplication was monitored 72 hours post exposure to 5 Gy.

F. Box plot showing a quantitation of the number of 53BP1 foci per nucleus in U2OS control or U2OS cells with deletions in RNF168, RNF8, or RIF1 one hour after exposure to 5 Gy. Each set represent the average of a minimum of 100 nuclei in three independent experiments.

3.6. DIRR is promoted by hyper resection at DSBs and RAD51-mediated strand invasion

We showed so far that IR-induced rereplication is stimulated as a result of the failure to recruit 53BP1 to DSBs. The 53BP1-RIF1 complex is recruited to DSBs to restrain DNA hyper resection, which is a long range 5'to 3' nucleolytic digestion of broken DNA ends required for HR-mediated repair, through the recruitment of the Shieldin Complex. Shieldin, a newly characterized four-subunit complex (REV7, SHLD1, SHLD2, SHLD3), is a downstream effector and the primary mediator of the 53BP1-RIF1-dependent DNA end protection that binds ssDNA and "shields" the free DNA ends from end resection exonucleases such as CtIP (CtBP-interacting protein) and EXO1 (Exonuclease 1). While CtIP is involved in the initiation of "short-range" end resection, the "long-range" hyper resection is carried out by a number of nucleases including EXO1 (Gupta et al. 2018; Dev et al. 2018; Mirman et al. 2018; Noordermeer et al. 2018; Ghezraoui et al. 2018; Scully et al. 2019). We found at the depletion of each of the Shieldin subunits SHLD1, SHLD2, or SHLD3 was sufficient to stimulate DIRR without affecting 53BP1 recruitment to DSBs (Fig. 4.8A-B). To directly test if DNA hyper resection plays a role in DIRR, we silenced the expression of CtIP or EXO1 by siRNA prior to irradiation and assessed rereplication. Depletion of each exonuclease in U2OS significantly suppressed rereplication induction following IR (Fig. 4.8C). These results highlight the role the end resection of broken DSBs plays in promoting DIRR.

Following hyper-resection, the long tracks of ssDNA generated are bound by RAD51 to initiate sequence homology search and mediate strand invasion (Scully et al. 2019). We found that the inhibition of strand exchange activity of RAD51 using the small

molecule inhibitor B02 significantly inhibited IR-induced rereplication in a dose dependent manner (Fig. 4.8D) (Huang et al. 2011). These results altogether demonstrate that hyper resection and RAD51-mediated strand invasion are required for DIRR, which is suppressed by the 53BP1-RIF1-mediated recruitment of the Shieldin complex to protect broken DSBs ends from DNA repair exonucleases.

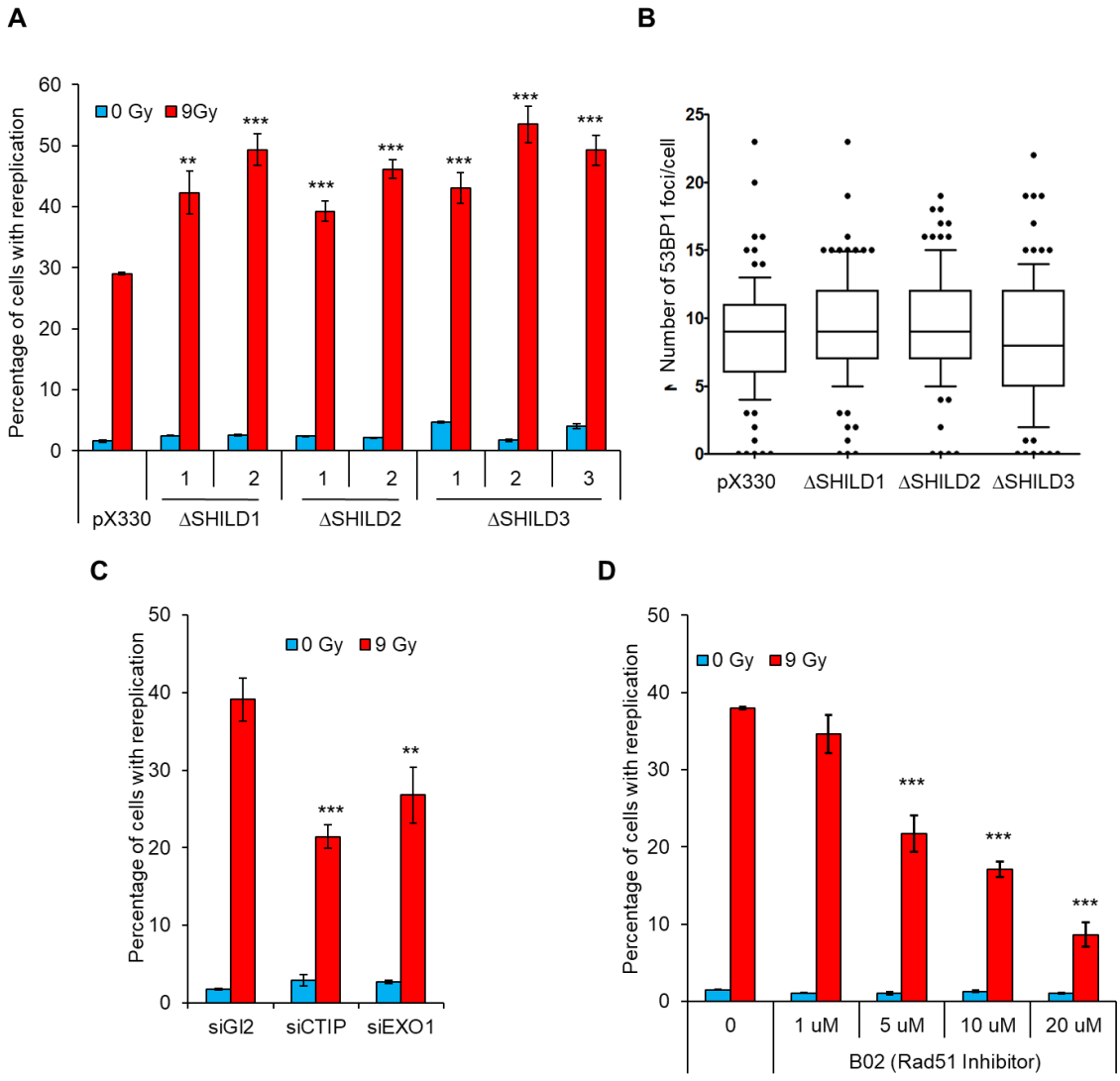
A
Percentage of cells with rereplication
0 Gy
9Gy
pX330
ΔSHILD1
ΔSHILD2
ΔSHILD3
B
Number of 53BP1 foci/cell
pX330
ΔSHILD1
ΔSHILD2
ΔSHILD3
C
Percentage of cells with rereplication
0 Gy
9 Gy
siGl2
siCTIP
siEXO1
D
Percentage of cells with rereplication
0 Gy
9 Gy
0
1 uM
5 uM
10 uM
20 uM
B02 (Rad51 Inhibitor)

Figure 4.8: DIRR is promoted by hyper-resection at DSBs and RAD51-mediated strand invasion:

A. Histogram showing the impact of the deletion of SHLD1, SHLD2, or SHLD3 in U2OS on DIRR. Rereplication was examined in multiple clones of each deletion compared to U2OS control (pX330) 72 hours post irradiation (9Gy).

B. Box plot showing a quantitation of the number of 53BP1 foci per nucleus in U2OS control or U2OS cells with deletions in SHLD1, SHLD2, SHLD3 one hour after exposure to 5 Gy. Each set represent the average of a minimum of 100 nuclei in three independent experiments.

C. Histogram showing the percentage of DIRR (72 hours post 9Gy) in U2OS with siRNA-mediated transient suppression in CTIP or EXO1 compared to G2 control.

D. Histogram showing the dose dependent suppression of IR-induced rereplication as a result of treatment with increasing doses of Rad51 inhibitor B02 on U2OS.

3.7. DIRR is most stimulated in cells incompetent of homologous repair

We have demonstrated that DIRR requires both hyper-resection and strand invasion, which promote HR-mediated repair and proceeds efficiently in the presence of a homologous template in late S-phase or G2. We have also shown that DIRR requires replicative polymerases whose activity is maximal in G1/S and S-phase and decreases as the cell exits S-phase due to CDK phosphorylation (Voitenleitner et al. 1999). Therefore, we anticipate that the extent of IR-induced rereplication is cell-cycle dependent, and DSBs are more susceptible to rereplication in early S-phase compared to late S and G2 where a fully synthesized homologous template is present. To test this hypothesis, synchronized U2OS cells were released from DTB block (G1/S transition) or Nocodazole (G2/M) and exposed to 9 Gy at various stages of the cell cycle (unreleased, 1h, 2h, 4h, 6h, and 8h post DTB release and 3h, 5h post Nocodazole release) (Figure 4.9A-B). Rereplication was assessed using Flow Cytometry 72hrs post irradiation (Figure 4.9C). We found that rereplication was maximal in early and mid S-phase (DTB, 1h, 2h, and 4h post release), then it decreases as cell cycle progresses to reach its lowest extent at early and mid G1 (3h and 5h post nocodazole release) (Figure 4.9C). These results indicate that DSBs are more susceptible to DIRR in the absence of a complete homologous template and the presence of active

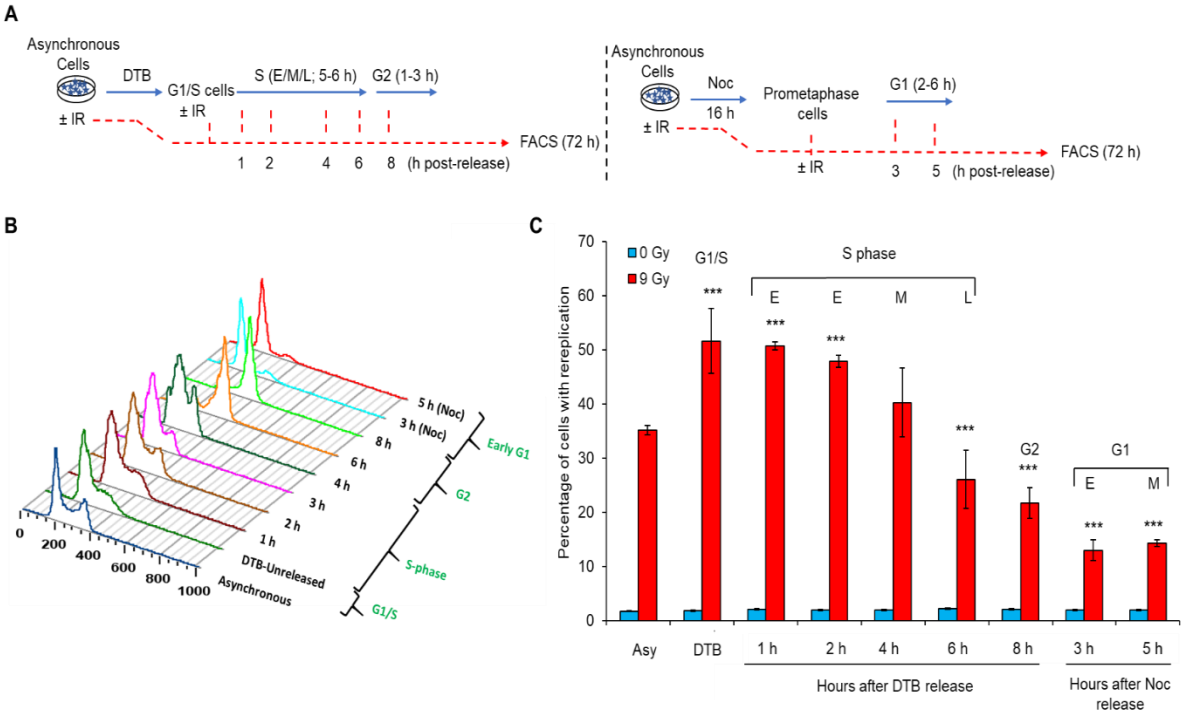
A
Asynchronous Cells
DTB
G1/S cells
S (E/M/L; 5-6 h)
G2 (1-3 h)
± IR
± IR
1 2 4 6 8 (h post-release)
FACS (72 h)
Asynchronous Cells
Noc 16 h
Prometaphase cells
G1 (2-6 h)
± IR
± IR
3 5 (h post-release)
FACS (72 h)
B
5 h (Noc)
3 h (Noc)
8 h
6 h
4 h
3 h
2 h
1 h
DTB-Unreleased
Asynchronous
0 200 400 600 800 1000
Early G1
G2
S-phase
G1/S
C
0 Gy
9 Gy
G1/S
S phase
E E M L
G2
G1
E M
Percentage of cells with rereplication
0 10 20 30 40 50 60 70
Asy DTB 1 h 2 h 4 h 6 h 8 h 3 h 5 h
Hours after DTB release
Hours after Noc release

Figure 4.9: Cell cycle dependence of DIRR in U2OS cells

A. Schematic of cell cycle synchronization using thymidine or nocodazole in U2OS.

B. Representative flow cytometry profiles of cells collected at the indicated time post release from DTB or nocodazole.

C. Histogram showing the percentage of rereplication in U2OS cells irradiated at the indicated times following release from DTB or nocodazole (as depicted in A and B). Asy: asynchronous U2OS, E: early, M: Mid, L: late. Rereplication was examined 72 hours post treatment with 9 Gy.

4. Discussion:

In this chapter we have described a previously uncharacterized mechanism of cytotoxicity that results from the exposure to ionizing radiation or agents that induce DSBs in cancer cells, namely the induction of DNA rereplication. DSB lesions are widely regarded as the primary contributor to IR-induced cell killing. The toxicity of radiation-induced DSBs is attributed to the generation of severe forms of genomic instability including chromosomal rearrangements, translocations, mutations, and genomic amplifications, that result from the erroneous joining of broken DNA ends (Mladenov et al. 2013; Hahn, Nevaldine, and Morgan 1990; Mavragani et al. 2017). In addition to chromosomal aberrations, a significant loss of DNA sequences with varying sizes is readily observed at many IR-induced DSB junctions due to the activity of DNA nucleases at breakpoints prior to joining or repair (Povirk 2006). Likewise, rereplication can be catastrophic to the cell due collapsed replication forks and the accumulation of harmful replication intermediates. Rereplication has been shown to lead to the generation of SSBs, DSBs, mutations, chromosome breakage, genomic amplifications, apoptosis, senescence, and oncogenesis (Abbas, Keaton, and Dutta 2013; Liontos et al. 2007; Bui and Li 2019; Truong and Wu 2011).

The observed increase in genomic DNA as a result of treatment with radiation or other DSB-inducing agents does not require mitotic entry nor it appears to be a result of chromosomal missegregation or failed cytokinesis. This phenomenon also cannot be attributed to repair-mediated DNA synthesis or region-specific genomic amplifications which are small in size whereas DIRR exhibits an extensive increase in genomic content

that is large enough to be readily detected by flow cytometry. In addition, the fact that IR-induced rereplication is enhanced in the absence of key DNA damage sensors and repair factors, such as ATM and DNA-PKcs, further uncouples DIRR from DNA repair synthesis. Moreover, since depletion of the catalytic subunit of polymerase delta POLD3, which is critical for DNA synthesis during break-induced replication (BIR), did not suppress rereplication, we believe that the DSB-induced DNA synthesis proceeds through a mechanism distinct from the one utilized by break-induced replication (BIR; Data not shown) (Kramara, Osia, and Malkova 2018). These results altogether, and in addition to the appearance of a significant CsCl fraction of DNA doubly labeled with Brdu (H:H) after exposure to IR for a single round of S-phase, and the requirement of DNA replicative polymerases further confirm this DSB-induced DNA synthesis as *bona fide* rereplication.

In Chapter Three, we have shown how rereplication induction as a result of deregulated origin licensing sensitizes cells to ionizing radiation and enhances IR-induced suppression of head and neck carcinoma tumors *in vivo* (Vanderdys et al. 2018). In this Chapter, we showed that cancer cells from various epithelial origins undergo varying extents of rereplication as a result of IR treatment, or other DSB-inducing agents. While some cancer cell lines underwent robust rereplication after exposure to IR, others underwent very little to no rereplication. We were unable to identify a clear correlation between the primary oncogenic drivers amongst the various cell lines we examined and their susceptibility to DIRR. However, the extent of IR-induced rereplication did correlate with IR-induced toxicity in melanoma and breast cancer cell line panels suggesting that

susceptibility to DIRR can be regarded as a key determinant of sensitivity to radiotherapy in cancer cells.

Our findings shed the light on fundamental differences between DSB-induced rereplication and the one that results from deregulated origin licensing, such as the one that results from the inactivation of $CRL4^{CDT2}$. While the latter is initiated at origins of replication, we speculate that DIRR is likely to be nucleated at DSBs, given that its extent correlates with the number of DSBs induced with increasing IR does. In fact, we found that, unlike the rereplication induced by abnormal origin re-firing, DIRR does not require the canonical ORC1/2-CDT1 origin licensing, and is surprisingly unaffected in cancer cells depleted of CDT1 or ORC1/2 (Benamar et al. 2016; Abbas and Dutta 2011). Depletion of the monomethyl transferase SET8, which suppresses rereplication induced by deregulated origin licensing, surprisingly stimulated DIRR instead (Benamar et al. 2016). This stimulation, observed also in cells depleted of the di-methyltransferase SUV4-20H1 but not SUV4-20H2, suggests that DIRR proceeds in cancer cells through an H4K20me2-dependent mechanism. Since de novo methylation of H4K20 at DSBs is essential, but not sufficient, to recruit 53BP1 to the damage site, we examined if the DNA repair machinery plays a role in regulating DIRR (Dulev et al. 2014). We found that depletion of key DNA repair factors, such as ATM, 53BP1, and DNA-PKcs, stimulated DIRR while not effecting rereplication induced after deregulated origin licensing. We demonstrated that DIRR is suppressed by the recruitment of the 53BP1-RIF1-Shieldin complex to DSBs to shield the exposed broken ends from various resection exonucleases needed to promote HR-mediated repair. Inhibition of RAD51-mediated strand invasion significantly suppressed

rereplication further highlighting the role HR-mediated repair play in promoting DIRR. Susceptibility to DIRR was found to be cell cycle dependent. Exposure to IR during early and mid S-phase resulted in maximal rereplication which decreases as the cell progresses through cell cycle. DIRR reached its minimum extent at early G1 which is consistent with the need of replicative polymerases and homologous recombination repair factors. The lack of complete homologous sequences early during S-phase and the sheer number of IR-induced DSBs compel the broken DNA ends to invade non-homologous sequences resulting in an HR-mediated aberrant long-range DNA synthesis (Model - Fig. 4.10).

In conclusion, our work presents DIRR as an origin-independent cytotoxic phenomenon in cancer cells that arise from the exposure to IR or other DSB-inducing agents. DIRR appears to be promoted by hyper resection of unshielded broken DSB ends that invade non-homologous sequences early in S-phase. Additional studies are needed to uncover more details on the mechanism underlying this phenomenon and how can DIRR be exploited clinically to enhance IR-based therapies.

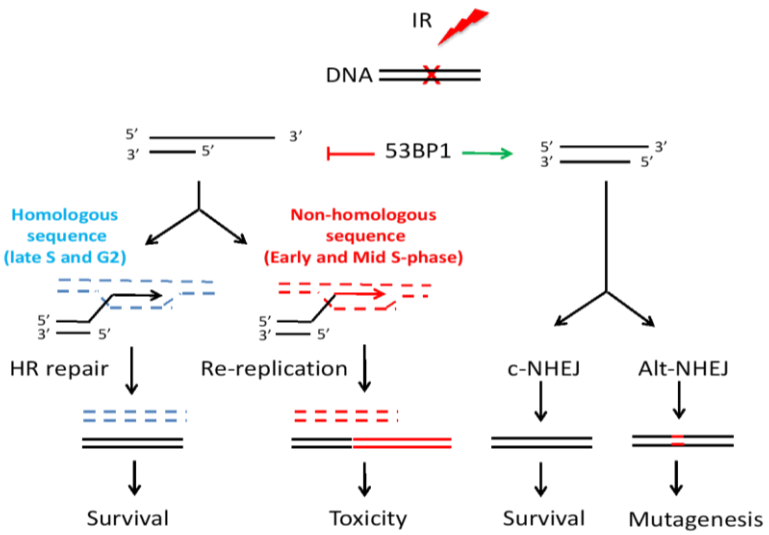

Figure 4.10: Proposed Model.

5. Materials and Methods:

5.1. Cell culture:

U2OS osteosarcoma cells, HEK 293T embryonic kidney cells, and breast cancer cells (MDA-MB-231 were maintained in Dulbecco's modified Eagle's medium (DMEM) supplemented with 10% fetal bovine serum (FBS) and 1% penicillin/streptomycin (P/S). The previously described A*si*SI-ER-U2OS cell line (Iacovoni et al. 2010) was maintained in the same culture media used for parental U2OS cells. The human melanoma cell lines VMM39, VMM1, VMM18, VMM5A, VMM15, and VMM12 were established from metastatic lesions of patients at the University of Virginia (IRB #5202, Dr. CL. Slingluff). DM93, DM331, DM13, DM112, DM6, and SLM2 melanoma cell lines were established from metastatic lesions by Dr. H.F. Seigler at Duke University (Hogan et al. 2005; Slingluff et al. 1993; Molhoek et al. 2008; Yamshchikov et al. 2001; 2005; Kittlesen et al. 1998; Huntington et al. 2004). SK-MEL-2 and SK-MEL-28 melanoma cells were obtained from the American Type Culture Collection (ATCC, Manassas, VA). All melanoma cells were grown in RPMI medium supplemented with 10% FBS and 1% P/S. Non-malignant human PIG3V melanocytes (Poole et al. 2000) were maintained in Media 254 (ThermoFisher Scientific) containing 1% human melanocyte growth supplement (HMGS), 5% FBS, and 1% P/S. The human head and neck squamous cell carcinoma (HNSCC) cell lines Cal27, FaDu, and SCC25 were obtained from ATCC (Manassas, Virginia). The UNC7 HNSCC cells were provided by Dr. Wendell Yarbrough (Vanderbilt University, Nashville, Tennessee). HNSCC cells were maintained in DMEM/Ham's nutrient mixture F12 (Sigma Aldrich) supplemented with 10% FBS and 1% P/S. Human h-Tert

immortalized keratinocytes (OKF6-TERT2) were obtained from Dr. James Rhienwald (Harvard Medical School), and were cultured in GIBCO keratinocyte serum-free medium (K-sfm) supplemented with 25 µg ml^{-1} BPE, 0.4 mM $CaCl_2$, 0.2 ng ml^{-1} EGF, and 1% P/S. The colorectal cancer HCT116 cell lines were obtained from Dr. Anindya Dutta (University of Virginia), and were maintained in McCoy's 5A (Modified) Medium supplemented with 10% FBS and 1% P/S. All cells were grown at 37°C in 5% CO_2, and were periodically tested for mycoplasma contamination (MycoAlert; Lonzo Group Ltd). The identity of the cells was validated by STR profiling (ATCC), by morphological examination, and in some cases, by analysis of chromosome number in metaphase spreads.

5.2. Flow cytometry:

The effect of IR and MLN4924 on the cell cycle and rereplication induction was assessed by flow cytometry with propidium iodide (PI) or bromodeoxyuridine (BrdU) staining. Cells were treated with various doses of MLN4924 (Active Biochem) or exposed to various doses of IR for different time points before harvesting. Cells were washed with ice-cold PBS and resuspended in ethanol (70%). Cells were subsequently treated with a PI staining buffer (50 µg ml^{-1} PI (Sigma Aldrich), 10 µg ml^{-1} DNase-free RNase A, 0.05% NP40). A FACscan (Becton Dickinson) flow cytometer was used to analyse the samples, and G_0/G_1, S, and G_2/M fractions were segmented. Subsequent analysis using FlowJo and ModFit software was used to determine the fraction of cells with genomic content of greater than G2/M (rereplication). For BrdU staining, cells were pulse-treated with BrdU (10 nM) for 1 h in the dark before harvesting. Cells were washed with PBS and staining

solution before they were fixed and permeabilized according to the manufacturer's instructions (BD Biosciences, San Diego, CA). Cells were subsequently stained with anti-BrdU antibody solution at room temperature for 20 min, washed, and stained with 7-AAD (BD Biosciences) for 30 min at 4°C. The cells were resuspended in 1 ml of staining buffer, and stored at 4°C overnight before analysis. Samples were analysed on a FACscan (Becton Dickinson) flow cytometer, and the fraction of BrdU positive cells was determined using FlowJo and ModFit software. Where indicated, cells were treated with ATM kinase inhibitor KU-55933, DNA-PKcs kinase inhibitor NU-7441, or Rad51 inhibitor B02 (all purchased from TOCRIS Bioscience) 24 h before irradiation. The DNA LIG4 inhibitor SCR7 (#SML1546, Sigma Aldrich) was added 24 h before irradiation, and was replenished every 24 h. Analysis of rereplication induction by FACS (PI staining) following the induction of DNA damage by etoposide (1 μg ml^{-1}, TOCRIS), doxorubicin (0.1 μM, Sigma Aldrich), or by UV (100 J m^{2-}) was performed 72 following treatment.

5.3. Cell synchronization and exposure to IR:

Asynchronously growing U2OS cells were synchronized at the G1/S boundary by double thymidine block (DTB) and release. Briefly, U2OS cells were treated with 2 mM thymidine (ACROS Organics) for 14 h, then washed with PBS, and fresh medium was added. After 9 h, cells were treated again with thymidine (2 mM), and incubated for another 14 h. Cells were released from G1/S arrest by washing with PBS and addition of fresh media. Cell synchronization was monitored by flow cytometry. Cells synchronized at various stages of the cell cycle were exposed to 9 Gy of X-ray (Gamma irradiation was performed at the University of Virginia Small Animal Radiation Research Platform

[SARRP; Xstrahl]), and were incubated for 48 or 72 h prior to analysis by FACS. In another scheme, U2OS cells were synchronized in prometaphase by treating the cells with nocodazole (0.5 µg ml^{-1}, M1404; Sigma Aldrich) for 24 h. Prometaphase cells were collected by mitotic shake off, counted, washed, and re-seeded with or without nocodazole, and exposed to 9 Gy at various time points following release from the nocodazole block. Parallel samples were collected for flow cytometric analysis to determine the phase in which the various cells were exposed to IR.

5.4. Meselson-Stahl Caesium Chloride Gradient Ultracentrifugation:

U2OS cells were synchronized at the G1/S boundary using double thymidine block (DTB). BrdU (100 µM) was added upon release. Eight hours post-release from the DTB, cells were either mock-treated or irradiated with 9 Gy, and were treated with nocodazole (0.5 µg ml^{-1}) and BrdU (100 µM) with or without aphidicolin (2 µM; EMD Millipore Corp). Cells were collected 36 h post-irradiation. A sample not treated with BrdU was collected in parallel, and served as an unstained negative control. Cells were lysed in lysis buffer (100 mM NaCl, 10 mM Tris-HCl pH 8, 25 mM EDTA, 0.5% SDS), and proteins were digested with 20 µg of proteinase K overnight at 55°C. Genomic DNA was extracted by Phenol/Chloroform/isoamyl alcohol extraction and ethanol precipitation. Purified DNA (50 µg in 200 µl total volume) was sheared by sonication for 2 sec into fragments ranging from 0.5 to 3 kb. Digested DNA was mixed with 0.96 g ml^{-1} Caesium Chloride in TE Buffer (giving a density of 1.71) in 13 ml Polyallomer Quick-Seal ultracentrifuge tubes (Beckman). Samples were spun at 44,000 g in a 70.1 Ti Rotor (Beckman) for 66 h. fractions (200 µl) were collected from the bottom of the tubes, and the DNA concentration

was measured using Qubit fluorometric quantification. The percentage of DNA exhibiting rereplication (containing H:H DNA) was calculated by measuring the area under the curves from three independent experiments using GraphPad Prism v.7.0.

5.5. Cell lysis, SDS-PAGE, and immunoblotting:

Cells were lysed with Radioimmunoprecipitation assay (RIPA) lysis buffer (50 mM Tris, pH 8.0; 150 mM NaCl, 1% NP-40; 0.5% sodium deoxycholate; 0.1% SDS) supplemented with 1X Halt Protease and Phosphatase Inhibitor Cocktail (Thermo-Scientific). Equal amounts of protein lysates were separated on polyacrylamide 8–12% gels (BioRad, Hercules, CA) by electrophoresis and transferred to nitrocellulose membranes. Membranes were blocked with 1X phosphate buffered saline, 1% Tween 20 (Sigma Aldrich; PBST) with 5% milk (or 5% BSA) for one hour at room temperature, and incubated with the appropriate primary antibodies in 1X PBST for 1 h at room temperature or overnight at 4°C. The membranes were washed 5 times with 1X PBST and incubated with horseradish peroxidase conjugated secondary anti-mouse or anti-rabbit IgG (1:5000, Cat # P0161 and P0448, respectively; DAKO) in 1X PBST for 1 h at room temperature. Immunoblot signals were detected by enhanced chemiluminescence (Millipore). Primary antibodies recognizing the following proteins were used: ATM (1:1000, ab78; Abcam), tubulin (1:1000, sc-53646; Santa Cruz), SET8 (1:1000, C18B7; Cell Signaling), mono-methyl Histone H4 (K20) (1:500, #9724; Cell Signaling), di-methyl Histone H4 (K20) (1:500, #9759; Cell Signaling), Tri-methyl Histone H4 (K20) (1:500, #5737; Cell Signaling), DNA-PKcs (1:1000, ab44815; Abcam), 53BP1 (1:5000, N100-304; Novus Biologicals) POLD3 (1:1000, H00010714-M01; Abnova), POLQ (1:1000, H00010721-M09; Abnova),

RIF1 (1:1000, A300-569A-M; Bethyl Laboratories), RNF8 (1:1000, sc-2711462; Santa Cruz), RNF168 (1:1000, ABE367; Millipore), CtIP (1:1000, sc-271339, Santa Cruz), EXO1 (1:1000, ab95012; Abcam), XRCC4 (1:1000, sc-271087; Santa Cruz), XLF (1:1000, A300-730A-M; Bethyl Laboratories), NBS1 (1:1000, ab32074; Abcam), MDC1 (1:25,000, ab11171; Abcam), LIG1 (1:1000, 18051-1-AP; Proteintech), and LIG4 (1:1000, HPA001334; Sigma Aldrich).

5.6. Immunofluorescence:

Cells were grown on coverslips and fixed in 4% Paraformaldehyde for 10 min (or 2% for 30 min). Slides were washed three times with PBS, then permeabilized in extraction buffer (0.1% Triton-X in PBS) for 10 minutes. Slides were washed 3X in wash buffer (0.5% BSA in 1X PBS) for 5 min, blocked in 2% BSA in PBS for 45 min, washed (3x 5 min each), and then incubated with anti-53BP1 (1:1000, N100-304; Novus Biologicals) in 0.5% BSA with 0.1% Triton-X overnight at 4°C. Slides were washed and incubated with Alexa Fluor 488 anti-IgG (1:500; Life Technologies) in 0.5% BSA in PBS for 1 h at room temperature. Slides were washed, dried, and mounted with 4′, 6′-diamidino-2-phenylindole (DAPI; #H-1200, Vector Laboratories, Inc.), and 53BP1 foci were visualized and quantified using EVOS FL cell imaging system fluorescence microscope (Advanced Microscopy Group). A minimum of 100 nuclei from random fields were examined for each group.

5.7. RNA interference:

Transfections with siRNAs were performed using Lipofectamine RNAi-max according to the manufacturer's protocol (Invitrogen, Carlsbad, CA). Cells were seeded at 25% confluence and transfected with the individual siRNAs (10 nM each) in the

appropriate growth media. Cells were harvested 48 and 96 h post-transfection for cell cycle analysis. The following siRNAs were used (sense strand): si-GL2 (control): 5′-AACGUACGCGGAAUACUUCGA-3′; si-CDT1: 5′-AACGUGGAUGAAGUACCCGAC-3′; si-SET8: 5′-GAUUGAAAGUGGGAAGGAA-3′; si-EXO1: 5'-CAAGCCUAUUCUCGUAUUU-3'; si-CtIP 5'-GCUAAAACAGGAACGAAUC-3'.

5.8. Gene targeting by CRISPR/Cas9, and establishment of individual knockout cell lines:

Two single guide-RNAs (sgRNAs) targeting the various genes at two proximal (within 300 bp) sites in early exons of each gene were cloned into pX330 vector (Addgene #42230) containing a human codon-optimized *Sp*Cas9 endonuclease using BbsI restriction enzyme to cut sites downstream of the U6 promoter. Plasmids were amplified in DH5□ bacteria (Invitrogen), purified using the QIAprep Spin Miniprep Kit according to the manufacturer's instructions (Qiagen), and verified by Sanger sequencing (Eurofins Scientific) using U6-specific primers. Various cell lines were transfected along with pMSCV vector containing the puromycin resistance gene (Clontech) using Lipofectamine 2000 according to the manufacturer's instructions (Invitrogen). At 24 h post-transfection, cells were incubated with puromycin (2 μg ml^{-1}) for 48 h, and were subsequently seeded at low density to obtain single colonies. Individual clones were propagated in culture in the appropriate growth medium, and aliquots were frozen. Samples of each clone were lysed overnight at 55°C in lysis buffer (100 mM NaCl, 10 mM Tris-HCl pH 8, 25 mM EDTA, 0.5% SDS) supplemented with 20 μg proteinase K. Genomic DNA was extracted by

phenol/chloroform/isoamyl alcohol followed by ethanol precipitation. Genotyping was performed using PCR amplification of the targeted locus with gene-specific primers followed by Sanger sequencing (Eurofins Scientific). The deletion of the various genes in the knockout-positive cell lines was further confirmed by immunoblotting. The following sg-RNAs (sense strand) were used to generate the various knockout clones: ATM: sg-ATM-1: 5'-TCAACTAGAACATGATAGAG-3', sg-ATM-2: 5'-GATTCGAGATCCTGAAACAA-3'; PRKDC: sg-DNA-PKcs-1: 5'-GAGCCGGTGTGCGTTGCTCC-3', DNA-PKcs-2: 5'-GCCGGTCATCAACTGATCCG-3'; TP53BP1: sg-53BP1-1: 5'-GACGCACAAAGAAAATCCTG-3', sg-53BP1-2: 5'-GAACGAGGAGACGGTAATAG-3'; XRCC4: sg-XRCC4-1: 5'-AGTATAACTCATTTTCTACA-3', sg-XRCC4-2: 5'-TTTGTTATTACACTTACTGA-3'; RIF1: sg-RIF1-1: 5'-CCTCGCGCCGCTGTTGGAGA-3', sg-RIF1-2: 5'-ACGCTTACCTGACTCTGACC-3'; RNF8: sg-RNF8-1: 5'-CCGGGGTCGAGTAGGCGATG-3', sg-RNF8-2: 5'-TTCGTCACAGGAGACCGCGC-3'; RNF168: sg-RNF168-1: 5'-TCGCTGTCCGAGTGCCAGTG-3', sg-RNF168-2: 5'-GGTATCGTCGTGGACTCGGT-3'; NHEJ1: sg-XLF-1: 5'-TGGGCGTGGCTACAGCTTGC-3', sg-XLF-2: 5'-TGAACAGGTGGACACTAGTG-3'; NBN: sg-NBS1-1: 5'-GCGTTGAGTACGTTGTTGGA-3', sg-NBS1-2: 5'-TAACTTTTCTGTAACCAACC-3'; MDC1: sg-MDC1-1: 5'-GGACACCCAGGCTATTGACT-3', sg-MDC1-2: 5'-GTAGGGCGGCTACATATCTT-3'; LIG1: sg-LIG1-1: 5'-AGAGTGACTCTCCGGTGAAG-3', sg-LIG1-2: 5'-TTAGCCCTGCTAAAGGCCAG-3'; LIG4: sg-LIG4-1: 5'-

CACAAACTTCACAAACTGTT-3', sg-LIG4-2: 5'-GCAATGAGACTAATTCTTCC-3'; POLQ: sg-POLQ-1: 5'-TGAATCTTCTGCGTCGGAGT-3', sg-POLQ-2: 5'-GATTCGTTCTCGGGAAGCGG-3'; KMT5B: sg-SUV4-20H1-1: 5'-TGACTAAATGCACCTGGGTC-3', sg-SUV4-20H1-2: 5'-AAAATTACAGCACACGGGGA-3'; KMT5C: sg-SUV4-20H2-1: 5'-GCCGGAAAGTGGCTTTACCA-3', sg-SUV4-20H2-2: 5'-AGATCGTGTCCACTCGTGCT-3'; SHLD1: sg-SHLD1-1: 5'-TCAGCGTGTGACATAAGAGA-3', sg- SHLD1-2: 5'-ACAGCGAGGCTTTCAGTTCT-3'; SHLD2: sg- SHLD2-1: 5'-ATTGGTTCTCCAGATCTTAG-3', sg- SHLD2-2: 5'-CTAGACTGAGTGATATAACT-3'; SHLD3: sg- SHLD3-1: 5'-TGTGAGAGTGATCCCACACA-3', sg- SHLD3-2: 5'-AGCTTCCACTCAGACCTAAA-3'.

5.9. Clonogenic survival assays:

Radiation sensitivity in the various cell clones was established using a clonogenic survival assay. Briefly, the various cell lines were trypsinized, counted using a Countess Automated Cell Counter (Invitrogen), and serial dilutions of cells were seeded in 10 cm dishes in triplicate. Twenty-four hours after seeding, cells were irradiated (1-9 Gy) and cultured for two weeks. Once colonies reached the appropriate size (>50 cells each), cells were washed in ice-cold PBS, fixed in cold methanol for 10 min, and stained with crystal violet (0.5%) for 10 min. Plates were washed with water, dried, and images were captured using Imagelab software (BioRad). QuantityOne software (BioRad) was used to quantitate the number of colonies, and survival curves were established based on the linear quadratic

model, using the formula $S=e^{-\alpha D-\beta D2}$; where S represents the surviving fraction and D represents the dose of irradiation. Results are represented as mean ± standard deviation (SD) from three independent experiments normalized to the corresponding non-irradiated plates for each group.

5.10. Statistical analyses:

All statistical analyses were performed using Excel and GraphPad Prism v. 7.0. At least three independent experiments were performed for each data set. No statistical methods were used to predetermine the sample size. Numerical data were expressed as mean ± standard deviation (SD) and the statistical significance in each case was calculated by two-tailed Student's *t*-test (Mann-Whitney *U*-test). *P*-values were determined for all analyses, and $p < 0.05$ was considered significant. *$p < 0.05$, **$p < 0.01$, ***$p < 0.001$. For correlations, a Spearman correlation was used, and *p*-values < 0.05 were considered significant.

6. References:

Abbas, Tarek, and Anindya Dutta. 2011. “CRL4Cdt2: Master Coordinator of Cell Cycle Progression and Genome Stability.” *Cell Cycle*. Taylor and Francis Inc. https://doi.org/10.4161/cc.10.2.14530.

Abbas, Tarek, Mignon A. Keaton, and Anindya Dutta. 2013. “Genomic Instability in Cancer.” *Cold Spring Harbor Perspectives in Biology* 5 (3): a012914. https://doi.org/10.1101/cshperspect.a012914.

Abbas, Tarek, Etsuko Shibata, Jonghoon Park, Sudhakar Jha, Neerja Karnani, and Anindya Dutta. 2010. “CRL4Cdt2 Regulates Cell Proliferation and Histone Gene Expression by Targeting PR-Set7/Set8 for Degradation.” *Molecular Cell* 40 (1): 9–21. https://doi.org/10.1016/j.molcel.2010.09.014.

Abbas, Tarek, Uma Sivaprasad, Kenta Terai, Virginia Amador, Michele Pagano, and Anindya Dutta. 2008. “PCNA-Dependent Regulation of P21 Ubiquitylation and Degradation via the CRL4Cdt2 Ubiquitin Ligase Complex.” *Genes and Development* 22 (18): 2496–2506. https://doi.org/10.1101/gad.1676108.

Beck, David B., Adam Burton, Hisanobu Oda, Céline Ziegler-Birling, Maria Elena Torres-Padilla, and Danny Reinberg. 2012. “The Role of PR-Set7 in Replication Licensing Depends on Suv4-20h.” *Genes and Development* 26 (23): 2580–89. https://doi.org/10.1101/gad.195636.112.

Benamar, Mouadh, Fadila Guessous, Kangping Du, Patrick Corbett, Joseph Obeid, Daniel Gioeli, Craig L. Slingluff, and Tarek Abbas. 2016. “Inactivation of the CRL4-CDT2-

SET8/P21 Ubiquitylation and Degradation Axis Underlies the Therapeutic Efficacy of Pevonedistat in Melanoma." *EBioMedicine* 10 (August): 85–100. https://doi.org/10.1016/j.ebiom.2016.06.023.

Blackford, Andrew N., and Stephen P. Jackson. 2017. "ATM, ATR, and DNA-PK: The Trinity at the Heart of the DNA Damage Response." *Molecular Cell*. Cell Press. https://doi.org/10.1016/j.molcel.2017.05.015.

Bui, Duyen T., and Joachim J. Li. 2019. "DNA Rereplication Is Susceptible to Nucleotide-Level Mutagenesis." *Genetics* 212 (2): 445–60. https://doi.org/10.1534/genetics.119.302194.

Dev, Harveer, Ting-Wei Will Chiang, Chloe Lescale, Inge de Krijger, Alistair G Martin, Domenic Pilger, Julia Coates, et al. 2018. "Shieldin Complex Promotes DNA End-Joining and Counters Homologous Recombination in BRCA1-Null Cells." *Nature Cell Biology* 20 (8): 954–65. https://doi.org/10.1038/s41556-018-0140-1.

Dulev, Stanimir, Johnny Tkach, Sichun Lin, and Nizar N Batada. 2014. "SET8 Methyltransferase Activity during the DNA Double-Strand Break Response Is Required for Recruitment of 53BP1." *EMBO Reports* 15 (11): 1163–74. https://doi.org/10.15252/embr.201439434.

Fouad, Shahd, Owen S. Wells, Mark A. Hill, and Vincenzo D'Angiolella. 2019. "Cullin Ring Ubiquitin Ligases (CRLs) in Cancer: Responses to Ionizing Radiation (IR) Treatment." *Frontiers in Physiology*. Frontiers Media S.A. https://doi.org/10.3389/fphys.2019.01144.

Ghezraoui, Hind, Catarina Oliveira, Jordan R Becker, Kirstin Bilham, Daniela Moralli, Consuelo Anzilotti, Roman Fischer, et al. 2018. “53BP1 Cooperation with the REV7-Shieldin Complex Underpins DNA Structure-Specific NHEJ.” *Nature* 560 (7716): 122–27. https://doi.org/10.1038/s41586-018-0362-1.

Gupta, Rajat, Kumar Somyajit, Takeo Narita, Elina Maskey, Andre Stanlie, Magdalena Kremer, Dimitris Typas, et al. 2018. “DNA Repair Network Analysis Reveals Shieldin as a Key Regulator of NHEJ and PARP Inhibitor Sensitivity.” *Cell* 173 (4): 972-988.e23. https://doi.org/10.1016/j.cell.2018.03.050.

Hahn, Peter, Barbara Nevaldine, and William F. Morgan. 1990. “X-Ray Induction of Methotrexate Resistance Due to Dhfr Gene Amplification.” *Somatic Cell and Molecular Genetics* 16 (5): 413–23. https://doi.org/10.1007/BF01233191.

Hogan, Kevin T., Jennifer N. Sutton, Kyo U. Chu, Jennifer A.C. Busby, Jeffrey Shabanowitz, Donald F. Hunt, and Craig L. Slingluff. 2005. “Use of Selected Reaction Monitoring Mass Spectrometry for the Detection of Specific MHC Class I Peptide Antigens on A3 Supertype Family Members.” *Cancer Immunology, Immunotherapy* 54 (4): 359–71. https://doi.org/10.1007/s00262-004-0592-y.

Huang, Fei, Nuzhat A. Motlekar, Chelsea M. Burgwin, Andrew D. Napper, Scott L. Diamond, and Alexander V. Mazin. 2011. “Identification of Specific Inhibitors of Human RAD51 Recombinase Using High-Throughput Screening.” In *ACS Chemical Biology*, 6:628–35. NIH Public Access. https://doi.org/10.1021/cb100428c.

Huntington, Jonathan T., Janiel M. Shields, Channing J. Der, Colby A. Wyatt, Ulrike

Benbow, Craig L. Slingluff, and Constance E. Brinckerhoff. 2004. “Overexpression of Collagenase 1 (MMP-1) Is Mediated by the ERK Pathway in Invasive Melanoma Cells. Role of BRAF Mutation and Fibroblast Growth Factor Signaling.” *Journal of Biological Chemistry* 279 (32): 33168–76. https://doi.org/10.1074/jbc.M405102200.

Iacovoni, Jason S, Pierre Caron, Imen Lassadi, Estelle Nicolas, Laurent Massip, Didier Trouche, and Gaëlle Legube. 2010. “High-Resolution Profiling of GammaH2AX around DNA Double Strand Breaks in the Mammalian Genome.” *The EMBO Journal* 29 (8): 1446–57. https://doi.org/10.1038/emboj.2010.38.

Jorgensen, S., G. Schotta, and C. S. Sorensen. 2013. “Histone H4 Lysine 20 Methylation: Key Player in Epigenetic Regulation of Genomic Integrity.” *Nucleic Acids Research* 41 (5): 2797–2806. https://doi.org/10.1093/nar/gkt012.

Kittlesen, D J, L W Thompson, P H Gulden, J C Skipper, T A Colella, J Shabanowitz, D F Hunt, V H Engelhard, C L Slingluff, and J A Shabanowitz. 1998. “Human Melanoma Patients Recognize an HLA-A1-Restricted CTL Epitope from Tyrosinase Containing Two Cysteine Residues: Implications for Tumor Vaccine Development.” *Journal of Immunology (Baltimore, Md. : 1950)* 160 (5): 2099–2106. http://www.ncbi.nlm.nih.gov/pubmed/9498746.

Kong, Xiangduo, Samarendra K Mohanty, Jared Stephens, Jason T Heale, Veronica Gomez-Godinez, Linda Z Shi, Jong-Soo Kim, Kyoko Yokomori, and Michael W Berns. 2009. “Comparative Analysis of Different Laser Systems to Study Cellular Responses to DNA Damage in Mammalian Cells.” *Nucleic Acids Research* 37 (9):

e68–e68. https://doi.org/10.1093/nar/gkp221.

Kramara, J, B Osia, and A Malkova. 2018. “Break-Induced Replication: The Where, The Why, and The How.” *Trends in Genetics : TIG* 34 (7): 518–31. https://doi.org/10.1016/j.tig.2018.04.002.

Kuo, Alex J., Jikui Song, Peggie Cheung, Satoko Ishibe-Murakami, Sayumi Yamazoe, James K. Chen, Dinshaw J. Patel, and Or Gozani. 2012. “The BAH Domain of ORC1 Links H4K20me2 to DNA Replication Licensing and Meier-Gorlin Syndrome.” *Nature* 484 (7392): 115–19. https://doi.org/10.1038/nature10956.

Limas, Juanita C., and Jeanette Gowen Cook. 2019. “Preparation for DNA Replication: The Key to a Successful S Phase.” *FEBS Letters* 593 (20): 2853–67. https://doi.org/10.1002/1873-3468.13619.

Lin, Jie Jessie, Michael A. Milhollen, Peter G. Smith, Usha Narayanan, and Anindya Dutta. 2010. “NEDD8-Targeting Drug MLN4924 Elicits DNA Rereplication by Stabilizing Cdt1 in S Phase, Triggering Checkpoint Activation, Apoptosis, and Senescence in Cancer Cells.” *Cancer Research* 70 (24): 10310–20. https://doi.org/10.1158/0008-5472.CAN-10-2062.

Liontos, Michalis, Marilena Koutsami, Maria Sideridou, Konstantinos Evangelou, Dimitris Kletsas, Brynn Levy, Athanassios Kotsinas, et al. 2007. “Deregulated Overexpression of HCdt1 and HCdc6 Promotes Malignant Behavior.” *Cancer Research* 67 (22): 10899–909. https://doi.org/10.1158/0008-5472.CAN-07-2837.

Massip, Laurent, Pierre Caron, Jason S Iacovoni, Didier Trouche, and Gaëlle Legube.

2010. “Deciphering the Chromatin Landscape Induced around DNA Double Strand Breaks.” *Cell Cycle* 9 (15): 3035–44. https://doi.org/10.4161/cc.9.15.12412.

Mavragani, Ifigeneia V, Zacharenia Nikitaki, Maria P Souli, Asef Aziz, Somaira Nowsheen, Khaled Aziz, Emmy Rogakou, and Alexandros G Georgakilas. 2017. “Complex DNA Damage: A Route to Radiation-Induced Genomic Instability and Carcinogenesis.” *Cancers* 9 (7): 91. https://doi.org/10.3390/cancers9070091.

Meselson, M., and F. W. Stahl. 1958. “The Replication of DNA in Escherichia Coli.” *Proceedings of the National Academy of Sciences* 44 (7): 671–82. https://doi.org/10.1073/pnas.44.7.671.

Meselson, M., F. W. Stahl, and J. Vinograd. 1957. “EQUILIBRIUM SEDIMENTATION OF MACROMOLECULES IN DENSITY GRADIENTS.” *Proceedings of the National Academy of Sciences* 43 (7): 581–88. https://doi.org/10.1073/pnas.43.7.581.

Mirman, Zachary, Francisca Lottersberger, Hiroyuki Takai, Tatsuya Kibe, Yi Gong, Kaori Takai, Alessandro Bianchi, Michal Zimmermann, Daniel Durocher, and Titia de Lange. 2018. “53BP1-RIF1-Shieldin Counteracts DSB Resection through CST- and Polα-Dependent Fill-In.” *Nature* 560 (7716): 112–16. https://doi.org/10.1038/s41586-018-0324-7.

Mladenov, Emil, and George Iliakis. 2011. “Induction and Repair of DNA Double Strand Breaks: The Increasing Spectrum of Non-Homologous End Joining Pathways.” *Mutation Research/Fundamental and Molecular Mechanisms of Mutagenesis* 711 (1–2): 61–72. https://doi.org/10.1016/J.MRFMMM.2011.02.005.

Mladenov, Emil, Simon Magin, Aashish Soni, and George Iliakis. 2013. "DNA Double-Strand Break Repair as Determinant of Cellular Radiosensitivity to Killing and Target in Radiation Therapy." *Frontiers in Oncology* 3 (May): 113. https://doi.org/10.3389/fonc.2013.00113.

Molhoek, Kerrington R., Heinrich Griesemann, Jianfen Shu, Jeffrey E. Gershenwald, David L. Brautigan, and Craig L. Slingluff. 2008. "Human Melanoma Cytolysis by Combined Inhibition of Mammalian Target of Rapamycin and Vascular Endothelial Growth Factor/Vascular Endothelial Growth Factor Receptor-2." *Cancer Research* 68 (11): 4392–97. https://doi.org/10.1158/0008-5472.CAN-07-5844.

Nishioka, Kenichi, Judd C Rice, Kavitha Sarma, Hediye Erdjument-Bromage, Janis Werner, Yanming Wang, Sergei Chuikov, et al. 2002. "PR-Set7 Is a Nucleosome-Specific Methyltransferase That Modifies Lysine 20 of Histone H4 and Is Associated with Silent Chromatin." *Molecular Cell* 9 (6): 1201–13. https://doi.org/10.1016/s1097-2765(02)00548-8.

Noordermeer, Sylvie M, Salomé Adam, Dheva Setiaputra, Marco Barazas, Stephen J Pettitt, Alexanda K Ling, Michele Olivieri, et al. 2018. "The Shieldin Complex Mediates 53BP1-Dependent DNA Repair." *Nature* 560 (7716): 117–21. https://doi.org/10.1038/s41586-018-0340-7.

Oda, Hisanobu, Michael R. Hübner, David B. Beck, Michiel Vermeulen, Jerard Hurwitz, David L. Spector, and Danny Reinberg. 2010. "Regulation of the Histone H4 Monomethylase PR-Set7 by CRL4Cdt2-Mediated PCNA-Dependent Degradation

during DNA Damage." *Molecular Cell* 40 (3): 364–76. https://doi.org/10.1016/j.molcel.2010.10.011.

Oda, Hisanobu, Ikuhiro Okamoto, Niall Murphy, Jianhua Chu, Sandy M Price, Michael M Shen, Maria Elena Torres-Padilla, Edith Heard, and Danny Reinberg. 2009. "Monomethylation of Histone H4-Lysine 20 Is Involved in Chromosome Structure and Stability and Is Essential for Mouse Development." *Molecular and Cellular Biology* 29 (8): 2278–95. https://doi.org/10.1128/MCB.01768-08.

Panier, Stephanie, and Simon J Boulton. 2013. "Double-Strand Break Repair: 53BP1 Comes into Focus." *Nature Reviews Molecular Cell Biology* 15 (1): 7–18. https://doi.org/10.1038/nrm3719.

Poole, I. Caroline Le, Raymond E. Boissy, Rangaprasao Sarangarajan, Jing Chen, Judith J. Forristal, Pranav Sheth, Wiete Westerhof, George Babcock, Pranab K. Das, and Catharine B. Saelinger. 2000. "PIG3V, an Immortalized Human Vitiligo Melanocyte Cell Line, Expresses Dilated Endoplasmic Reticulum." *In Vitro Cellular & Developmental Biology - Animal 2000 36:5* 36 (5): 309–19. https://doi.org/10.1290/1071-2690(2000)036<0309:PAIHVM>2.0.CO;2.

Povirk, Lawrence F. 2006. "Biochemical Mechanisms of Chromosomal Translocations Resulting from DNA Double-Strand Breaks." *DNA Repair* 5 (9–10): 1199–1212. https://doi.org/10.1016/j.dnarep.2006.05.016.

Santivasi, Wil L, and Fen Xia. 2014. "Ionizing Radiation-Induced DNA Damage, Response, and Repair." *Antioxidants & Redox Signaling* 21 (2): 251–59.

https://doi.org/10.1089/ars.2013.5668.

Scully, Ralph, Arvind Panday, Rajula Elango, and Nicholas A. Willis. 2019. “DNA Double-Strand Break Repair-Pathway Choice in Somatic Mammalian Cells.” *Nature Reviews Molecular Cell Biology*. Nature Publishing Group. https://doi.org/10.1038/s41580-019-0152-0.

Shibata, Etsuko, Manjari Kiran, Yoshiyuki Shibata, Samarendra Singh, Shashi Kiran, and Anindya Dutta. 2016. “Two Subunits of Human ORC Are Dispensable for DNA Replication and Proliferation.” *ELife* 5 (December): e19084. https://doi.org/10.7554/eLife.19084.

Slingluff, C L, A L Cox, R A Henderson, D F Hunt, and V H Engelhard. 1993. “Recognition of Human Melanoma Cells by HLA-A2.1-Restricted Cytotoxic T Lymphocytes Is Mediated by at Least Six Shared Peptide Epitopes.” *The Journal of Immunology* 150 (7): 2955–63.

Tardat, Mathieu, Julien Brustel, Olivier Kirsh, Christine Lefevbre, Mary Callanan, Claude Sardet, and Eric Julien. 2010. “The Histone H4 Lys 20 Methyltransferase PR-Set7 Regulates Replication Origins in Mammalian Cells.” *Nature Cell Biology* 12 (11): 1086–93. https://doi.org/10.1038/ncb2113.

Truong, Lan N., and Xiaohua Wu. 2011. “Prevention of DNA Re-Replication in Eukaryotic Cells.” *Journal of Molecular Cell Biology* 3 (1): 13–22. https://doi.org/10.1093/JMCB/MJQ052.

Tuzon, Creighton T, Tanya Spektor, Xiaodong Kong, Lauren M Congdon, Shumin Wu,

Gunnar Schotta, Kyoko Yokomori, and Judd C Rice. 2014. “Concerted Activities of Distinct H4K20 Methyltransferases at DNA Double-Strand Breaks Regulate 53BP1 Nucleation and NHEJ-Directed Repair.” *Cell Reports* 8 (2): 430–38. https://doi.org/10.1016/j.celrep.2014.06.013.

Vanderdys, Vanessa, Amir Allak, Fadila Guessous, Mouadh Benamar, Paul W. Read, Mark J. Jameson, and Tarek Abbas. 2018. “The Neddylation Inhibitor Pevonedistat (MLN4924) Suppresses and Radiosensitizes Head and Neck Squamous Carcinoma Cells and Tumors.” *Molecular Cancer Therapeutics* 17 (2): 368–80. https://doi.org/10.1158/1535-7163.MCT-17-0083.

Vaziri, Cyrus, Sandeep Saxena, Yesu Jeon, Charles Lee, Kazutaka Murata, Yuichi Machida, Nikhil Wagle, Deog Su Hwang, and Anindya Dutta. 2003. “A P53-Dependent Checkpoint Pathway Prevents Rereplication.” *Molecular Cell* 11 (4): 997–1008. https://doi.org/10.1016/s1097-2765(03)00099-6.

Voitenleitner, Christian, Christoph Rehfuess, Melissa Hilmes, Lynda O’Rear, Pao-Chi Liao, Douglas A. Gage, Robert Ott, Heinz-Peter Nasheuer, and Ellen Fanning. 1999. “Cell Cycle-Dependent Regulation of Human DNA Polymerase α-Primase Activity by Phosphorylation.” *Molecular and Cellular Biology* 19 (1): 646–56. https://doi.org/10.1128/mcb.19.1.646.

Wang, Chen, and Susan P Lees-Miller. 2013. “Detection and Repair of Ionizing Radiation-Induced DNA Double Strand Breaks: New Developments in Nonhomologous End Joining.” *International Journal of Radiation Oncology, Biology, Physics* 86 (3): 440–

49. https://doi.org/10.1016/j.ijrobp.2013.01.011.

Yamshchikov, Galina, Lee Thompson, William G. Ross, Holly Galavotti, William Aquila, Donna Deacon, Jennifer Caldwell, James W. Patterson, Donald F. Hunt, and Craig L. Slingluff. 2001. "Analysis of a Natural Immune Response against Tumor Antigens in a Melanoma Survivor: Lessons Applicable to Clinical Trial Evaluations." *Clinical Cancer Research* 7 (3): 909s-916s.

Yamshchikov, Galina V., David W. Mullins, Chien-Chung Chang, Takeshi Ogino, Lee Thompson, Jennifer Presley, Holly Galavotti, et al. 2005. "Sequential Immune Escape and Shifting of T Cell Responses in a Long-Term Survivor of Melanoma." *The Journal of Immunology* 174 (11): 6863–71. https://doi.org/10.4049/jimmunol.174.11.6863.

Zhou, Yi, Pierre Caron, Gaëlle Legube, and Tanya T Paull. 2014. "Quantitation of DNA Double-Strand Break Resection Intermediates in Human Cells." *Nucleic Acids Research* 42 (3): e19–e19. https://doi.org/10.1093/nar/gkt1309.

x.

Chapter V:

Perspectives, Outstanding Questions, and Concluding Remarks

1. The Oncogenic Potential of CDT2

CDT2 has been shown to be overexpressed in various cancer types including breast and gastric cancers, Ewing sarcoma, gastric carcinoma, hepatocellular carcinoma, head and neck squamous cell carcinoma, and melanoma (Benamar et al. 2016; Vanderdys et al. 2018; Kobayashi et al. 2015; Mackintosh et al. 2012; Li et al. 2009; Ueki et al. 2008; Pan et al. 2006). In certain tumors such as melanoma, gastric cancer, and hepatocellular carcinoma, CDT2 overexpression correlates with poor patient survival (Kobayashi et al. 2015; Pan et al. 2006; Benamar et al. 2016). It is not clear whether deregulated overexpression of CDT2 can exert oncogenic properties sufficient to drive tumorigenesis. The observed correlation with poor prognosis can be attributed to its substrates p21 and SET8 which are crucial to DNA damage response and cell cycle regulation, and their degradation upon Cdt2 overexpression provides survival advantage to cells with oncogenic properties (Panagopoulos et al. 2020). DNA replication licensing aberration has been linked to oncogene-induced replication stress highlighting the role licensing factor regulation plays in tumorigenesis (Halazonetis, Gorgoulis, and Bartek 2008; Petropoulos et al. 2019).

Unscheduled proteolysis of licensing factors as a result of overexpression of CDT2 can lead to decrease occupancy at origin sites and therefore origin under-licensing. This could leave parts of the DNA under-replicated and can therefore promote genome instability and tumorigenesis (Petropoulos et al. 2019; Panagopoulos et al. 2020). However, CDT2 overexpression is unlikely to contribute to significant under-licensing due

to the PCNA requirement of $CRL4^{CDT2}$-mediated proteolysis and most origins are licensed before S-phase under normal conditions.

Another observation that highlights the potential oncogenic role of CDT2 is stabilization in high-risk HPV induced cancers. In short, E6 oncoproteins promote the selective recruitment of the deubiquitinase USP46 to stabilize CDT2, leading to the increased $CRL4^{CDT2}$ activity, increased degradation of Set8, and the subsequent cell cycle deregulation and tumor growth. The elevated expression of CDT2 in HPV-transformed cells was found to be dependent on USP46. Therefore, high-risk HPV-infection is suggested to "rewire" the cell so that cellular proliferation is more dependent on USP46 and potentially CDT2 (Kiran et al. 2018; Panagopoulos et al. 2020).

2. Rereplication and Region-Specific Amplification:

It has been reported in Chapter One that only about 20% of all metazoans available origin sites initiate DNA replication during an unperturbed S-phase while the rest remain "dormant." The presence of dormant origins is believed to play an essential role in genome preservation and may act as backup origins during replication stress (Cayrou et al. 2015; Marks, Fu, and Aladjem 2017; Fragkos et al. 2015). Does rereplication induced after deregulated origin licensing, whether as a result of genetic or pharmacological disruption of licensing control, make use of the dormant sites and increase occupancy of both active and dormant origins? or simply increase helicase loading on the same origins already in use during the same cell cycle? In addition, since metazoan origins of replication exhibit high heterogeneity (Fragkos et al. 2015), are there specific chromatin or epigenetic features

or chromosomal structures that provide a favorable environment permissive of rereplication induction? Furthermore, gene amplification and increased copy variants has been observed in rereplicating cells in budding yeast (Green, Finn, and Li 2010). We wonder if there are specific regions in the human genome that are selectively enriched as a result of rereplication?

3. DSB-induced Rereplication: Potent Driver of Genomic Amplification:

In Chapter Three, we revealed a previously unrecognized mechanism by which IR-induced DSBs result in repair-associated cytotoxic DNA synthesis. Rereplication has been shown to be a potent inducer of the early steps of gene amplification and increase in copy number variations (Green, Finn, and Li 2010). Our detailed findings provide a mechanism that is consistent with earlier observations that free double strand DNA ends lead to gene amplifications under various conditions including radiation, endonucleases, and antineoplastic agents. Earlier studies have shown that treatment of cells with X-rays or pharmacological agents that induce DSBs, such as Methotrexate (MTX), stimulate gene amplification (Hahn, Nevaldine, and Morgan 1990; Schimke 1984b). For instance, treatment of mouse EMT-6 cells with these agents resulted in MTX resistance due to the amplification of DHFR (dihydrofolate reductase), whose gene amplification was detected by metaphase spread and pulsed-field gel electrophoresis of radiation-induced double minutes (DMs) (Hahn, Nevaldine, and Morgan 1990). Gene amplification often produces two major structures: intrachromosomal homogeneously staining regions (HSR) that can be generated after religation of the broken ends of the two sister chromatids (breakage-

fusion-bridge model); and extra chromosomal double minutes (DMs) (Chiara Mondello, Smirnova, and Giulotto 2010; Cai et al. 2019).

Similarly, treatment of Chinese hamster cells with gamma radiation was shown to increase gene amplification of CAD (carbamyl-p-synthetase aspartate transcarbamylase dihydro-orotase). Gene amplification was measured by treatment-induced resistance to PALA (*N*-(phosphonacetyl)-l-aspartate) achieved after CAD amplification (Chiara Mondello et al. 2002). When I-SceI target sequence was inserted into the genome in close proximity to the DHFR gene, ectopic expression of the restriction endonuclease was found to trigger DHFR amplification through I-SceI-induced DSBs (Pipiras et al. 1998). We speculate that DIRR is the underlying mechanism that contribute to the observed gene amplification observed after ionizing radiation and DSB-inducing treatments.

None of these studies have looked at the cell population with greater than 4N DNA to observe excessive replication or amplification and relied primarily on conferred resistance to antineoplastic agents such as MTX. However, it would be informative to perform a chromosome or metaphase spread on IR or MLN4924-treated cells and isolate, examine, or sequence the resulting extrachromosomal double minutes and further investigate genomic regions or potential hot spots that are selectively rereplicated or amplified upon treatment.

Consistently with our findings that deficiency in the NHEJ pathway and 53BP1 recruitment to DSBs stimulate DIRR, deficiency in NHEJ factors such as ATM and DNA-PKcs enhances gene amplification propensity. Chinese hamster V3 cells, which are deficient in the NHEJ repair process due to a mutation in DNA-PKcs, showed increased

gene amplification after irradiation compared to the parental AA8 cells with unperturbed DNA repair pathway (Chiara Mondello et al. 2002). The same result was observed in immortalized mouse embryo fibroblasts derived from mice with a mutation that decreases DNA-PKcs protein expression, and human tumor cells treated with shRNA against DNA-PKcs, but not in primary mouse fibroblasts derived from knockout mice (Taccioli et al. 1998; C Mondello et al. 2001; Salzano et al. 2009). Deficiency in the p53 pathway, which stimulates DIRR, also leads to increased gene amplification even in non-permissive cells independent of tumorigenesis (Yin et al. 1992; Livingstone et al. 1992). Gene amplification is viewed as a result of the persistence of unrepaired DSBs and the disruption of the NHEJ pathway delays the joining of broken ends and favor gene amplification.

Our results demonstrated that HR, and more precisely hyper resection and strand invasion, promotes DIRR. Consistent with our earlier observations, HR was found to promote gene amplification in culture cells. BRCA1, which plays an integral role in HR by facilitating 53BP1 dephosphorylation, promoting end resection and RAD51-dependent strand invasion, was also shown to promote gene amplification in MTX-resistant cells. Silencing BRCA1, which results in downregulation of MRE11 and reduction in Rad51 foci formation, was found to markedly decrease gene amplification and reduce the number of extrachromosomal double minutes in cancer cells (Cai et al. 2019).

Gene amplification has been shown to promote oncogenesis and drug-resistance in various tumor models (Turner et al. 2017). Further understanding the molecular basis of DSB-induced rereplication will provide insight on the underlying mechanism that facilitate

the gene amplification of oncogenes and acquired resistance that often lead to cancer therapy failure.

4. The Role of SET8 in Rereplication:

The mono-methyl transferase SET8 is found to be critical in rereplication induced after deregulated replicative control. Our results in Chapter Two demonstrated that, unlike CDT1 and p21, SET8 is both necessary and sufficient to promote rereplication in melanoma cells and Set8 deficient cells fail to undergo extensive rereplication post MLN4924 treatment. The exact mechanism by which deregulated SET8 expression promotes rereplication may not be clear, but methylation of histone H4K20 may be critical for this activity (Abbas et al. 2010; Tardat et al. 2010). In fact, H4K20me2, which was found to be enriched at origins of replication, was shown to enhance both ORC1 and MCM2-7 loading and occupancy at origins and would therefore facilitate relicensing leading to rereplication (Kuo et al. 2012; Brustel et al. 2017). On the other hand, Set8 appears to play an antagonizing role in the origin-licensing independent IR-induced rereplication. This is due to the fact that Set8-mediated H4K20 dimethylation enhances 53BP1 binding at DSBs which blocks the hyper end-resection needed to promote IR-induced rereplication.

5. Rereplication Regulation in Endocycling Cells:

Not all forms of rereplication results in cell death and genomic instability. Endoreplication, which refers the doubling of the entire genome in the absence of mitosis resulting in polyploid cells, is a normal process that occurs regularly during the

development of certain cell types such as megakarocytes and trophoblastic cells (Zybina and Zybina 2005; Deutsch and Tomer 2006). How does the cell differentiate between an abnormal rereplication and a normal endoreplication required for tissue development? A number of studies have attempted to investigate the difference in the regulation and response to these two atypical forms of DNA replication. One study demonstrated that the canonical ORC complex is dispensable for DNA replication in endoreplicating cells (Asano 2009). Another study in *Drosophila* have shown that the tight control of Geminin expression and its proteolysis by APC/C after S-phase is required for rereplication control in endoreplicating cells (Zielke et al. 2008). In addition to that, further studies are needed to shed the light on how cell cycle checkpoint respond differently to these two physiologically distinct phenomena (Truong and Wu 2011).

6. Rereplication and Tumorigenesis

Various studies have demonstrated the tight association between deregulated origin licensing control and tumorigenesis, further emphasizing the significance of understanding rereplication in tumor development. Even though the overexpression of CDT1 has been shown to promote tumor growth, **there is still no direct correlation between rereplication and tumorigenesis** (Truong and Wu 2011). Even though studies have shown that overexpression of licensing factors, such as CDT1 or CDC6, can act as a main driver of oncogenesis, independent of its pro-proliferation effect, there is still not enough evidence to further support the role rereplication per se plays in the observed tumor development (Liontos et al. 2007). Given that CDC6 was implemented in the repression of tumor suppressors such as p15, p16, and ARF (Gonzalez et al. 2006), **could the observed**

oncogenic potential of CDT1 and CDC6 overexpression be independent of their role in promoting rereplication?

The rereplication-induced genomic instability promotes apoptosis and senescence, which are anti-tumor barriers. It has been reported that p53-inactivation and similar deficiencies in apoptotic and senescence pathways synergize with deregulated overexpression of CDT1 and CDC6 to increase rereplication and tumor formation (Seo et al. 2005; Karakaidos et al. 2004). Therefore, **is the oncogenic potential of rereplication dependent solely on the subsequent accumulation of mutations and, consequently, inactivation of the checkpoint pathways?** Is rereplication sufficient to permit cells to escape checkpoint machinery and anti-tumor barriers? Are other forms of genomic instability that contribute to the observed rereplication-induced tumorigenesis? It is worth noting that gene amplification and chromosomal rearrangements as a result of stalled replication forks have been implicated in cancer and can potentially be among the mechanisms that promote this rereplication-induced tumorigenesis (Brison 1993; Schimke 1984a; Albertson 2006).

Given all the studies that illustrate the potential role rereplication plays in the early stages of tumorigenesis, **is long-term continuous treatment with sub-lethal doses of MLN4924 sufficient to transform primary cell and promote tumor growth?** This would not be surprising since many low doses of anti-cancer therapies that exert DNA damage have been shown to promote tumorigenesis.

7. References:

Abbas, Tarek, Etsuko Shibata, Jonghoon Park, Sudhakar Jha, Neerja Karnani, and Anindya Dutta. 2010. "CRL4Cdt2 Regulates Cell Proliferation and Histone Gene Expression by Targeting PR-Set7/Set8 for Degradation." *Molecular Cell* 40 (1): 9–21. https://doi.org/10.1016/j.molcel.2010.09.014.

Albertson, Donna G. 2006. "Gene Amplification in Cancer." *Trends in Genetics*. https://doi.org/10.1016/j.tig.2006.06.007.

Asano, Maki. 2009. "Endoreplication: The Advantage to Initiating DNA Replication without the ORC?" *Fly* 3 (2): 173–75. https://doi.org/10.4161/fly.8087.

Benamar, Mouadh, Fadila Guessous, Kangping Du, Patrick Corbett, Joseph Obeid, Daniel Gioeli, Craig L. Slingluff, and Tarek Abbas. 2016. "Inactivation of the CRL4-CDT2-SET8/P21 Ubiquitylation and Degradation Axis Underlies the Therapeutic Efficacy of Pevonedistat in Melanoma." *EBioMedicine* 10 (August): 85–100. https://doi.org/10.1016/j.ebiom.2016.06.023.

Brison, Olivier. 1993. "Gene Amplification and Tumor Progression." *BBA - Reviews on Cancer*. https://doi.org/10.1016/0304-419X(93)90020-D.

Brustel, Julien, Nina Kirstein, Fanny Izard, Charlotte Grimaud, Paulina Prorok, Christelle Cayrou, Gunnar Schotta, et al. 2017. "Histone H4K20 Tri-methylation at Late-firing Origins Ensures Timely Heterochromatin Replication." *The EMBO Journal* 36 (18): 2726–41. https://doi.org/10.15252/embj.201796541.

Cai, Mengdi, Huishu Zhang, Liqing Hou, Wei Gao, Ying Song, Xiaobo Cui, Chunxiang Li, et al. 2019. "Inhibiting Homologous Recombination Decreases Extrachromosomal Amplification but Has No Effect on Intrachromosomal Amplification in Methotrexate-Resistant Colon Cancer Cells." *International Journal of Cancer* 144 (5): 1037–48. https://doi.org/10.1002/ijc.31781.

Cayrou, Christelle, Benoit Ballester, Isabelle Peiffer, Romain Fenouil, Philippe Coulombe,

Jean Christophe Andrau, Jacques Van Helden, and Marcel Méchali. 2015. “The Chromatin Environment Shapes DNA Replication Origin Organization and Defines Origin Classes.” *Genome Research* 25 (12): 1873–85. https://doi.org/10.1101/gr.192799.115.

Deutsch, Varda R., and Aaron Tomer. 2006. “Megakaryocyte Development and Platelet Production.” *British Journal of Haematology*. https://doi.org/10.1111/j.1365-2141.2006.06215.x.

Fragkos, Michalis, Olivier Ganier, Philippe Coulombe, and Marcel Méchali. 2015. “DNA Replication Origin Activation in Space and Time.” *Nature Reviews Molecular Cell Biology*. Nature Publishing Group. https://doi.org/10.1038/nrm4002.

Gonzalez, Susana, Peter Klatt, Sonia Delgado, Esther Conde, Fernando Lopez-Rios, Montserrat Sanchez-Cespedes, Juan Mendez, Francisco Antequera, and Manuel Serrano. 2006. “Oncogenic Activity of Cdc6 through Repression of the INK4/ARF Locus.” *Nature*. Nature Publishing Group. https://doi.org/10.1038/nature04585.

Green, Brian M., Kenneth J. Finn, and Joachim J. Li. 2010. “Loss of DNA Replication Control Is a Potent Inducer of Gene Amplification.” *Science* 329 (5994): 943–46. https://doi.org/10.1126/science.1190966.

Hahn, Peter, Barbara Nevaldine, and William F. Morgan. 1990. “X-Ray Induction of Methotrexate Resistance Due to Dhfr Gene Amplification.” *Somatic Cell and Molecular Genetics* 16 (5): 413–23. https://doi.org/10.1007/BF01233191.

Halazonetis, Thanos D., Vassilis G. Gorgoulis, and Jiri Bartek. 2008. “An Oncogene-Induced DNA Damage Model for Cancer Development.” *Science*. American Association for the Advancement of Science. https://doi.org/10.1126/science.1140735.

Karakaidos, Panagiotis, Stavros Taraviras, Leandros V. Vassiliou, Panayotis Zacharatos, Nikolaos G. Kastrinakis, Dionysia Kougiou, Mirsini Kouloukoussa, et al. 2004. “Overexpression of the Replication Licensing Regulators HCdt1 and HCdc6

Characterizes a Subset of Non-Small-Cell Lung Carcinomas: Synergistic Effect with Mutant P53 on Tumor Growth and Chromosomal Instability - Evidence of E2F-1 Transcriptional Control over HCdt1." *American Journal of Pathology* 165 (4): 1351–65. https://doi.org/10.1016/S0002-9440(10)63393-7.

Kiran, Shashi, Ashraf Dar, Samarendra K. Singh, Kyung Yong Lee, and Anindya Dutta. 2018. "The Deubiquitinase USP46 Is Essential for Proliferation and Tumor Growth of HPV-Transformed Cancers." *Molecular Cell* 72 (5): 823-835.e5. https://doi.org/10.1016/j.molcel.2018.09.019.

Kobayashi, Hiroki, Shuhei Komatsu, Daisuke Ichikawa, Tsutomu Kawaguchi, Shoji Hirajima, Mahito Miyamae, Wataru Okajima, et al. 2015. "Overexpression of Denticleless E3 Ubiquitin Protein Ligase Homolog (DTL) Is Related to Poor Outcome in Gastric Carcinoma." *Oncotarget* 6 (34): 36615–24. https://doi.org/10.18632/oncotarget.5620.

Kuo, Alex J., Jikui Song, Peggie Cheung, Satoko Ishibe-Murakami, Sayumi Yamazoe, James K. Chen, Dinshaw J. Patel, and Or Gozani. 2012. "The BAH Domain of ORC1 Links H4K20me2 to DNA Replication Licensing and Meier-Gorlin Syndrome." *Nature* 484 (7392): 115–19. https://doi.org/10.1038/nature10956.

Li, J., E. K.O. Ng, Y. P. Ng, C. Y.P. Wong, J. Yu, H. Jin, V. Y.Y. Cheng, et al. 2009. "Identification of Retinoic Acid-Regulated Nuclear Matrix-Associated Protein as a Novel Regulator of Gastric Cancer." *British Journal of Cancer* 101 (4): 691–98. https://doi.org/10.1038/sj.bjc.6605202.

Liontos, Michalis, Marilena Koutsami, Maria Sideridou, Konstantinos Evangelou, Dimitris Kletsas, Brynn Levy, Athanassios Kotsinas, et al. 2007. "Deregulated Overexpression of HCdt1 and HCdc6 Promotes Malignant Behavior." *Cancer Research* 67 (22): 10899–909. https://doi.org/10.1158/0008-5472.CAN-07-2837.

Livingstone, Laura R., Alicia White, Jason Sprouse, Elizabeth Livanos, Tyler Jacks, and Thea D. Tlsty. 1992. "Altered Cell Cycle Arrest and Gene Amplification Potential

Accompany Loss of Wild-Type P53." *Cell* 70 (6): 923–35. https://doi.org/10.1016/0092-8674(92)90243-6.

Mackintosh, C., J. L. Ordóñez, D. J. García-Domínguez, V. Sevillano, A. Llombart-Bosch, K. Szuhai, K. Scotlandi, et al. 2012. "1q Gain and CDT2 Overexpression Underlie an Aggressive and Highly Proliferative Form of Ewing Sarcoma." *Oncogene* 31 (10): 1287–98. https://doi.org/10.1038/onc.2011.317.

Marks, Anna B., Haiqing Fu, and Mirit I. Aladjem. 2017. "Regulation of Replication Origins." In *Advances in Experimental Medicine and Biology*, 1042:43–59. Springer New York LLC. https://doi.org/10.1007/978-981-10-6955-0_2.

Mondello, C, P Rebuzzini, M Dolzan, S Edmonson, G E Taccioli, and E Giulotto. 2001. "Increased Gene Amplification in Immortal Rodent Cells Deficient for the DNA-Dependent Protein Kinase Catalytic Subunit." *Cancer Research* 61 (11): 4520–25. http://www.ncbi.nlm.nih.gov/pubmed/11389084.

Mondello, Chiara, Valentina Guasconi, Elena Giulotto, and Fiorella Nuzzo. 2002. "γ-Ray and Hydrogen Peroxide Induction of Gene Amplification in Hamster Cells Deficient in DNA Double Strand Break Repair." *DNA Repair* 1 (6): 483–93. https://doi.org/10.1016/S1568-7864(02)00035-6.

Mondello, Chiara, Alexandra Smirnova, and Elena Giulotto. 2010. "Gene Amplification, Radiation Sensitivity and DNA Double-Strand Breaks." *Mutation Research - Reviews in Mutation Research*. Elsevier. https://doi.org/10.1016/j.mrrev.2010.01.008.

Pan, Hung Wei, Han Yi E. Chou, Shu Hsiang Liu, Shian Yang Peng, Chao Lien Liu, and Hey Chi Hsu. 2006. "Role of L2DTL, Cell Cycle-Regulated Nuclear and Centrosome Protein, in Aggressive Hepatocellular Carcinoma." *Cell Cycle* 5 (22): 2676–87. https://doi.org/10.4161/cc.5.22.3500.

Panagopoulos, Andreas, Stavros Taraviras, Hideo Nishitani, and Zoi Lygerou. 2020. "CRL4Cdt2: Coupling Genome Stability to Ubiquitination." *Trends in Cell Biology*. Elsevier Ltd. https://doi.org/10.1016/j.tcb.2020.01.005.

Petropoulos, Michalis, Spyridon Champeris Tsaniras, Stavros Taraviras, and Zoi Lygerou. 2019. “Replication Licensing Aberrations, Replication Stress, and Genomic Instability.” *Trends in Biochemical Sciences*. Elsevier Ltd. https://doi.org/10.1016/j.tibs.2019.03.011.

Pipiras, E., A. Coquelle, A. Bieth, and M. Debatisse. 1998. “Interstitial Deletions and Intrachromosomal Amplification Initiated from a Double-Strand Break Targeted to a Mammalian Chromosome.” *EMBO Journal* 17 (1): 325–33. https://doi.org/10.1093/emboj/17.1.325.

Salzano, Alberto, Nino Kochiashvili, Solomon G. Nergadze, Lela Khoriauli, Alexandra Smirnova, Aurora Ruiz-Herrera, Chiara Mondello, and Elena Giulotto. 2009. “Enhanced Gene Amplification in Human Cells Knocked down for DNA-PKcs.” *DNA Repair* 8 (1): 19–28. https://doi.org/10.1016/j.dnarep.2008.08.015.

Schimke, Robert T. 1984a. “Gene Amplification, Drug Resistance, and Cancer.” *Cancer Research* 44 (5): 1735–42.

Schimke, Robert T. 1984b. “Gene Amplification in Cultured Animal Cells Review.” *Cell*. Vol. 37.

Seo, Junghee, Yun S. Chung, Girdhar G. Sharma, Eunpyo Moon, Walter R. Burack, Tej K. Pandita, and Kyunghee Choi. 2005. “Cdt1 Transgenic Mice Develop Lymphoblastic Lymphoma in the Absence of P53.” *Oncogene* 24 (55): 8176–86. https://doi.org/10.1038/sj.onc.1208881.

Taccioli, Guillermo E., Aldo G. Amatucci, Heather J. Beamish, David Gell, Xie H. Xiang, Maria I. Torres Arzayus, Ann Priestley, et al. 1998. “Targeted Disruption of the Catalytic Subunit of the DNA-PK Gene in Mice Confers Severe Combined Immunodeficiency and Radiosensitivity.” *Immunity* 9 (3): 355–66. https://doi.org/10.1016/S1074-7613(00)80618-4.

Tardat, Mathieu, Julien Brustel, Olivier Kirsh, Christine Lefevbre, Mary Callanan, Claude Sardet, and Eric Julien. 2010. “The Histone H4 Lys 20 Methyltransferase PR-Set7

Regulates Replication Origins in Mammalian Cells." *Nature Cell Biology* 12 (11): 1086–93. https://doi.org/10.1038/ncb2113.

Truong, Lan N., and Xiaohua Wu. 2011. "Prevention of DNA Re-Replication in Eukaryotic Cells." *Journal of Molecular Cell Biology* 3 (1): 13–22. https://doi.org/10.1093/JMCB/MJQ052.

Turner, Kristen M., Viraj Deshpande, Doruk Beyter, Tomoyuki Koga, Jessica Rusert, Catherine Lee, Bin Li, et al. 2017. "Extrachromosomal Oncogene Amplification Drives Tumour Evolution and Genetic Heterogeneity." *Nature* 543 (7643): 122–25. https://doi.org/10.1038/nature21356.

Ueki, T., T. Nishidate, J. H. Park, M. L. Lin, A. Shimo, K. Hirata, Y. Nakamura, and T. Katagiri. 2008. "Involvement of Elevated Expression of Multiple Cell-Cycle Regulator, DTL/RAMP (Denticleless/RA-Regulated Nuclear Matrix Associated Protein), in the Growth of Breast Cancer Cells." *Oncogene* 27 (43): 5672–83. https://doi.org/10.1038/onc.2008.186.

Vanderdys, Vanessa, Amir Allak, Fadila Guessous, Mouadh Benamar, Paul W. Read, Mark J. Jameson, and Tarek Abbas. 2018. "The Neddylation Inhibitor Pevonedistat (MLN4924) Suppresses and Radiosensitizes Head and Neck Squamous Carcinoma Cells and Tumors." *Molecular Cancer Therapeutics* 17 (2): 368–80. https://doi.org/10.1158/1535-7163.MCT-17-0083.

Yin, Yuxin, Michael A. Tainsky, Farideh Z. Bischoff, Louise C. Strong, and Geoffrey M. Wahl. 1992. "Wild-Type P53 Restores Cell Cycle Control and Inhibits Gene Amplification in Cells with Mutant P53 Alleles." *Cell* 70 (6): 937–48. https://doi.org/10.1016/0092-8674(92)90244-7.

Zielke, Norman, Silvia Querings, Carmen Rottig, Christian Lehner, and Frank Sprenger. 2008. "The Anaphase-Promoting Complex/Cyclosome (APC/C) Is Required for Rereplication Control in Endoreplication Cycles." *Genes and Development* 22 (12): 1690–1703. https://doi.org/10.1101/gad.469108.

Zybina, Tatiana G., and Eugenia V. Zybina. 2005. “Cell Reproduction and Genome Multiplication in the Proliferative and Invasive Trophoblast Cell Populations of Mammalian Placenta.” *Cell Biology International*. https://doi.org/10.1016/j.cellbi.2005.10.015.